

1 **Answers to reviewer 1**

2

3 We thank the reviewer for carefully reading our manuscript and for their thoughtful responses. The recommendations they
4 gave were very valuable and have helped us to improve the paper. We have made many changes to the paper per the reviewer's
5 request. Notably, we added information on the comparison of our results to the literature and proposed additional
6 parameterizations for an easier use from the community. However, the conclusions and main message of the paper did not
7 change.

8

9 Before proceeding to specific comments, we first will describe the changes made to the calculation of surface area normalized
10 INP concentrations, as this is the basis for the rest of the changes to the manuscript.

11 First, we calculated adjusted daily mean particle size distribution based on sampling time intervals from the differential
12 mobility particle sizer (DMPS) that aligned better with when the filters later analyzed by the Dynamic filter processing chamber
13 (DFPC) were collecting particles. In our original manuscript, daily means of DMPS data were calculated on a 24-hour time
14 interval beginning and ending at midnight. As DFPC filter samples were not collected at these exact times, there existed a
15 small misalignment between DMPS and DFPC sampling intervals. We therefore re-calculated the DMPS daily mean across
16 each DFPC sampling period. We also did the same adjustment for daily means of underway data when comparing underway
17 data to the DFPC INP concentrations. We added error bars to represent the standard deviation throughout each sampling period
18 to the resulting size distributions, produced from the bubbling system during each DFPC sampling period, shown in Figure
19 R1. This figure has been added to the supporting information as Figure S3 on line 18.

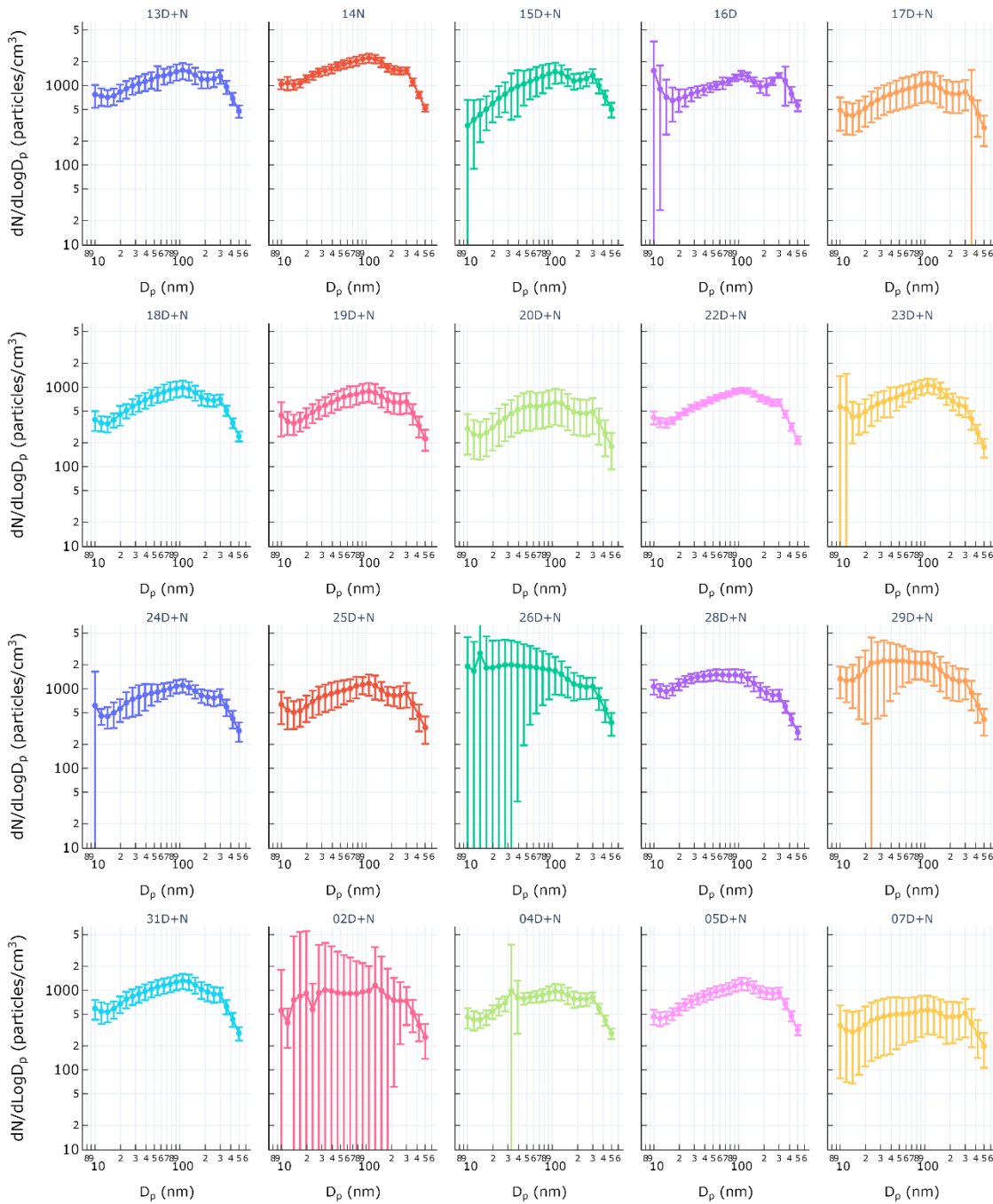


Figure R1.

20

21 Average size distributions of SSA produced by the plunging apparatus as observed by DMPS across each DFPC sampling
 22 period. Error bars represent standard deviation.

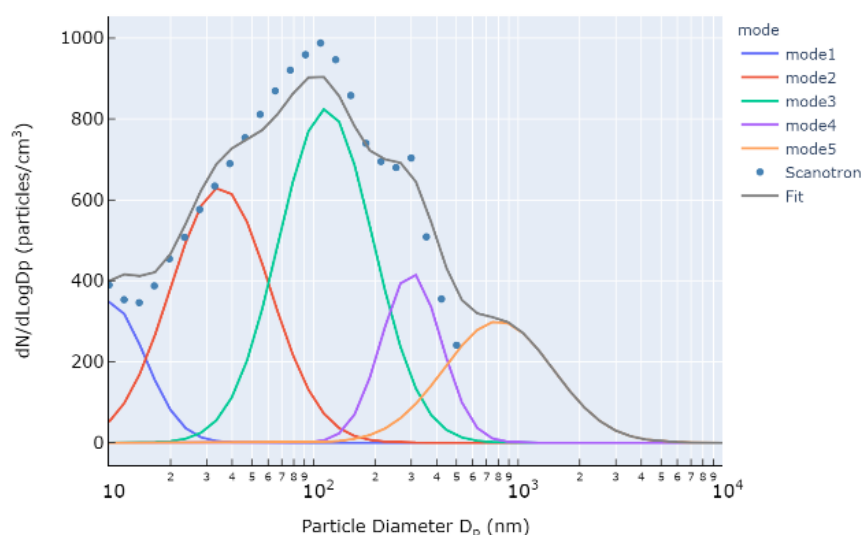
23 Both reviewers expressed concern that the DMPS data used to calculate surface area of SSA that did not include particles
 24 above 500 nm in diameter. The reviewers correctly pointed out that an additional mode at 800 nm exists, which contains a
 25 large portion of SSA surface area. Ovadneveite et al. (2014) developed a sea spray aerosol source function consisting of 5 log-
 26 normal modes based on in-situ particle number concentration measurements at Mace Head and open-ocean eddy correlation
 27 flux measurements from the Eastern Atlantic. Comparison of parameters from their fit with those from the fit of our number-
 28 size distribution revealed good agreement between the two. The parameters are shown in Table R1 below. This table has been
 29 added to the SI on line 1 as Table S1.

30 **Table R1.** Lognormal parameters for a sea spray source function parameterization from Ovadneveite et al. (2013) and for the
 31 fit of observed particle counts during the PEACETIME cruise. For each mode (i), a geometric standard deviation (σ_i), count-
 32 median diameter (CMD_i), and total number flux (F_i) or amplitude is shown. For the fit from the literature (Ovadnevaite et al.,

33 2014). F_i is a function of Reynolds number Re_{HW} which we selected as 3.1×10^6 based on the air flow across the surface of the
 34 water in our bubbling apparatus.

i	σ_i	CMD_i	$F_i/\text{Amplitude}$
Ovadneveite et al. (2013)			
1	1.37	0.018	$104.5(Re_{HW} - 1 \times 10^5)^{0.556}$
2	1.5	0.041	$0.0442(Re_{HW} - 1 \times 10^5)^{1.08}$
3	1.42	0.09	$149.6(Re_{HW} - 1 \times 10^5)^{0.545}$
4	1.53	0.23	$2.96(Re_{HW} - 1 \times 10^5)^{0.79}$
5	1.85	0.83	$0.51(Re_{HW} - 1 \times 10^5)^{0.87}$
PEACETIME Cruise			
1	1.5	0.01	0.01
2	1.75	0.035	0.025
3	1.7	0.115	0.031
4	1.4	0.300	0.01

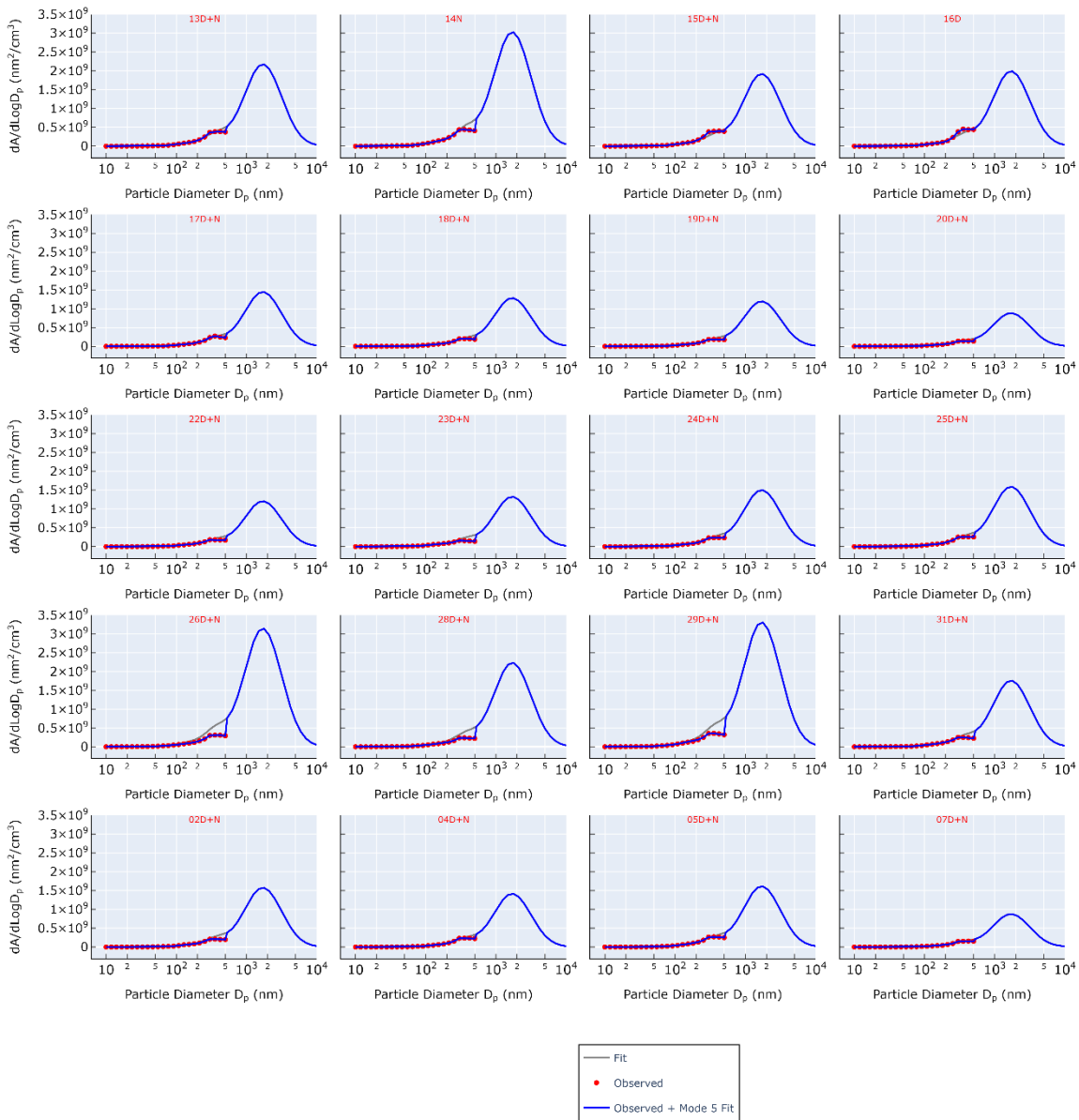
35 We next took the ratio of mode 5 to mode 3 from the Ovadneveite (2014) fit and applied it to our fit to calculate a fifth mode
 36 accounting for particles ranging in size between 500 nm and 10 μm . Figure R2 shows an example of the result of this process
 37 using daily mean data from March 18. The total fit is shown in gray, which consists of modes 1-4 as calculated from our DMPS
 38 data, as well as mode 5 calculated as described above. Blue circles represent observed values.



39 **Figure R2.** Example of resulting size distribution fit based on comparison of fit from observed PEACETIME particle counts
 40 with a 5 lognormal-mode fit from the literature (Ovadneveite et al., 2014). Blue markers denote particle counts by the DMPS
 41 instrument (named Scanotron). Modes 1-4 are fit based on onserved data. Mode 5 is calculated by taking the ratio of Mode 5/3
 42 from the Ovadneveite et al. (2014) fit and applying it to our observed mode 3.

43 We applied this calculation to the mean data from the DMPS for each DFPC sampling period. From the resulting fits, we
 44 calculated aerosol surface area distribution, shown in Figure R3 (also found on line 22 of the Supporting Information as Figure
 45 S4). Finally, we used this adjusted surface area value to re-calculate surface area normalized INP concentrations. We have
 46 added description of this calculation to the main text on line 172.

47 Where relevant throughout the remainder of this text, we will refer readers to this initial comment.



48

49 **Figure R3.** Daily average of adjusted SSA surface area distributions. Sampling time is indicated in red text at the top of each
 50 plot, where numbers indicate the day of the month and D/N indicates whether sampling was conducted at day/night,
 51 respectively. The gray line shows the combined fit of modes 1-4 from observed data with the additional contribution of mode
 52 5 as calculated using the Ovadnevaite et al. (2013) fit . Red circles represent observed values and blue line represents the
 53 surface area from observed values through 500nm plus theoretical contribution from mode 5 from the gray fit. The small
 54 difference between blue and gray lines indicates the goodness of the fit.

55

56

57 General Comments: The paper Trueblood et al. 2020 is a nice study which considers INP data from oligotrophic/Mediterranean
 58 waters and shows that eutrophic parameterisations (W15 and MC18) result in over-prediction. The occurrence of a dust
 59 deposition event over the measurement periods, in conjunction with measurements from the SML, SSW, and SSA, makes for
 60 very interesting reading, although it is a shame that the dataset ends before INPSSA concentrations reached a clear maximum.
 61 However, this brings up the question can the two-component temperature dependent parameterisation from this study be
 62 relevant to much larger bodies of water? I am happy that the authors themselves addressed this in the need for future work
 63 relating INPSSA to POC and NCBL measurements in the Southern Ocean. However, the difficulty in choosing POC and
 64 NCBL in relationship to INP is that all variables must be directly measured.

65 **We now propose a new parameterization based on OC and WIOC in SSA, which is more easily measurable or predictable.**

66 The authors give no indication how to apply this parameterisation in a global model.

67 POC classes can be retrieved from satellite data (Rasse et al., 2017) or from Biogeochemical models such as PISCES (Aumont
68 et al., 2015). SSA OC and WIOC characteristics can be taken from existing parameterizations and observations (Albert et al.,
69 2010). This information is now added to line 528 of the manuscript.

70

71 The largest problem with the current study is that no uncertainties or error in the INP measurements (or biological
72 measurements for that matter) are shown or discussed. This paper should not be published without the addition or evaluation
73 of the inherent errors and uncertainties in the measurements themselves and the application of the measurements to creating a
74 parameterisation.

75 As mentioned in the initial comment above, we have included error bars for particle size and surface area distributions. We
76 have also included error bars for data from the DFPC and LINDA instruments. See relevant sections below for details and
77 Figure 1 on line 180, Figure 2 on line 203, and Figure 6 on line 305 of the main text.

78 Also, the authors have not convincingly shown that the temperature dependent parameterisations are necessary to model INP
79 concentrations, although they have shown that oligotrophic waters may need different parameterisations to eutrophic waters.

80 To ensure selection of the model that best fits the data, we formulated various parameterizations consisting of different
81 time periods, features, and number of components for temperature ranges. Predictor features were chosen based upon their
82 correlation with INP concentrations as described in the previous section. Single component parameterizations in which INP
83 across all three temperatures were linked with the same features were compared with two-component parameterizations in
84 which INP were split into warm and cold categories, each having their own predictor features. Finally, we developed and
85 compared altered versions of the W15 and MC18 models to account for the oligotrophic seawater of the Mediterranean Sea,
86 as the existing models were formulated from observations of eutrophic waters. Each parameterization was recalculated using
87 data across all days of the cruise as well as for only days before the dust deposition event in order to determine the impact of
88 the dust event on the ability to predict INP. The complete set of parameterizations and their associated fit metrics (R^2 and $R_{adj.}^2$)
89 are given in Table R2.

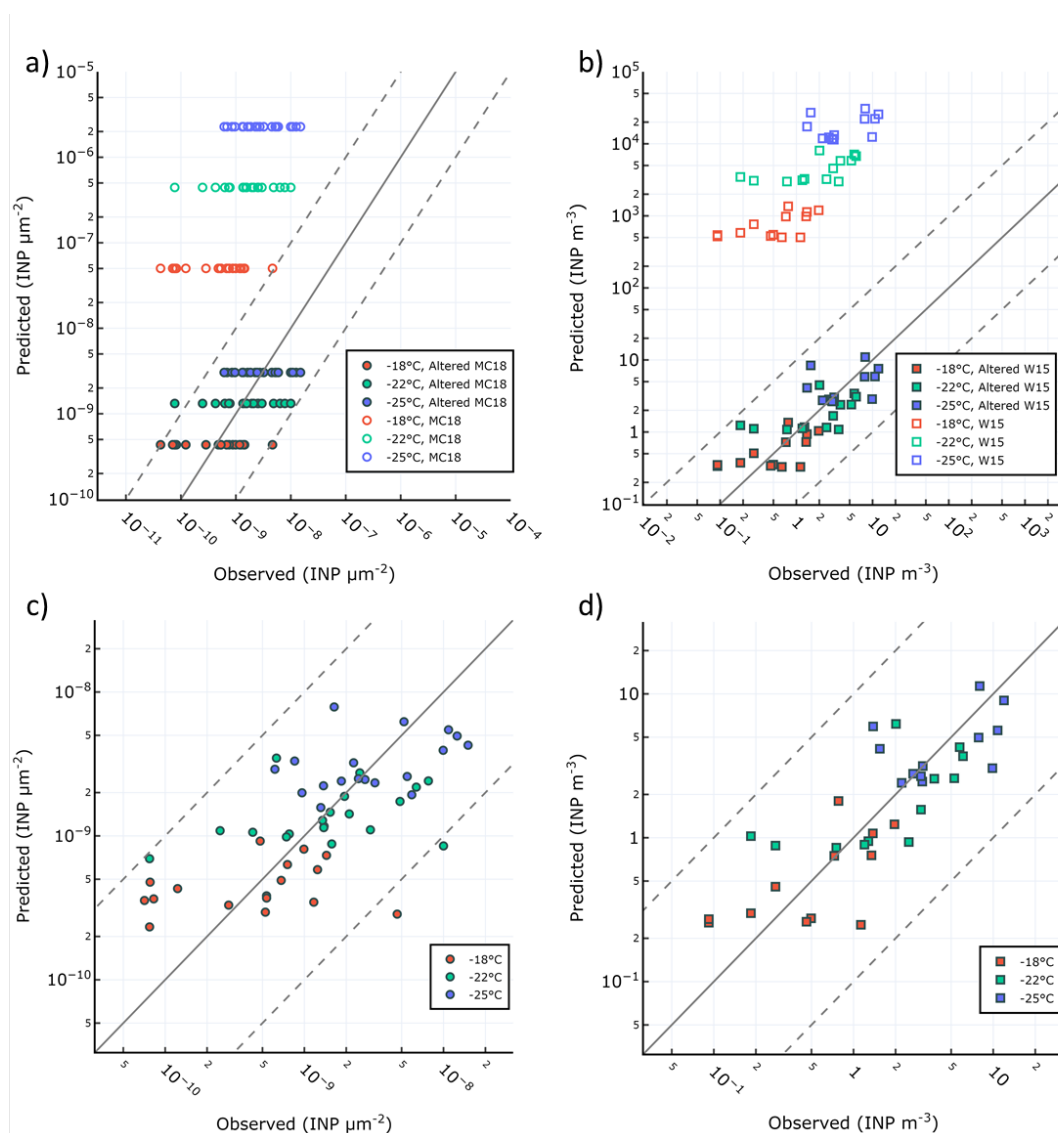
90 Figure R4a shows observed vs predicted INP_{SSA} for the W15 model, while Figure R4b shows the same but using the
91 MC18 parameterization. Similar to our results for seawater INP, a large overprediction is found relative to our observations
92 when using W15. Figure R4b shows that while MC18 is a slight improvement over the W15 approach, it still overpredicts INP
93 by two orders of magnitude. We also present re-calculated best-fit-lines to data using the same features as in W15 and MC18
94 (i.e., OC and SSA surface area) in order to account for possible changes due to the oligotrophic nature of the Mediterranean
95 Sea. We term these two parameterizations the altered Wilson fit for oligotrophy, which is given by:

$$\frac{INP}{m^3} = \exp(-7.332 - (0.2989 * T) + (0.3792 * OC_{SSA}))$$

96 and the altered McCluskey fit for oligotrophy, given as:

$$\frac{INP}{\mu m^2} = \exp(-26.57 - (0.2782 * T))$$

97 The results for these fits are shown in Figure R5a,b alongside the results of the original W15 and MC18 parameterizations.
 98 Both altered models offer improvements over the original parameterizations. The adjusted R^2 of the altered Wilson fit for
 99 oligotrophy on log-transformed INP abundance was $R_{adj}^2=0.59$ and was $R_{adj}^2=0.32$ for the altered McCluskey fit for
 100 oligotrophy. Interestingly, the adjusted Wilson fit for oligotrophy performs better than the adjust McCluskey fit for
 101 oligotrophy, which is the opposite of what was found when comparing the original models.
 102



103 **Figure R54** Different parameterizations for prediction of INP in SSA. a) W15 and refit of same method using PEACETIME
 104 observations b) MK18 and refit of same method using PEACETIME observations c) single-component parameterization for
 105 INP/ μm^2 SSA surface area where INP at all temperatures are related to POC_{SSW} d) two-component parameterization for INP/ m^3
 106 where $\text{INP} \geq -22^\circ\text{C}$ are related to OC and $\text{INP} < -22^\circ\text{C}$ are related to WIOC.

107 We also tried a range of novel parameterizations based on the observed correlations between INP_{SSA} with seawater
 108 and SSA properties. Below we describe two parameterizations which offered good fits to the data. The single-component
 109 parameterization assumes the abundance of INP per unit surface area of total SSA at each temperature can be predicted from
 110 POC_{SSW} concentrations:

$$\frac{INP}{\mu m^2} = \exp(-28.5324 - (0.2729 * T) + (0.0361 * POC_{SSW}))$$

111 The second parameterization separates INP into warm and cold classes, where warm INP ($\geq -22^\circ\text{C}$) are related to SSA
 112 OC and cold INP ($< -22^\circ\text{C}$) are related to the concentration of SSA WIOC. This two-component parameterization predicts the
 113 concentration of INP/ m^3 through the following equations:

$$\frac{INP_{T \geq -22^\circ\text{C}}}{\text{m}^3} = \exp(-7.9857 - (0.3178 * T) + (0.4643 * OC_{SSA}))$$

$$\frac{INP_{T < -22^\circ\text{C}}}{\text{m}^3} = \exp(-6.6606 - (0.2712 * T) + (0.5755 * WIOC_{SSA}))$$

114 Figure R4c,d shows the results of our single-component model using POC_{SSW} and the two-part model which uses SSA WIOC
 115 and OC and considers the separate temperature classes of INP. The adjusted R^2 for each model on the log-transformed INP
 116 abundance were $R_{adj}^2=0.404$ for the single component model using POC_{SSW} and $R_{adj}^2=0.60$ for the two-component model using
 117 OC and WIOC. This result reveals that they both fit the observations better than the altered McCluskey parameterization for
 118 oligotrophy, while the two-component method performs as well as the altered Wilson parameterization. Each
 119 parameterization's fit to the data is improved when considering pre-dust days only ($R_{adj}^2=0.63$ for the two-component
 120 parameterization and $R_{adj}^2=0.57$ for the single-component parameterization). The improvement is more pronounced for the
 121 single-component parameterization using POC_{SSW} , further pointing to the fact that such dust deposition events can alter the
 122 INP properties of surface waters and the subsequent SSA, either through
 123 .

124 **Table R2.** Summary of tested parameterizations to the PEACETIME dataset.

Model Name	INP Units	Days	# Cat.	Features	Warm Features	Cold Features	R^2	R_{adj}^2
PD-2TC_OC_WIOC	INP/ m^3	Pre-Dust	2		OC_{SSA}	WIOC	0.66	0.63
PD-1TC_OC	INP/ m^3	Pre-Dust	1	OC_{SSA}			0.63	0.61
PD-1TC_WSOC_WIOC	INP/ m^3	Pre-Dust	1	WSOC, WIOC			0.64	0.60
AD-2TC_OC_WIOC	INP/ m^3	All Days	2		OC_{SSA}	WIOC	0.63	0.60
AD-1TC_OC	INP/ m^3	All Days	1	OC_{SSA}			0.61	0.59
PD-2TC_POC_PHYTO-L	INP/ μm^2	Pre-Dust	2		POC_{SSW}	Micro-NCBL	0.62	0.59
AD-1TC_WSOC_WIOC	INP/ m^3	All Days	1	WSOC, WIOC			0.62	0.58
PD-1TC_POC	INP/ μm^2	Pre-Dust	1	POC			0.59	0.57
PD-1TC_POC_PHYTO-L	INP/ μm^2	Pre-Dust	1	POC, Micro-NCBL			0.58	0.53
PD-2TC_WSOC_WIOC	INP/ m^3	Pre-Dust	2		WSOC	WIOC	0.53	0.49
AD-2TC_WSOC_WIOC	INP/ m^3	All Days	2		WSOC	WIOC	0.45	0.41
AD-1TC_POC	INP/ μm^2	All Days	1	POC_{SSW}			0.43	0.40
AD-2TC_POC_PHYTO-L	INP/ μm^2	All Days	2		POC_{SSW}	Micro-NCBL	0.43	0.39
AD-2TC_POC_PHYTO-LM	INP/ μm^2	All Days	2		POC_{SSW}	Micro-, Nano-NCBL	0.43	0.38
AD-1TC_T	INP/ μm^2	All Days	1	Temperature			0.33	0.32

125 We have added this discussion to line 411 of the manuscript.

126

127 A question also arises of whether INPSSA increases after the dust event are really to do with the dust event or not? INPSSA
 128 did not seem to be very connected with SML conditions (which surprised the authors and may therefore necessitate more
 129 attention).

130 A more in depth discussion of the relationship between INP concentrations and the dust event has been added to the manuscript.

131 See line 264 of the main text.

132 Lastly, throughout the text, Figure and Table descriptions are kept too short and often do not fully describe what is shown.

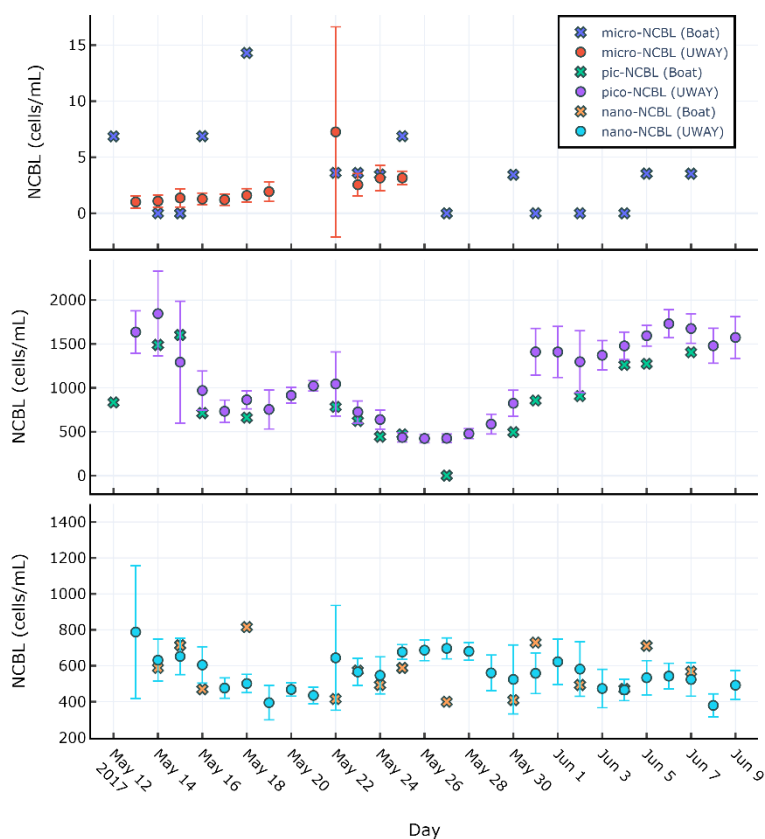
133 We have corrected the captions related to figures and tables. Details are seen in the relevant sections below.

134 Specific Comments: Temperature nomenclature (TM) varies throughout the text, sometimes for example as -15C or -15 C.
135 Please keep consistency and it is suggested to use the proper format of e.g. -15°C. All figures appear blurry, this should be
136 corrected.

137 **We have corrected this throughout the text.**

138 Line 102 – SSW properties were obtained from two depths 20 cm and 5 m, why this is done at two depths is never explained.
139 It is important as POC is measured at 5 m depth while SML and 20 m depth SSW samples were measured simultaneously and
140 both calculated NCBL.

141 **This question is linked to the question regarding Line 204 (see below). SSW properties were measured at two depths because
142 multiple analysis methods were available. The first method was an underway system that continuously monitored 5 m water
143 with a high time resolution. The second method was a workboat which was used to collect discrete samples both the SML and
144 the underlying seawater (at 20 cm, not 20 m). By measuring SSW properties from multiple methods (i.e., the workboat and
145 underway), we were able to compare results from the two and be sure of the results. Figure R5 below shows that there was
146 reasonable agreement between the two SSW sampling methods. Larger phytoplankton species (i.e., microphytoplankton)
147 showed greater variability between the two methods than did smaller species (i.e., picophytoplankton), with workboat
148 measured microphytoplankton values at times higher than those measured from the underway. Additionally, after May 25, the
149 underway system stopped monitoring microphytoplankton.**



150 **Figure R5. Daily average of continuous NCBL measurements from the underway (UWAY) system, where error bars**
151 **represent standard deviation compared with discrete daily samples from the workboat.**

152 Line 110 – Why is there a specific empirical relationship for PEACETIME? Will this affect other estimations of POC used for
153 the parameterization?

154 **POC was determined both continuously using optical methods and on discrete samples via high performance liquid**
155 **chromatography. The discrete samples were then used to calibrate the optical determination of POC, as optical proxies have**
156 **been found to vary from one region to another (Cetinić et al., 2012).**

157 Line 126 – methodology should be described in brief, or else simply cited if it is the only established measurement practice.

158 We make reference to the method as described in the literature (Tovar-Sanchez 2019), on line 124 of the main manuscript.
 159 Line 140 – calculation should be described in brief. What are the associated errors/uncertainties of this methodology using
 160 LINDA?
 161 The calculation for INP from the LINDA instrument follows Stopelli (2014) which was originally formulated by Vali (1971):
 162
$$\frac{INP}{volume} = \frac{\ln(N_{total}) - \ln(N_{unfrozen})}{V_{tube}}$$

 163 where N_{total} is the total number of tubes, $N_{unfrozen}$ the total number of unfrozen tubes, and V_{tube} the volume of sample in each
 164 tube. The number of unfrozen tubes is calculated by first blank correcting the number of frozen tubes, and then subtracting
 165 that value from the total number of tubes.
 166 We calculate uncertainty as the binomial proportion confidence interval (95%) using the Wilson score interval.
 167 This information has been added to the main text on line 134.
 168 Line 153 – You talk about bin size or 100-500 nm, but what is this? Is it the dry particle (electrical?) mobility diameter? This
 169 must be stated explicitly.
 170 For particle size distributions, we used a custom-made system referred to as Scanotron, which consists of a DMPS and a size
 171 segregated cloud condensation nuclei counter system in parallel. The Scanotron measures dry particle electrical mobility
 172 diameter. Data is inverted with the szdist algorithm developed at LaMP and available online (<https://hal.archives-ouvertes.fr/hal-01883795>). The inversion assumes a theoretical transfer function for the differential mobility analyzer
 173 (DMA) and considers the condensation particle counter (CPC) efficiency and the charge equilibrium state. It also includes
 174 multiple charge correction and accounts for diffusion losses in the instrument. Data quality is regularly checked during
 175 inter-calibration procedures and inter-comparison workshops, initially conducted in the frame of the EUSAAR 210
 176 project (European Supersites for Atmospheric Research) and since 2011 within the ACTRIS project (Wiedensohler et
 177 al., 2012).
 178 We have added the information regarding particle diameter to line 175 of the main text.
 179 Line 161-164. Confusing description of how measurement of WSOC was measured vs how TOC was measured. Then how
 180 was WIOC measured?
 181 WSOC was measured after water extraction using a high-temperature catalytic oxidation instrument (Shimadzu; TOC 5000
 182 A). TOC was measured using a Multi N/C 2100 elemental analyzer (Analytik Jena, Germany) with a furnace solids module.
 183 The analysis was performed on an 8 mm diameter filter punch, pre-treated with 40 μ L of H_3PO_4 (20% v/v) to remove
 184 contributions from inorganic carbon. WIOC was determined as the difference between TOC and WSOC.
 185 We have added this to line 155 of the main text.
 186 Line 166-175. It seems that no measurements of ambient INP were taken. This seems concerning as often tank and ambient
 187 measurements do not always compare well to one another. Do you have evidence that the plunging jet SSA measurements
 188 were similar to that of the ambient SSA over the Mediterranean?
 189 Our goal in this experiment is to determine the contribution of INP to sea spray aerosols. As ambient sources are expected to
 190 contain additional aerosols beyond sea spray, our bubbling setup was necessary in order to restrict our analysis. The
 191 characteristics of the setup were selected to mimic Fuentes et al. (2010). These parameters (water flow rates, plunging water
 192 depth, etc.) have been shown to mimic well nascent SSA. Using this setup, our group has previously effectively mimicked the
 193 SSA size distribution of nascent SSA (Schwier et al., 2015; 2017). Furthermore, our distribution matches well with modes 1-
 194 4 of Ovadnevaite et al. (2014) (see initial comments at top of this file).
 195 We have added this information to line 142 of the main text.
 196 Line 166-175. What are the associated errors/uncertainties of this methodology using DFPC?

198 During an intercomparison study of the DFPC with other INP measurement systems (DeMott et al., 2018) the DFPC was found
199 to have uncertainties for temperature and water supersaturation of about 0.1 °C and 0.02%, respectively, leading to an overall
200 INP concentration uncertainty of ±30%.

201 We have thus added 30% error bars on the observations of DFPC measured INP (Figure 1B on line 189 in the main text). We
202 also now note this uncertainty in line 172 of the main text. For greater explanation of the DFPC as well as how a description
203 of its use in other studies, see our response to reviewer 2.

204 Line 178 – 183. How are INP from SSW measured (I assume it is LINDA – but this is not included in your methodology)?
205 Which SSW measurement is tested for INP?

206 Correct, it is LINDA. The test is for SSW water from the workboat. We now make note of this in line 129 of the main text.

207 Line 191 – 192. The use of the term ‘peak’ here is a bit confusing in two ways. Purely graphically it is true that INPSSA,-25C
208 peaked on May 12, however, the implication that it is truly peaking is false as this is the first measurement it could have been
209 higher before measurements commenced. Has contamination of the plunger tank system been ruled out as it is by far the
210 greatest disparity between different temperatures for INPSSA?

211 Data point on May 13 (erroneously reported as May 12) has been corrected. See initial comment on changes to SSA surface
212 area and averaging intervals. By correcting sampling intervals, the peak on May 13 has been corrected. See Figure 2b in the
213 text on line 189.

214 Regarding potential contamination: the plunging jet system was cleaned at the same time as the ship’s underway system and
215 the comparison of the biological measurements from the underway seawater system show agreement with workboat samplings,
216 indicating no contamination across the voyage. The plunging jet systems were additionally cleaned every day for being used
217 in discrete seawater generation experiments. Generated SSA concentrations were found correlated to the nanophytoplankton
218 cell number concentration measured online from the underway seawater system (Sellegri et al., 2020 in review) indicating no
219 contamination of the plunging jet system itself.

220 We have also altered the text describing the INP timeseries starting on line 175.

221 Line 196. Again the use of the word peak is a bit misleading as measurements ended before the true peak could be observed.
222 In this case can you really comment on the time difference between one peak in SML and SSA?

223 See response to the comment above on line 191.

224 Line 204. Were there any differences in cell counts between SSW at 5 m or 20 cm depth?

225 Overall, the agreement was reasonable between SSW at 5 m and 20 cm depth. See response above to comment on line 143 of
226 this file and associated Figure R5 for a comparison of cell counts from underway vs workboat.

227 Line 206-207. Are these the ranges associated with Pujo-Pay et al. 2011, or the ranges for this study? If the latter than perhaps
228 give the expected range as well.

229 These are ranges associated with this study. Pujo-Pay gives range of 45.3-72.4 uM for DOC and 0.80-8.70 for POC. More
230 specifically, Western Basin DOC ranges between 45.3-69.4 with mean of 58.7 and sigma of 7.4. Eastern Basin ranges between
231 49.4-72.4 with average of 61.5 and sigma of 5.9. Western Basin POC ranges between 1.45-8.70 with mean of 4.31 and sigma
232 of 1.73 while Eastern Basin POC ranges between 0.80-5.41 with mean of 3.08 and sigma of 0.90.

233 We have added the following:

234 *Observed DOC and POC values ranged between 700-900 µgC/L and POC between 42-80 µgC/L and were within the range*
235 *of expected values for the oligotrophic Mediterranean (540–860 µgC/L for DOC and 9.6-104 µgC/L for POC)(Pujo-Pay et*
236 *al., 2011).*

237 Line 209. How are you calculating enrichment factor? It is good to state as sometimes confusion arises.

238 Enrichment factor is calculated as the ratio of SML to SSW:

239
$$EF = \frac{SML}{SSW}$$

240 We have added this to line 129 of the main text.

241 Line 236-240. This paragraph feels like it is out of place as a discussion paragraph crammed between the synopsis of the results
242 in the same Figure. It does not add much to the discussion. What do these two studies mean for your results? If anything they
243 imply that you must compare INPSSA to SSA bacterial abundance.

244 See response to the comment below.

245 Line 250. DOC EF is positively correlated with $INP_{SML,-15C}$, and you state this is due to the dust event, and in the next
246 statement say that the fraction DOC enriched in the SML during the dust event has specific IN properties. It seems possible
247 that the DOC came from non-marine originating bacteria and that the deposition event also deposited terrestrial DOC which
248 is the origin of increased IN ability. Or more so, could the correlation be coincidental with another correlating factors from the
249 dust event (i.e. Fe)? No indication is given of why the authors believe it to be ‘likely connected to the CSP abundance, albeit
250 not to the TEP’, which if given may add value to the statement.

251 We have altered the text to the following, which can be found on line 275:

252 *“Figure 4 shows scatterplots of statistically significant relationships between $INP_{SML,-15C}$ concentrations and various SML
253 properties. $INP_{SML,-15C}$ were most strongly positively correlated with dissolved iron ($r=0.99$), TEP EF ($r=0.95$), and bacteria
254 EF ($r=0.93$). However, these relationships are skewed by the outlier due to the drastic increase in iron observed on June 4
255 (Figure S2a) from the dust deposition event, as described previously. It is difficult to segregate between the dust and biological
256 impact on the $INP_{SML,-15C}$, as dust is known to have good INP properties while being capable of fertilizing the surface ocean
257 with dissolved iron, leading to concomitant increases in biological activity. It is also possible that the dust deposition led to
258 increased abundance of terrestrial OC, which would exhibit different INP activity. When considering days before the dust
259 event, $INP_{SML,-15C}$ is only significantly correlated with dissolved iron ($r=0.91$) and TOC in the SML ($r=-0.93$). We note that
260 while no longer statistically significant for pre-dust days, moderate correlations were still observed between $INP_{SML,-15C}$ and
261 total NCBL ($r=0.48$), HNA bacteria ($r=0.78$), and total bacteria ($r=0.64$). Previous reports examining the correlation between
262 INP and microbial abundance have yielded mixed results. For example, a report of INP in Arctic SML and SSW found no
263 statistically significant relationship between the temperature at which 10% of droplets had frozen and bacteria or
264 phytoplankton abundances in bulk SSW and SML samples (Irish et al., 2017). However, recent mesocosm studies using
265 nutrient-enriched seawater found that INP abundances between $-15^{\circ}C$ and $-25^{\circ}C$ in the aerosol phase were positively
266 correlated with aerosolized bacterial abundance (McCluskey et al., 2017). “*

267 Line 291-293. What are the total particle counts referred to in Line 292? How are they measured and how do they match well
268 with SSA counts in the range? In terms of SSA surface area: (1) how was SSA calculated from D_p ? (2) SSA have two
269 noticeable modes larger than 500 nm, one is a submicron mode and the other is the jet-drop mode which are found to have
270 mean dry mobility diameters near at 0.83 (Ovadnevaite et al. 2014) and $\sim 2 \mu m$ (Wang et al. 2017, Lewis & Schwartz 2004),
271 respectively. According to Figure S3, most of the surface area distributions have already peaked by $0.5 \mu m$ particle diameter
272 (with the possible exception of 2017-05-17), yet a significant portion of surface area for particles with $D_p > 0.5 \mu m$ seems to
273 be lost. It seems an overstatement to say ‘most of the surface area of sea spray is comprised between this size range’.
274 Ovadnevaite, J., Manders, A., de Leeuw, G., Ceburnis, D., Monahan, C., Partanen, A. I., Korhonen, H., and O’Dowd, C. D.:
275 A sea spray aerosol flux parameterization encapsulating wave state, Atmos. Chem. Phys., 14, 1837-1852, 10.5194/acp-14-
276 1837-2014, 2014. Wang, X., Deane, G. B., Moore, K. A., Ryder, O. S., Stokes, M. D., Beall, C. M., Collins, D. B., Santander,
277 M. V., Burrows, S. M., Sultana, C. M., and Prather, K. A.: The role of jet and film drops in controlling the mixing state of
278 submicron sea spray aerosol particles, Proceedings of the National Academy of Sciences, 114, 6978-6983,
279 10.1073/pnas.1702420114, 2017. Lewis, E. R., and Schwartz, S. E.: Sea Salt Aerosol Production: Mechanisms, Methods,
280 Measurements and Models-A Critical Review, American Geophysical Union, 2004.

281 We refer to the initial opening comment as our response to the first portions of this comment. We do not compare our particle
282 size distribution to Wang et al. (2017) as the size distributions shown in their paper are created from electrolysis bubbles,

283 which was used to investigate the role of jet drops in submicron aerosol formation. As the electrolysis bubbler created hydrogen
284 bubbles with size less than 100 μm and a mean radius between 20-40 μm , no film drops would be expected to contribute to
285 these SSA since only bubbles of radius greater than 500 μm create film drops. This method would therefore not be expected
286 to accurately represent SSA. Indeed, the authors state “It is important to note that the nucleation bubbler is an artificial source
287 of jet drops that was convenient to unambiguously illustrate the differences in electrical mobility between jet and film drops,
288 but is not representative of wave breaking.” Wang et al. (2017) does also show a particle size distribution for SSA generated
289 using a plunging waterfall in a marine aerosol reference tank, but this is only for particles with diameter less than 1 μm and
290 thus cannot be used as a reference for supermicron particle counts.

291 Line 313. What is the difference between SSA OC and TOC here? How is OC calculated from the SSA?

292 Here, SSA OC is defined as the organic carbon content found within the aerosol phase for PM1 particles. Earlier in the
293 manuscript this was defined as TOC, and so we will change this to make it more clear. Section 2.3.2 describes how TOC was
294 calculated by acidifying filter punches to remove inorganic carbon, leaving only TOC.

295 Line 326/327. It would be good to state the relevant conclusions of Freney et al. 2020.

296 We have added the following to line 406 of the main text:

297 *“A separate manuscript discusses the trend and controls on SSA chemical composition, linking the different classes of organic
298 carbon in submicron SSA to seawater chemical and biological properties (Freney et al., 2020). In this work, OMSS was linked
299 to POC_{SSW} and the coccolithophores cell abundance. In light of this and given the correlation of $\text{INP}_{\text{SSA},-25\text{C}}$ with seawater
300 microbial abundance and with SSA OMSS and WIOC, it seems likely that INP_{SSA} at this temperature are related to the exudates
301 of phytoplankton which are concentrated at the SML and then emitted into the SSA as WIOC.”*

302 Line 368. How are you calculating OMSS? Why is this in agreement with Cochran et al. 2017?

303 OMSS is calculated as the fraction of $\text{OM}/(\text{OM}+\text{SeaSalt})$, where SeaSalt is the sum of SO_4^{2-} , NO_3^- , NH_4^+ , Na^+ , Cl^- , K^+ , Mg^{2+} ,
304 Ca^{2+} as determined using ICP-MS and OM is the sum of WSOM and WIOM, which are each calculated as $\text{WSOM} = \text{WSOC}$
305 $\times 1.8$ and $\text{WIOM} = \text{WIOC} \times 1.4$ (where WIOC and WSOC are calculated using the method described on line 164 of this text).
306 We have added this description to line 163 of the text.

307 Furthermore, we have altered the text on line 400 of the manuscript to the following:

308 *“Table 4 and Figure 7 shows the significant correlations between INP_{SSA} and SSA properties. A positive correlation exists
309 between $\text{INP}_{\text{SSA},-18\text{C}}$ and SSA organic carbon (OC) as well as the ratio of SSA water-soluble organic carbon to organic carbon
310 (WSOC/OC). The correlation between WSOC/OC and $\text{INP}_{\text{SSA},-18\text{C}}$ makes sense given the finding that $\text{INP}_{\text{SSA},-18\text{C}}$ was correlated
311 with POC_{SSW} , as a higher WSOC/OC value would suggest a higher fraction of soluble organics which would be expected to
312 transfer to the atmosphere from the bulk SSW rather than the SML due to their high solubility. $\text{INP}_{\text{SSA},-25\text{C}}$ had a significant
313 correlation with WIOC and OMSS. We note that $\text{INP}_{\text{SSA},-25\text{C}}$ was also found to be correlated with various microbes in the SSW,
314 specifically *Prochlorococcus*, coccolithophores, nano- and micro-NCBL (previous section). Phytoplankton are known for their
315 ability to produce extracellular polymeric substances (Thornton, 2014), and a previous mesocosm experiment showed
316 microbially-derived long-chain fatty acids were efficiently ejected from the seawater as SSA, increasing the fraction of highly-
317 aliphatic, WIOC (Cochran et al., 2017). A separate manuscript discusses the trend and controls on SSA chemical composition,
318 linking the different classes of organic carbon in submicron SSA to seawater chemical and biological properties (Freney et
319 al., 2020). In this work, OMSS was linked to POC_{SSW} and the coccolithophores cell abundance. In light of this and given the
320 correlation of $\text{INP}_{\text{SSA},-25\text{C}}$ with seawater microbial abundance and with SSA OMSS and WIOC, it seems likely that INP_{SSA}
321 at this temperature are related to the exudates of phytoplankton which are concentrated at the SML and then emitted into the
322 SSA as WIOC.”*

323 Line 413. It is stated that ‘. . .the INP concentrations measured in the SSW are in line with the INP measured in the SML. . .’.
324 There is only one comparison of INP shown of the two (figure 2a) and only one temperature is shown for the SSW. Is there
325 further evidence to back this statement? Indicate what evidence is referred to in the text.

326 This statement was vague and has been removed.

327 Table 1 – Description of table needs to state what p, R(R2) and n are. Is the p value of NCBL EF 0.78? This looks like a typo.

328 Review the rest of the table to double check for other typographical issues. Why does it say CSPabundance, when in there is

329 no explanation of the difference between CSP and CSPabundance?

330 All tables and scatter plots in the manuscript have been altered to account for these requests. We have recalculated all

331 correlations after calculating adjusted averaged underway values to better line up with DFPC filter sampling time and adjusted

332 IN_{SSA} normalized by particle surface area values (explained above). This did not impact the INP_{SML} correlations with seawater

333 properties, as daily averages were retained. Please see Table 1 on line 262, Table 2 on line 351, Table 3 on line 360, and Table

334 4 on line 384.

335 Table 2. Description of table needs to state what p, R(R2) and n are. The table is stretched over a page break. This should be

336 corrected to be on one page. Change POC to POCSSW.

337 Please see comment above and Table 2 on line 351.

338 Table 3. Description of table needs to state what p, R(R2) and n are.

339 See comment above and Table 3 on line 360.

340 Figure 1. The image is blurry. The points indicated on the map are names with abbreviations that are never explained nor

341 referred to in the text. If these refer to the dates mentioned in other graphs, this should be made clear. If not, then why are they

342 there?

343 We have removed this figure from the manuscript.

344 Figure 2. Why is there no uncertainty associated with each measurement? INP measurements have some of the largest

345 uncertainties in aerosol science, this can't be neglected. How do you explain why $INP_{SSA,-25C}$ and $INP_{SSA,-22C}$ are

346 sometimes anti-correlated and sometimes not? Some other minor corrections are needed. This graph is blurry and should be

347 higher resolution. It would be nice to have different keys for a) and b). The y-axis in a) should be written scientifically – i.e.

348 either 10,000 or 1×10^4 . It is difficult to differentiate the colours, effort should be taken to use different markers. The bottom

349 access should probably be the 'Date' not 'Day Number' (see same issue in other graphs).

350 See responses above. We have updated the figure accordingly, which can be seen on line 192 of the manuscript.

351 Figure 3. This figure is also blurry with no error/uncertainty on the measurements shown.

352 We have updated this chart, please see Figure 4 on line 275.

353 Figure 4. Y-axis scale is difficult to interpret, should be written for example 108 not 108. On the x-axis the authors might

354 consider writing Temperature ($^{\circ}C$) rather than (C). Again error/uncertainties should be shown, or else noted that the error bars

355 are not larger than the data points. The description of Figure 4 is on a different page than the figure, this should be corrected.

356 It is difficult to tell day=2017-05-24 from day=2017-06-06. The authors could probably omit the 'day=' in the key and make

357 the text larger.

358 Error bars have been added to account for INP counting errors. We included all temperature rather than single degree averaged

359 values. Please see Figure 6 on line 319.

360 Figure 5. Description does not mention INP normalised to SSA. Why use $/cm^3$ rather than $/nm^2$ which is what the surface area

361 is shown in in Figure S3? When you normalise INP to SSA, should it not still be in term of $(/m^3 \text{ of air } \hat{=} SSA \text{ cm}^2)$? Top

362 left panel, should read ' 3×10^{-4} ' not ' 3×10^{-4} '.

363 We have updated the scatterplot figures based on this and the requests below. Please see Figures 8, 9, and 10 on lines 355,

364 375, and 410 of the main text.

365 Figure 6. Description should be below figure, and should include some more details of the graph. The figure is blurry, and

366 need to be corrected. OMSS not explained.

367 This figure has been moved to the SI and can be found on line 27 of the SI.

368 Figure 7. Description should mention only significant correlations shown. Text should not state that these panels are a matrix.
369 The scatter plots are blurry and should be corrected to higher resolution. The authors may choose to add r-values to each panel
370 to make it easier for readers to study the results.

371 **See comments above.**

372 Figure 8. Graph should be made larger and enhanced to be less blurry. Y-axis scale is difficult to interpret, should be written
373 for example 101 not 101. It is difficult to read the axes. Your 3 panel axes seem to be in different units, some per L and some
374 per m³. These are all SSA INP so they should be terms of their atmospheric concentration. This should be explained in the
375 description. Additionally, it seems clear from the graphs that while both the W15 and MC18 models over predict INP
376 concentrations the over prediction is not really temperature dependent. The graph seems to show more of the difference
377 between oligotrophic waters and eutrophic waters. How much does the authors' own parameterizations differ if only the colder
378 (eq. 2) or warmer (eq. 1) parameterization is applied to all the results? Are there any data of eutrophic waters which suggest a
379 temperature dependence might improve the agreement?

380 **Please see response on line 81 of this file.**

381 Supplementary Info – consider adding a schematic of measurements taken from the tank.

382 Table S1. Usually tables come before Figures. Description of table needs to state what p, R(R²) and n are. Place a '0' before
383 all values in column p.

384 **This table has been removed.**

385 Figure S1. Where possible, missing data should be deleted rather than shown as a line jumping from the last measured point
386 to the next. There should be graph panel specific keys as each factor is not shown on every graph. It would be nice if more
387 detail could be given in the description of where/how these measurements were taken. A description of what POC or biovolume
388 covers here could also be useful.

389 **Figure S1 has been updated and is found on line 11 of the SI.**

390 Figure S2. Grey outline squares around a) and b) are somewhat off centre and cut-off the a) and b). Fe axis should be shown
391 on the same scale in a) and b). It would be nice to see INPSSA measurement overlaid in time with those SML and SSW
392 conditions considered to be contributing most prominently to INPSSA concentrations.

393 Figure S3. It is nearly impossible to tell some of these 'variable' apart as the same color is used for multiple days. Please graph
394 in such a way that the surface area spectrums can be identified for each variable. If they are daily averages than the stdev
395 should also be graphed. Y-axis, change from '(nm²/(cm³))' to '(nm²/cm³)'. The authors could probably omit the 'variable='
396 in the key. Also, it is low resolution. What is a scanotron? Were these not measured by the DMPS as stated in the methodology?

397 **Please see Figure S3 of the supporting information on line 19.**

398 Figure S4. Color of 'variables' again overlap for multiple days. Please graph in such a way that the number size distribution
399 spectrums can be identified for each variable. If they are daily averages than the stdev should also be graphed. The y-axis
400 shows dN/dlogDp in '(particles/(cm³ nm))' the extra nm is likely a typo? It should be '(/cm³)'. The authors could probably
401 omit the 'variable=' in the key. Also, the graph resolution is low. What is a scanotron? Were these not measured by the DMPS
402 as stated in the methodology?

403 **See the answer regarding Line 153 for description of DMPS (i.e., scanotron). See Figure R1 of this text. This has been updated
404 in the manuscript accordingly.**

405 Technical corrections:

406 **We have corrected all of the concerns listed below and they are highlighted in the manuscript.**

407 Line 22 – delete the 's' after INP, as INP is defined plural earlier.

408 Line 29 - delete the 's' after INP. This occurs many more times so check throughout the text.

409 Line 33 – delete extra space '. . .' to SSW parameters (POCSSW. . .'. Add an 'and' or a ',' between '(POCSSW INPSSW,-
410 16C)'.

411 Line 56 – delete ‘)(’ between references and replace with ‘;’. Delete ‘-’ after SSA.

412 Line 62/63 – refer to study simply as ‘Wilson et al. 2015 identified a temperature-dependent. . .’. Either delete the ‘s’ from the
413 end of the word entities or from concentrations.

414 Line 68 – TM (see specific comments).

415 Line 85 - delete the ‘s’ after INP. Delete the ‘the’ before title of study. Here is it the title of the cruise or study? I suggest
416 replace the word ‘cruise’ with ‘study’ and delete ‘study’ from the end.

417 Line 87 – add space, ‘May 10 – June 10, 2017’. Line 88 – delete ‘were’.

418 Line 92 – what is ‘R/V’? Here ‘Pourquoi Pas?’ is written differently than later. Keep consistency.

419 Line 94 – replace ‘fashion from 35° to 42°’ to ‘fashion between 35° to 42°’.

420 Line 109 – HPLC acronym not explained.

421 Line 113 – FWS and SWS acronym not needed as never used again.

422 Line 124 – ICP-MS acronym not explained. Replace with full title as acronym not needed.

423 Line 130 – MQ acronym not explained. Replace with full title as acronym not needed.

424 Line 131 – add space between ‘0.5L’

425 Line 132 – HCL acronym not explained, although it is well known as Hydrochloric acid. Authors may choose to spell it out
426 as it is not repeated.

427 Line 135 - add space, ‘May 22 - June 7’.

428 Line 137 – TM (see specific comments).

429 Line 146 – change meter to ‘m’

430 Line 147 – ACSM acronym not described. DMPS and CPC acronym used before description.

431 Line 153 – correct to ‘10-500 nm’.

432 Line 159 – MSA acronym not explained. Replace with full title as acronym not needed.

433 Line 160 – KOH acronym not explained. Replace with full title as acronym not needed.

434 Line 161 – WSOC acronym used for first time and is not defined. Line 166 – ‘24h’ change to ‘24-hour’ to keep consistency.

435 Line 167 – delete the ‘s’ after INP, as INP is defined plural earlier.

436 Line 169 – change to ‘47 mm’ with space.

437 Line 173 – TM (see specific comments). Add ‘. . .(for air temperatures of . . . -22.3 C, respectively)’. Line 175 – add
438 ‘INP/volume of air’

439 Line 181/182 – TM (see specific comments). June 4 not 4th.

440 Line 192 – use scientific notation for INP/m³ (i.e. 1.47x10⁻² not 14.7x10⁻³).

441 Line 196 – the peak in INPSSA occurred three days after INPSML peaked, not one day. Unless the authors meant to suggest
442 that INPSSA only saw an increase begin a full day after the INPSML peak? Line 200 – Delete ‘(SI)’.

443 Line 204/205 – keep same scientific notation for describing cells/mL.

444 Line 209 – add ‘Enrichment factors (EF). . .’

445 Line 214 – delete ‘next’ (optional).

446 Line 220 – consider adding in ‘. . .positive or negative correlations. . .’

447 Line 254 – uppercase L for litre, such that ‘TOC µgC/L’. Replace ‘particulate organic carbon’ with POC.

448 Line 255 – Replace ‘dissolved organic carbon’ with DOC.

449 Line 256 – Should be ‘(INP per gram of TOC)’ not ‘OC’. Is this cumulative INP as in W15, or is this INP/mL?

450 Line 282 – Do you mean ‘. . .between seawater OC’ or ‘TOC’?

451 Line 291 – add space between ‘500’ and ‘nm’.

452 Line 294 – Only normalised size distribution shown in Figure S4, not number concentration. Perhaps add it in the graph key?

453 Replace ‘dependence of’ with ‘dependence on’.

454 Line 298 – add space between ‘500’ and ‘nm’. Line 300 – add ‘in’ ahead of ‘Table 2’.

455 Line 307 – Give correlation stats for INPSSW,-16C

456 Line 351 – replace ‘the’ with ‘that’.

457 Line 353 – Replace ‘At this C8 ACPD Interactive comment Printer-friendly version Discussion paper temperature, INPSSA’

458 with just ‘INPSSA,-25C. . .’

459 Line 361 – some overlap issue with graph and line numbering.

460 Line 362 – change ‘R=.84’ to ‘R=0.84’. Check for other numbering mistakes throughout the text.

461 Line 380/381 – TM (see specific comments).

462 Line 392 & equations – Warm INP defined as $\geq -24\text{C}$, but in eq. (1) says -22. Also, in eq. (1) ‘POC’ should be rewritten

463 ‘POCSSW’ to keep clarity (unless authors want any POC to be used in which case more explanation should be given).

464 Line 393 – this entire line should come before eq. (1) and (2).

465 Line 425 –INPSWL? Change ‘INPSWL and INPSML’ to ‘INPSSW and INPSML’.

466 Line 430 – Is INPSSA measured at -16C or it -18C? Leave and ‘and’ or ‘,’ between POC and INP.

467 Line 436 – ‘. . .seawater POC and SSW microbial abundance’ seems redundant or repetitive.

468 Line 446 – it is written here ‘RV’ but elsewhere ‘R/V’. ‘Pourquoi Pas ?’ is also written differently elsewhere. Please also note

469 the supplement to this comment: [https://www.atmos-chem-phys-discuss.net/acp-2020-487/acp-2020-487-RC1-](https://www.atmos-chem-phys-discuss.net/acp-2020-487/acp-2020-487-RC1-supplement.pdf)

470 [supplement.pdf](https://www.atmos-chem-phys-discuss.net/acp-2020-487/acp-2020-487-RC1-supplement.pdf)

471

472 Albert, M. F. M. A., Schaap, M., de Leeuw, G., and Bultjes, P. J. H.: Progress in the determination of the sea spray

473 source function using satellite data, *Journal of Integrative Environmental Sciences*, 7, 159-166,

474 [10.1080/19438151003621466](https://doi.org/10.1080/19438151003621466), 2010.

475 Aumont, O., Ethé, C., Tagliabue, A., Bopp, L., and Gehlen, M.: PISCES-v2: an ocean biogeochemical model for

476 carbon and ecosystem studies, *Geosci. Model Dev.*, 8, 2465-2513, [10.5194/gmd-8-2465-2015](https://doi.org/10.5194/gmd-8-2465-2015), 2015.

477 Cetinić, I., Perry, M. J., Briggs, N. T., Kallin, E., D'Asaro, E. A., and Lee, C. M.: Particulate organic carbon and inherent

478 optical properties during 2008 North Atlantic Bloom Experiment, *Journal of Geophysical Research: Oceans*, 117,

479 [10.1029/2011JC007771](https://doi.org/10.1029/2011JC007771), 2012.

480 DeMott, P. J., Möhler, O., Cziczo, D. J., Hiranuma, N., Petters, M. D., Petters, S. S., Belosi, F., Bingemer, H. G.,

481 Brooks, S. D., Budke, C., Burkert-Kohn, M., Collier, K. N., Danielczok, A., Eppers, O., Felgitsch, L., Garimella, S.,

482 Grothe, H., Herenz, P., Hill, T. C. J., Höhler, K., Kanji, Z. A., Kiselev, A., Koop, T., Kristensen, T. B., Krüger, K., Kulkarni,

483 G., Levin, E. J. T., Murray, B. J., Nicosia, A., O'Sullivan, D., Peckhaus, A., Polen, M. J., Price, H. C., Reicher, N.,

484 Rothenberg, D. A., Rudich, Y., Santachiara, G., Schiebel, T., Schrod, J., Seifried, T. M., Stratmann, F., Sullivan, R. C.,

485 Suski, K. J., Szakáll, M., Taylor, H. P., Ullrich, R., Vergara-Temprado, J., Wagner, R., Whale, T. F., Weber, D., Welti,

486 A., Wilson, T. W., Wolf, M. J., and Zenker, J.: The Fifth International Workshop on Ice Nucleation phase 2 (FIN-02):

487 laboratory intercomparison of ice nucleation measurements, *Atmospheric Measurement Techniques*, 11, 6231-

488 6257, [10.5194/amt-11-6231-2018](https://doi.org/10.5194/amt-11-6231-2018), 2018.

489 Freney, E., Sellegri, K., Nicosia, A., Trueblood, J. V., Bloss, M., Rinaldi, M., Prevot, A., Slowik, J. G., Thyssen, M.,

490 Gregori, G., Engel, A., Zanker, B., Desboeufs, K., Asmi, E., Lefevre, D., and Guieu, C.: High Time Resolution of

491 Organic Content and Biological Origin of Mediterranean Sea Spray Aerosol, *ACP*, 2020.

492 Fuentes, E., Coe, H., Green, D., de Leeuw, G., and McFiggans, G.: Laboratory-generated primary marine aerosol

493 via bubble-bursting and atomization, *Atmos. Meas. Tech.*, 3, 141-162, [10.5194/amt-3-141-2010](https://doi.org/10.5194/amt-3-141-2010), 2010.

494 Irish, V. E., Elizondo, P., Chen, J., Chou, C., Charette, J., Lizotte, M., Ladino, L. A., Wilson, T. W., Gosselin, M.,

495 Murray, B. J., Polishchuk, E., Abbatt, J. P. D., Miller, L. A., and Bertram, A. K.: Ice-Nucleating Particles in Canadian

496 Arctic Sea-Surface Microlayer and Bulk Seawater, *Atmos. Chem. Phys.*, 17, 10583-10595,

497 <https://doi.org/10.5194/acp-17-10583-2017>, 2017.

498 McCluskey, C. S., Hill, T. C. J., Malfatti, F., Sultana, C. M., Lee, C., Santander, M. V., Beall, C. M., Moore, K. A.,

499 Cornwell, G. C., Collins, D. B., Prather, K. A., Jayarathne, T., Stone, E. A., Azam, F., Kreidenweis, S. M., and DeMott,

500 P. J.: A Dynamic Link between Ice Nucleating Particles Released in Nascent Sea Spray Aerosol and Oceanic

501 Biological Activity during Two Mesocosm Experiments, *J. Atmos. Sci.*, 74, 151-166, [https://doi.org/10.1175/JAS-](https://doi.org/10.1175/JAS-D-16-0087.1)

502 [D-16-0087.1](https://doi.org/10.1175/JAS-D-16-0087.1), 2017.

503 Ovadnevaite, J., Manders, A., de Leeuw, G., Ceburnis, D., Monahan, C., Partanen, A. I., Korhonen, H., and O'Dowd,
504 C. D.: A sea spray aerosol flux parameterization encapsulating wave state, *Atmospheric Chemistry and Physics*,
505 *14*, 1837-1852, [10.5194/acp-14-1837-2014](https://doi.org/10.5194/acp-14-1837-2014), 2014.

506 Pujo-Pay, M., Conan, P., Oriol, L., Cornet-Barthaux, V. C., Falco, C., Ghiglione, J.-F., Goyet, C., Moutin, T., and
507 Prieur, L.: Integrated Survey of Elemental Stoichiometry (C, N, P) from the Western to Eastern Mediterranean Sea,
508 *Biogeosciences*, *8*, 883-899, <https://doi.org/10.5194/bg-8-883-2011>, 2011.

509 Rasse, R., Dall'Olmo, G., Graff, J., Westberry, T. K., van Dongen-Vogels, V., and Behrenfeld, M. J.: Evaluating Optical
510 Proxies of Particulate Organic Carbon across the Surface Atlantic Ocean, *Frontiers in Marine Science*, *4*, 367, 2017.
511
512

Answers to reviewer 2

We thank the reviewer for carefully reading our manuscript and for providing us with their helpful insight. We have adjusted our manuscript based on their recommendations, which we believe has strengthened the manuscript's overall impact. Our responses to specific comments are shown below in red.

Review of "A Two-Component Parameterization of Marine Ice Nucleating Particles Based on Seawater Biology and Sea Spray Aerosol Measurements in the Mediterranean Sea" by Trueblood et al.

General comment

This study investigated the ice-nucleating abilities of surface microlayer (SML), surface seawaters (SSW), and sea spray aerosol (SSA) particles collected/generated in the Mediterranean Sea. In parallel to the evaluation of the ice-nucleating abilities of the different samples, a large set of biogeochemical analysis were performed on the samples to understand the relationship between ocean biology and marine ice nucleating particles (INP). While the ice nucleation analysis of the SML and SSW samples was performed with a LED based Ice Nuclei Detection Apparatus (LINDA), the analysis for the SSA samples was performed using a Dynamic Filter Processing Chamber (DFPC). Taking into account the collected information, the authors developed a new two-component parametrization. Although the information collected/derived by the authors is very rich and valuable, in addition that they were collected in a poorly explored region on Earth, the manuscript is not easy to follow, it lacks important information, and the conclusions are not clearly supported by the provided data. The manuscript fits with the ACP scope, but the current version cannot be accepted for its publication.

Major Comment 1. Two different techniques were used to analyze the ice nucleating abilities of the samples, i.e., the LINDA and the DFPC. While the LINDA determines the INP concentrations via the immersion freezing mode, the DFPC does it via condensation freezing. Given that both data sets were used to develop the parametrization, I am wondering if the INP concentration delivered by both instruments are directly comparable. For example, I am wondering about the very low concentration of INPs reported for the SSA samples in comparison to literature data. It is a true number or is it an artifact related to the used method?

Only the DFPC IN data was used to develop the parameterization. The LINDA instrument was only used on seawater (SSW and SML) samples, and the results were used to help guide the selection of features for the parameterization of SSA INP based on their correlation with biological features. A more in-depth response regarding the process of using the DFPC and its comparison with immersion freezing methods is given in the response below.

2. I was unable to fully understand how the INP concentrations for the SSA samples were obtained as the DFPC was not properly described. Is this a new custom-made instrument? Is this the first data delivered/published by this instrument? If this is the case, a much deeper description needs to be provided. If this is not the case, how good is the agreement of the data delivered by the DFPC against other well-known ice nucleation instruments?

The method for the DFPC is as follows: aerosols are collected onto a filter which is then placed on a metallic support covered with a layer of paraffin. The paraffin is heated slightly (60-80°C) for ~10 seconds and then rapidly cooled to allow the paraffin to penetrate the filter pores. This process is done to modify the color of the filter from white to black for optical processing and to improve thermal conductivity. The filter is then placed inside the DFPC on top of a Peltier cooler plate. The filter is then continuously swept by humid and cool air. Upon activation, ice nuclei grow into ice crystals with size around 0.4 mm. The ice crystals are then recorded using a camera.

In this study, the DFPC was used at water saturation, S_w , of 1.02 and $T = -22, -25, \text{ and } -18^\circ\text{C}$. Under these conditions, we expect to see condensation freezing mode. It has been reported (Vali et al., 2015) that condensation freezing and immersion freezing are not distinguishable as unique.

The DFPC has been used in multiple previous studies and found to agree well with other INP monitoring instruments (DeMott et al., 2018; Hiranuma et al., 2019; McCluskey et al., 2018).

556 We have updated the methods section starting at line 167 of the main text to account for this added information.

557 3. I am surprised that the INPs concentrations of the SML, SSW, and SSA are not compared to literature data. Actually, a
558 recent study by Gong et al. (2020) who also studied the SML, SSW, and SSA is not cited/discussed here. There are also other
559 studies in marine environment performed at subtropical and tropical latitudes that deserved to be discussed in the context of
560 the present study.

561 We have added Figure 2 and Figure 3 to the manuscript, along with discussion starting on line 222 to compare seawater and
562 SSA INP concentrations to previous studies.

563 4. Given that the chemical composition of the SSA is linked to the size of the aerosol particles (e.g., O'Dowd et al. 2004;
564 Prather et al. 2013), I am wondering how well the used apparatus to generate the SSA, reproduces the proper size distribution
565 of the natural SSA. Also, the authors only provided the particle size distribution and the chemical characterization for particles
566 smaller than 500 nm and 1000 nm, respectively. There is a big problem here because while the chemical analysis was
567 performed for submicron particles only, but the INP concentration took into account total suspended particles. It has been
568 shown that the aerosol particles with the highest potential to act as INP are those larger than 500 nm (DeMott et al. 2010), and
569 especially the super-micron particles (Mason et al. 2015; Gong et al. 2020) ignored in the present study.

570 We agree that replicating the production mechanism of SSA is certainly an important and difficult task. The plunging apparatus
571 used in this study has been well characterized in previous studies (Schwier et al., 2015; Schwier et al., 2017). Furthermore, the
572 characteristics of the setup (water flow rates, plunging water depth, etc.) were selected to mimic Fuentes et al. (2010), which
573 have been shown to mimic quite well the production of nascent SSA. To this end, we are confident that the SSA analyzed in
574 this study are an accurate representation of natural SSA.

575 It is not yet clear whether INP from sea spray are mainly from super or submicron sizes. While Gong et al. (2020) reported
576 high concentrations of INP for supermicron particles, they also note these likely came from dust particles rather than marine
577 aerosols. As studies have shown that the IN active components of SSA are typically of biogenic origin (DeMott et al., 2016),
578 and that the organic mass fraction of SSA is greatest for submicron particles (Gantt and Meskhidze, 2013), it would seem
579 likely that the INP characteristics of SSA can be well described in terms of the submicron regime. Indeed, comparison of INP
580 concentrations in PM1 and PM10 filter samples of both clean marine air and continental land-mass air at Mace Head in the
581 North Atlantic have recently provided evidence that the majority of SSA INP are in the submicron regime and that terrestrial
582 aerosol INP are in the supermicron regime (McCluskey et al., 2018). Field campaigns in the equatorial Pacific and Gulf of
583 Mexico have also found the marine INPs are most abundant for particle diameters less than 500 nm (Rosinski et al., 1986,
584 1987; Rosinski et al., 1988). However, we want to stress here that our INP measurements are performed over the full range of
585 SSA sizes, and we do not ignore its supermicronic fraction.

586

587 For a response to the concern of particle size distributions, please see our response to comment number 5 below.

588 Concerning the chemical analysis of SSA, it is correct that only the submicron concentration of SSA has been measured.
589 However, previous analysis of the chemical composition of marine aerosol have shown that most of the organic matter is found
590 in the submicron fraction (O'Dowd et al. 2004, Gantt and Meskhidze 2013 for a review). Therefore, we base our analysis that
591 the WIOC, WSOC and OC concentrations provided in this work are representative of the whole size range of SSA. This is
592 now mentioned line 698-700 of the manuscript.

593 Given that we have taken steps to accurately mimic the SSA production mechanism, extended our SSA surface calculation to
594 include particle with diameters smaller than 10 μm , and clearly mention the hypothesis that organic carbon in submicron SSA
595 is representative of the OC in the totality of the SSA, we are confident that our approach is sufficient to characterize total SSA
596 INP concentrations. However, future studies are needed to better constraint the characteristics of SSA in sub and supermicron
597 regimes.

598 5. INPSSA was normalized by the particle surface area. However, the NPSSA were derived from samples with total suspended
599 particles, but the particle surface area was derived from particles ranging between 10 and 500 nm only. There is a big mismatch
600 here that can hide important information or can even conduct the authors to deliver wrong conclusion. That is why the following
601 was found: “no statistically significant correlations were seen between total submicron particle counts or total SSA surface
602 area and INPSSA at all three temperatures”. Actually, it would have been more appropriate to use the size distribution of super-
603 micron particles to calculate the particles surface area.

604 **Please see below our response to reviewer 1 who had the same concern:**

605 **First, we calculated adjusted daily mean particle size distribution based on sampling time intervals from the differential**
606 **mobility particle sizer (DMPS) that aligned better with when the filters later analyzed by the Dynamic filter processing chamber**
607 **(DFPC) were collecting particles. In our original manuscript, daily means of DMPS data were calculated on a 24-hour time**
608 **interval beginning and ending at midnight. As DFPC filter samples were not collected at these exact times, there existed a**
609 **small misalignment between DMPS and DFPC sampling intervals. We therefore re-calculated the DMPS daily mean across**
610 **each DFPC sampling period. We also did the same adjustment for daily means of underway data when comparing underway**
611 **data to the DFPC INP concentrations. We added error bars to represent the standard deviation throughout each sampling period**
612 **to the resulting size distributions, produced from the bubbling system during each DFPC sampling period, shown in Figure**
613 **R1. This figure has been added to the supporting information as Figure S3 on line 18.**

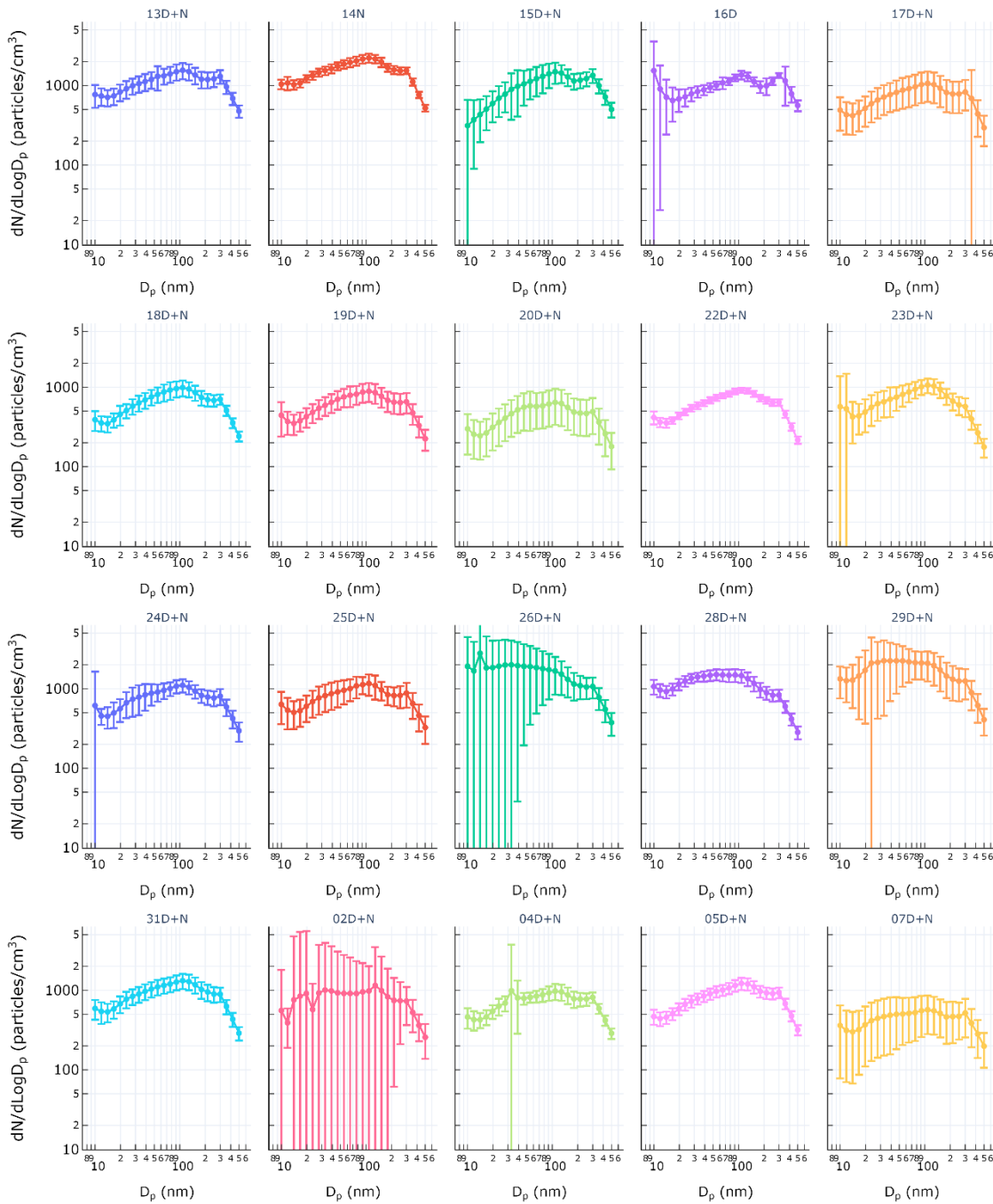


Figure R1.

Average size distributions of SSA produced by the plunging apparatus as observed by DMPS across each DFPC sampling period. Error bars represent standard deviation.

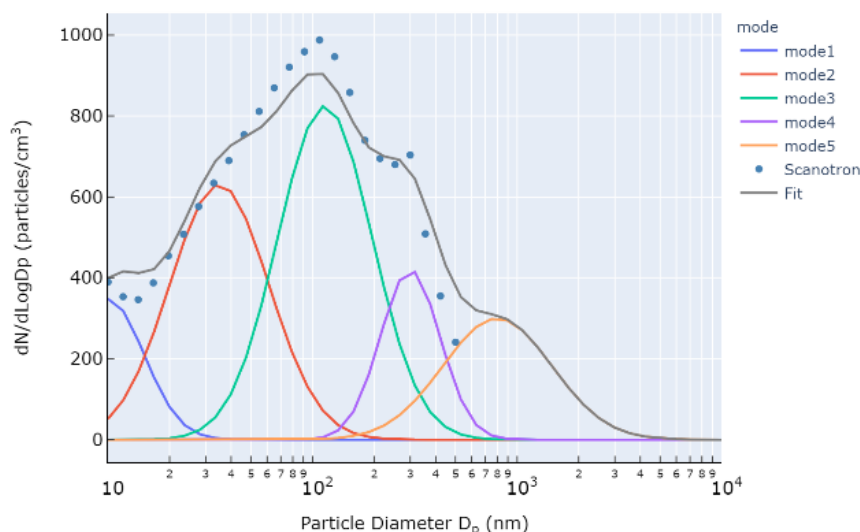
Both reviewers expressed concern that the DMPS data used to calculate surface area of SSA did not include particles above 500 nm in diameter. The reviewers correctly pointed out that an additional mode at 800 nm exists, which contains a large portion of SSA surface area. Ovadnevaite et al. (2014) developed a sea spray aerosol source function consisting of 5 log-normal modes based on in-situ particle number concentration measurements at Mace Head and open-ocean eddy correlation flux measurements from the Eastern Atlantic. Comparison of parameters from their fit with those from the fit of our number-size distribution revealed good agreement between the two. The parameters are shown in Table R1 below. This table has been added to the SI on line 1 as Table S1.

Table R1. Lognormal parameters for a sea spray source function parameterization from Ovadnevaite et al. (2013) and for the fit of observed particle counts during the PEACETIME cruise. For each mode (i), a geometric standard deviation (σ_i), count-median diameter (CMD_i), and total number flux (F_i) or amplitude is shown. For the fit from the literature (Ovadnevaite et al.,

627 2014). F_i is a function of Reynolds number Re_{HW} which we selected as 3.1×10^6 based on the air flow across the surface of the
 628 water in our bubbling apparatus.

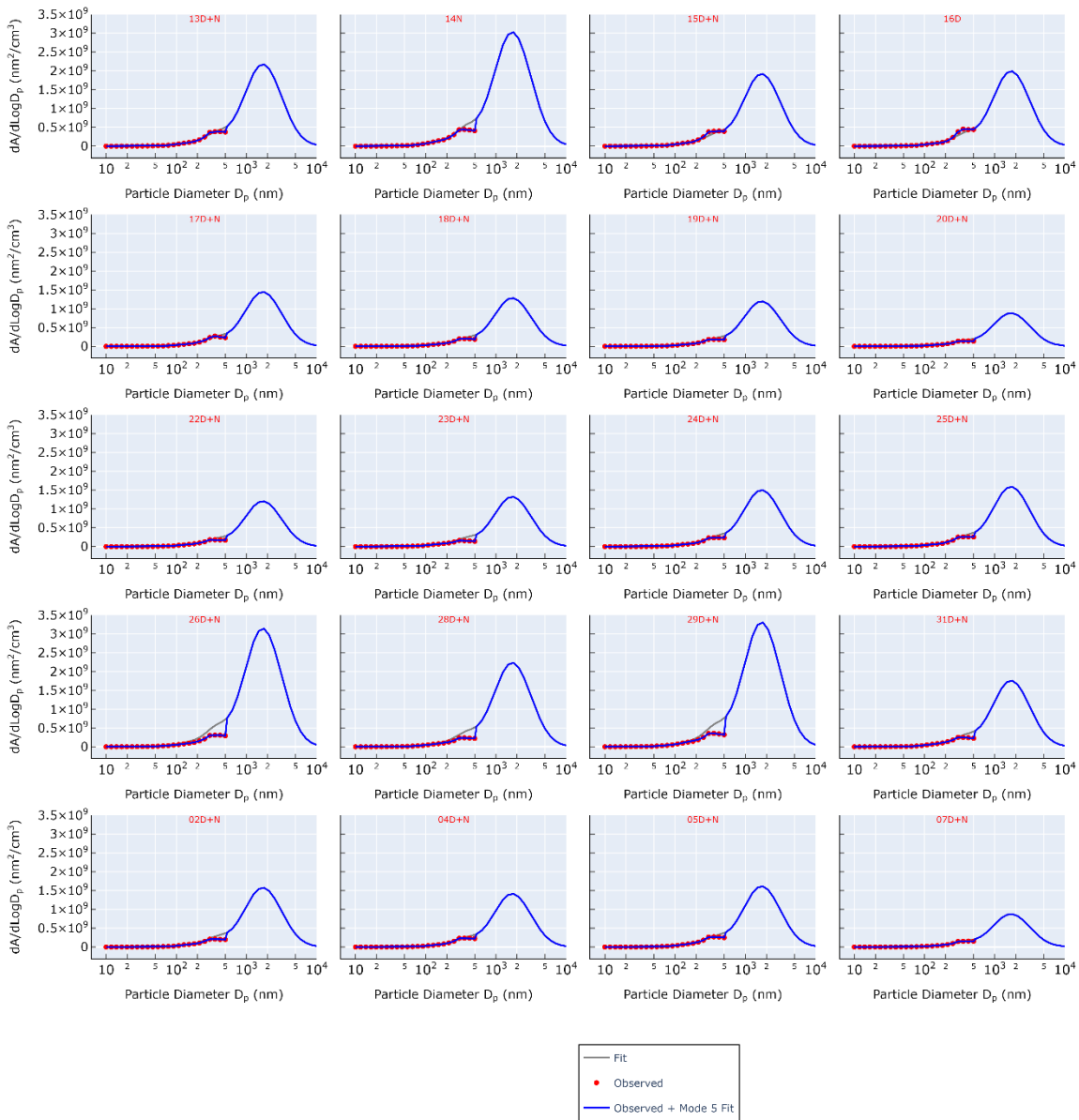
i	σ_i	CMD_i	$F_i/\text{Amplitude}$
Ovadneveite et al. (2013)			
1	1.37	0.018	$104.5(Re_{HW} - 1 \times 10^5)^{0.556}$
2	1.5	0.041	$0.0442(Re_{HW} - 1 \times 10^5)^{1.08}$
3	1.42	0.09	$149.6(Re_{HW} - 1 \times 10^5)^{0.545}$
4	1.53	0.23	$2.96(Re_{HW} - 1 \times 10^5)^{0.79}$
5	1.85	0.83	$0.51(Re_{HW} - 1 \times 10^5)^{0.87}$
PEACETIME Cruise			
1	1.5	0.01	0.01
2	1.75	0.035	0.025
3	1.7	0.115	0.031
4	1.4	0.300	0.01

629 We next took the ratio of mode 5 to mode 3 from the Ovadneveite (2014) fit and applied it to our fit to calculate a fifth mode
 630 accounting for particles ranging in size between 500 nm and 10 μm . Figure R2 shows an example of the result of this process
 631 using daily mean data from March 18. The total fit is shown in gray, which consists of modes 1-4 as calculated from our DMPS
 632 data, as well as mode 5 calculated as described above. Blue circles represent observed values.



633 **Figure R2.** Example of resulting size distribution fit based on comparison of fit from observed PEACETIME particle counts
 634 with a 5 lognormal-mode fit from the literature (Ovadneveite et al., 2014). Blue markers denote particle counts by the DMPS
 635 instrument (named Scanotron). Modes 1-4 are fit based on onserved data. Mode 5 is calculated by taking the ratio of Mode 5/3
 636 from the Ovadneveite et al. (2014) fit and applying it to our observed mode 3.

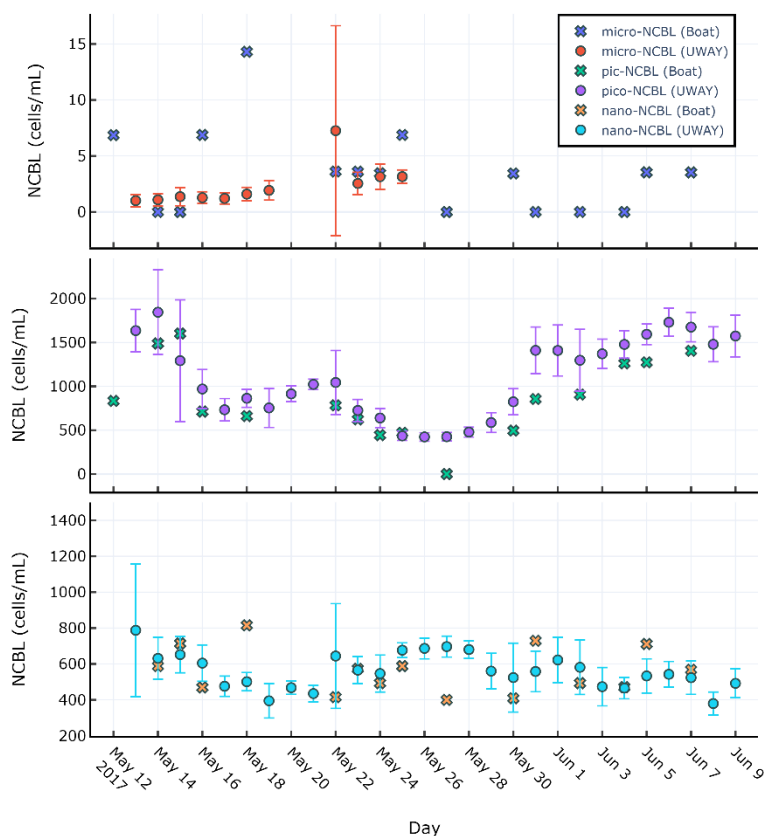
637 We applied this calculation to the mean data from the DMPS for each DFPC sampling period. From the resulting fits, we
 638 calculated aerosol surface area distribution, shown in Figure R3 (also found on line 22 of the Supporting Information as Figure
 639 S4). Finally, we used this adjusted surface area value to re-calculate surface area normalized INP concentrations. We have
 640 added description of this calculation to the main text on line 172.



641
 642 **Figure R3.** Daily average of adjusted SSA surface area distributions. Sampling time is indicated in red text at the top of each
 643 plot, where numbers indicate the day of the month and D/N indicates whether sampling was conducted at day/night,
 644 respectively. The gray line shows the combined fit of modes 1-4 from observed data with the additional contribution of mode
 645 5 as calculated using the Ovadnevaite et al. (2013) fit . Red circles represent observed values and blue line represents the
 646 surface area from observed values through 500nm plus theoretical contribution from mode 5 from the gray fit. The small
 647 difference between blue and gray lines indicates the goodness of the fit.

648 6. It is unclear if the SSW samples are really superficial waters (as defined by the authors), bulk waters, or deep waters. I could
 649 not find the depth at which those samples were collected. Also, the SSA was generated from waters collected at 5 m depth.
 650 Would not have been more relevant to use superficial waters instead? How comparable are the ice-nucleating abilities of the
 651 SSA particles (from “deep” waters, 5 m) with those from the superficial SML and SSW samples?

652 We do mention the sampling depth of discrete SSW samples and underway continuous seawater (respectively 20 cm and 5 m).
653 As the 5 m waters showed similar properties to SSW collected from 20 cm (see Figure R4), we are confident that they can be



654 considered similar in nature.

655 **Figure R4.** Daily average of continuous NCBL measurements from the underway (UWAY) system, where error bars represent
656 standard deviation compared with discrete daily samples from the workboat at 20 cm.

657 7. Section 4, the most important, is extremely short and too general without the required information to follow it. Two
658 parametrizations were developed, one for temperatures above -22°C and one for temperatures below -22°C. Therefore, this
659 means that the INPSSA were included in both parametrizations as the INP concentration for temperatures between -18°C and
660 -25°C were obtained for the SSA samples. However, as mentioned above the chemical analysis for the SSA samples was
661 performed for submicron particles only. C3 Therefore, this parametrizations may be valid for submicron SSA particles only
662 and are not representative for marine aerosol particles.

663 Concerning the chemical analysis of SSA, see our answer at point 4.

664 Reviewer 1 rose similar concerns regarding Section 4. Please see our response below:

665 To ensure selection of the model that best fits the data, we formulated various parameterizations consisting of different
666 time periods, features, and number of components for temperature ranges. Predictor features were chosen based upon their
667 correlation with INP concentrations as described in the previous section. Single component parameterizations in which INP
668 across all three temperatures were linked with the same features were compared with two-component parameterizations in
669 which INP were split into warm and cold categories, each having their own predictor features. Finally, we developed and
670 compared altered versions of the W15 and MC18 models to account for the oligotrophic seawater of the Mediterranean Sea,
671 as the existing models were formulated from observations of eutrophic waters. Each parameterization was recalculated using
672 data across all days of the cruise as well as for only days before the dust deposition event in order to determine the impact of
673 the dust event on the ability to predict INP. The complete set of parameterizations and their associated fit metrics (R^2 and $R_{adj.}^2$)
674 are given in Table R2.

675 Figure R5a shows observed vs predicted INP_{SSA} for the W15 model, while Figure R5b shows the same but using the
676 MC18 parameterization. Similar to our results for seawater INP, a large overprediction is found relative to our observations

677 when using W15. Figure 5b shows that while MC18 is a slight improvement over the W15 approach, it still overpredicts INP
 678 by two orders of magnitude. We also present re-calculated best-fit-lines to data using the same features as in W15 and MC18
 679 (i.e., OC and SSA surface area) in order to account for possible changes due to the oligotrophic nature of the Mediterranean
 680 Sea. We term these two parameterizations the altered Wilson fit for oligotrophy, which is given by:

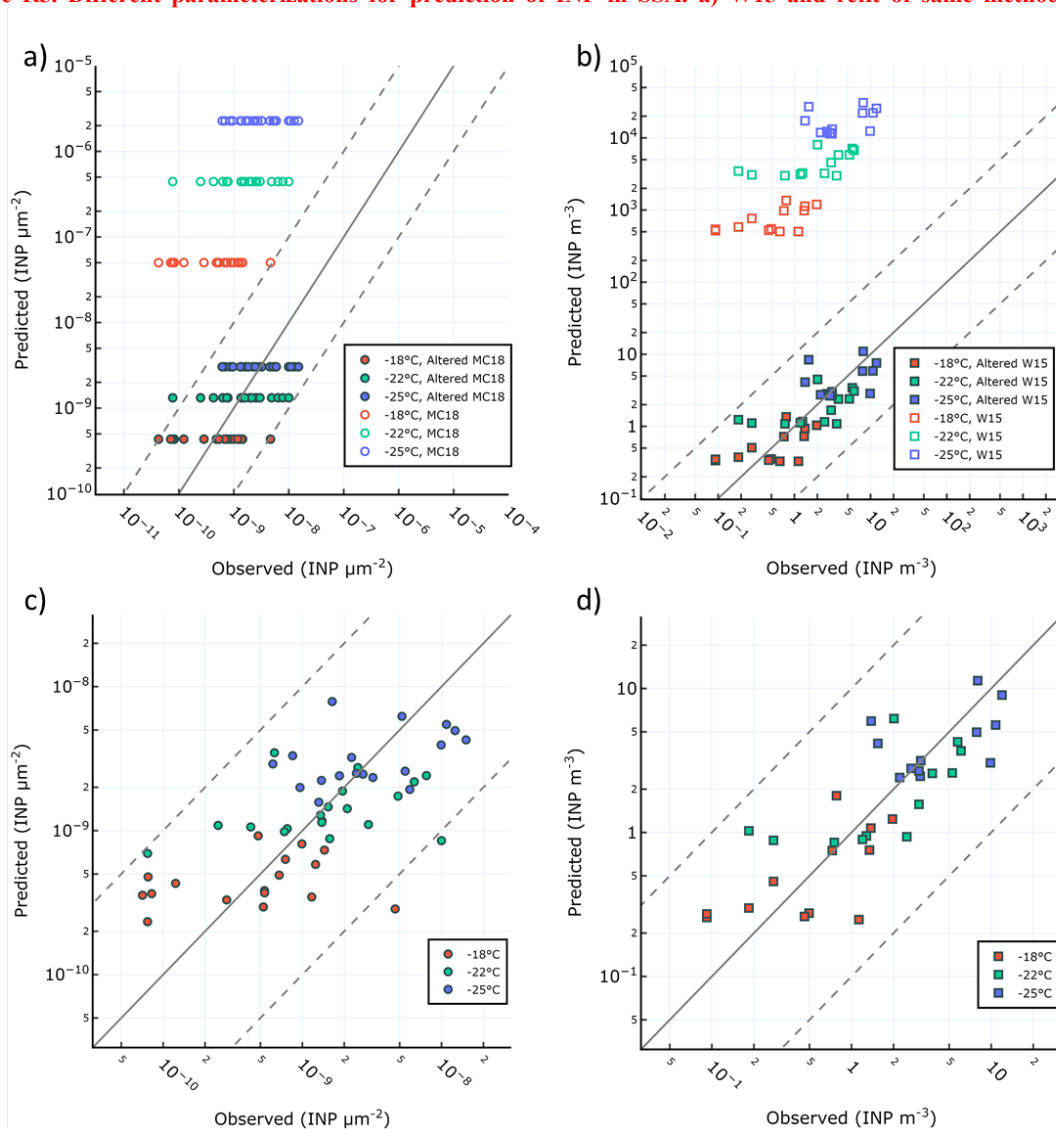
$$\frac{INP}{m^3} = \exp(-7.332 - (0.2989 * T) + (0.3792 * OC_{SSA}))$$

681 and the altered McCluskey fit for oligotrophy, given as:

$$\frac{INP}{\mu m^2} = \exp(-26.57 - (0.2782 * T))$$

682 The results for these fits are shown in Figure R5a,b alongside the results of the original W15 and MC18 parameterizations.
 683 Both altered models offer improvements over the original parameterizations. The adjusted R² of the altered Wilson fit for
 684 oligotrophy on log-transformed INP abundance was R_{adj}²=0.59 and was R_{adj}²=0.32 for the altered McCluskey fit for
 685 oligotrophy. Interestingly, the adjusted Wilson fit for oligotrophy performs better than the adjust McCluskey fit for
 686 oligotrophy, which is the opposite of what was found when comparing the original models.

687 **Figure R5. Different parameterizations for prediction of INP in SSA. a) W15 and refit of same method using PEACETIME**



688 observations b) MK18 and refit of same method using PEACETIME observations c) single-component parameterization for
 689 INP/μm² SSA surface area where INP at all temperatures are related to POC_{SSW} d) two-component parameterization for INP/m³
 690 where INP ≥ -22°C are related to OC and INP < -22°C are related to WIOC.

691 We also tried a range of novel parameterizations based on the observed correlations between INP_{SSA} with seawater
 692 and SSA properties. Below we describe two parameterizations which offered good fits to the data. The single-component

693 parameterization assumes the abundance of INP per unit surface area of total SSA at each temperature can be predicted from
 694 POC_{SSW} concentrations:

$$\frac{INP}{\mu m^2} = \exp(-28.5324 - (0.2729 * T) + (0.0361 * POC_{SSW}))$$

695 The second parameterization separates INP into warm and cold classes, where warm INP ($\geq -22^\circ C$) are related to SSA
 696 OC and cold INP ($< -22^\circ C$) are related to the concentration of SSA WIOC. This two-component parameterization predicts the
 697 concentration of INP/m³ through the following equations:

$$\frac{INP_{T \geq -22^\circ C}}{m^3} = \exp(-7.9857 - (0.3178 * T) + (0.4643 * OC_{SSA}))$$

$$\frac{INP_{T < -22^\circ C}}{m^3} = \exp(-6.6606 - (0.2712 * T) + (0.5755 * WIOC_{SSA}))$$

698 Figure R5c,d shows the results of our single-component model using POC_{SSW} and the two-part model which uses SSA WIOC
 699 and OC and considers the separate temperature classes of INP. The adjusted R² for each model on the log-transformed INP
 700 abundance were R_{adj}²=0.404 for the single component model using POC_{SSW} and R_{adj}²=0.60 for the two-component model using
 701 OC and WIOC. This result reveals that they both fit the observations better than the altered McCluskey parameterization for
 702 oligotrophy, while the two-component method performs as well as the altered Wilson parameterization. Each
 703 parameterization's fit to the data is improved when considering pre-dust days only (R_{adj}²=0.63 for the two-component
 704 parameterization and R_{adj}²=0.57 for the single-component parameterization). The improvement is more pronounced for the
 705 single-component parameterization using POC_{SSW}, further pointing to the fact that such dust deposition events can alter the
 706 INP properties of surface waters and the subsequent SSA, either through

707 .

708 **Table R2.** Summary of tested parameterizations to the PEACETIME dataset.

Model Name	INP Units	Days	# Cat.	Features	Warm Features	Cold Features	R ²	R _{adj} ²
PD-2TC_OC_WIOC	INP/m ³	Pre-Dust	2		OC _{SSA}	WIOC	0.66	0.63
PD-1TC_OC	INP/m ³	Pre-Dust	1	OC _{SSA}			0.63	0.61
PD-1TC_WSOC_WIOC	INP/m ³	Pre-Dust	1	WSOC, WIOC			0.64	0.60
AD-2TC_OC_WIOC	INP/m ³	All Days	2		OC _{SSA}	WIOC	0.63	0.60
AD-1TC_OC	INP/m ³	All Days	1	OC _{SSA}			0.61	0.59
PD-2TC_POC_PHYTO-L	INP/μm ²	Pre-Dust	2		POC _{SSW}	Micro- NCBL	0.62	0.59
AD-1TC_WSOC_WIOC	INP/m ³	All Days	1	WSOC, WIOC			0.62	0.58
PD-1TC_POC	INP/μm ²	Pre-Dust	1	POC			0.59	0.57
PD-1TC_POC_PHYTO-L	INP/μm ²	Pre-Dust	1	POC, Micro- NCBL			0.58	0.53
PD-2TC_WSOC_WIOC	INP/m ³	Pre-Dust	2		WSOC	WIOC	0.53	0.49
AD-2TC_WSOC_WIOC	INP/m ³	All Days	2		WSOC	WIOC	0.45	0.41
AD-1TC_POC	INP/μm ²	All Days	1	POC _{SSW}			0.43	0.40
AD-2TC_POC_PHYTO-L	INP/μm ²	All Days	2		POC _{SSW}	Micro- NCBL	0.43	0.39
AD-2TC_POC_PHYTO-LM	INP/μm ²	All Days	2		POC _{SSW}	Micro- ,Nano- NCBL	0.43	0.38
AD-1TC_T	INP/μm ²	All Days	1	Temperature			0.33	0.32

709

710 We have added this discussion to line 411 of the manuscript.

711

References

- 715 DeMott, P. J., Hill, T. C. J., McCluskey, C. S., Prather, K. A., Collins, D. B., Sullivan, R. C., Ruppel, M. J., Mason,
716 R. H., Irish, V. E., Lee, T., Hwang, C. Y., Rhee, T. S., Snider, J. R., McMeeking, G. R., Dhaniyala, S., Lewis, E.
717 R., Wentzell, J. J. B., Abbatt, J., Lee, C., Sultana, C. M., Ault, A. P., Axson, J. L., Martinez, M. D., Venero, I.,
718 Santos-Figueroa, G., Stokes, D. M., Deane, G. B., Mayol-Bracero, O. L., Grassian, V. H., Bertram, T. H., Bertram,
719 A. K., Moffett, B. F., and Franc, G. D.: Sea Spray Aerosol as a Unique Source of ice Nucleating Particles, *PNAS*,
720 113, 5797-5803, <https://doi.org/10.1073/pnas.1514034112>, 2016.
- 721 DeMott, P. J., Möhler, O., Cziczo, D. J., Hiranuma, N., Petters, M. D., Petters, S. S., Belosi, F., Bingemer, H. G.,
722 Brooks, S. D., Budke, C., Burkert-Kohn, M., Collier, K. N., Danielczok, A., Eppers, O., Felgitsch, L., Garimella,
723 S., Grothe, H., Herenz, P., Hill, T. C. J., Höhler, K., Kanji, Z. A., Kiselev, A., Koop, T., Kristensen, T. B., Krüger,
724 K., Kulkarni, G., Levin, E. J. T., Murray, B. J., Nicosia, A., O'Sullivan, D., Peckhaus, A., Polen, M. J., Price, H.
725 C., Reicher, N., Rothenberg, D. A., Rudich, Y., Santachiara, G., Schiebel, T., Schrod, J., Seifried, T. M., Stratmann,
726 F., Sullivan, R. C., Suski, K. J., Szakáll, M., Taylor, H. P., Ullrich, R., Vergara-Temprado, J., Wagner, R., Whale,
727 T. F., Weber, D., Welti, A., Wilson, T. W., Wolf, M. J., and Zenker, J.: The Fifth International Workshop on Ice
728 Nucleation phase 2 (FIN-02): laboratory intercomparison of ice nucleation measurements, *Atmospheric*
729 *Measurement Techniques*, 11, 6231-6257, 10.5194/amt-11-6231-2018, 2018.
- 730 Fuentes, E., Coe, H., Green, D., de Leeuw, G., and McFiggans, G.: Laboratory-generated primary marine aerosol
731 via bubble-bursting and atomization, *Atmos. Meas. Tech.*, 3, 141-162, 10.5194/amt-3-141-2010, 2010.
- 732 Gantt, B., and Meskhidze, N.: The physical and chemical characteristics of marine primary organic aerosol: a
733 review, *Atmospheric Chemistry and Physics*, 13, 3979-3996, 10.5194/acp-13-3979-2013, 2013.
- 734 Gong, X., Wex, H., van Pinxteren, M., Triesch, N., Fomba, K. W., Lubitz, J., Stolle, C., Robinson, T.-B., Müller,
735 T., Herrmann, H., and Stratmann, F.: Characterization of aerosol particles at Cabo Verde close to sea level and at
736 the cloud level – Part 2: Ice-nucleating particles in air, cloud and seawater, *Atmospheric Chemistry and Physics*,
737 20, 1451-1468, 10.5194/acp-20-1451-2020, 2020.
- 738 Hiranuma, N., Adachi, K., Bell, D. M., Belosi, F., Beydoun, H., Bhaduri, B., Bingemer, H., Budke, C., Clemen,
739 H.-C., Conen, F., Cory, K. M., Curtius, J., DeMott, P. J., Eppers, O., Grawe, S., Hartmann, S., Hoffmann, N.,
740 Höhler, K., Jantsch, E., Kiselev, A., Koop, T., Kulkarni, G., Mayer, A., Murakami, M., Murray, B. J., Nicosia, A.,
741 Petters, M. D., Piazza, M., Polen, M., Reicher, N., Rudich, Y., Saito, A., Santachiara, G., Schiebel, T., Schill, G.
742 P., Schneider, J., Segev, L., Stopelli, E., Sullivan, R. C., Suski, K., Szakáll, M., Tajiri, T., Taylor, H., Tobo, Y.,
743 Ullrich, R., Weber, D., Wex, H., Whale, T. F., Whiteside, C. L., Yamashita, K., Zelenyuk, A., and Möhler, O.: A
744 comprehensive characterization of ice nucleation by three different types of cellulose particles immersed in water,
745 *Atmospheric Chemistry and Physics*, 19, 4823-4849, 10.5194/acp-19-4823-2019, 2019.
- 746 McCluskey, C. S., Ovadnevaite, J., Rinaldi, M., Atkinson, J., Belosi, F., Ceburnis, D., Marullo, S., Hill, T. C. J.,
747 Lohmann, U., Kanji, Z. A., O'Dowd, C., Kreidenweis, S. M., and DeMott, P. J.: Marine and Terrestrial Organic
748 Ice-Nucleating Particles in Pristine Marine to Continentally Influenced Northeast Atlantic Air Masses, *J. Geophys*
749 *Res. Atmos.*, 123, 6196-6212, <https://doi.org/10.1029/2017JD028033>, 2018.
- 750 O'Dowd CD, Facchini MC, Cavalli F, Ceburnis D, Mircea M, Decesari S, Fuzzi S, Yoon YJ, Putaud JP. Biogenically driven
751 organic contribution to marine aerosol. *Nature*. 2004 Oct 7;431(7009):676-80. doi: 10.1038/nature02959. PMID: 15470425.
- 752 Ovadnevaite, J., Manders, A., de Leeuw, G., Ceburnis, D., Monahan, C., Partanen, A. I., Korhonen, H., and
753 O'Dowd, C. D.: A sea spray aerosol flux parameterization encapsulating wave state, *Atmospheric Chemistry and*
754 *Physics*, 14, 1837-1852, 10.5194/acp-14-1837-2014, 2014.
- 755 Rosinski, J., Haagenson, P. L., Nagamoto, C. T., and Parungo, F.: Ice-forming nuclei of maritime origin, *Journal*
756 *of Aerosol Science*, 17, 23-46, [https://doi.org/10.1016/0021-8502\(86\)90004-2](https://doi.org/10.1016/0021-8502(86)90004-2), 1986.
- 757 Rosinski, J., Haagenson, P. L., Nagamoto, C. T., and Parungo, F.: Nature of ice-forming nuclei in marine air masses,
758 *Journal of Aerosol Science*, 18, 291-309, [https://doi.org/10.1016/0021-8502\(87\)90024-3](https://doi.org/10.1016/0021-8502(87)90024-3), 1987.
- 759 Rosinski, J., Haagenson, P. L., Nagamoto, C. T., Quintana, B., Parungo, F., and Hoyt, S. D.: Ice-forming nuclei in
760 air masses over the Gulf of Mexico, *Journal of Aerosol Science*, 19, 539-551, [https://doi.org/10.1016/0021-](https://doi.org/10.1016/0021-8502(88)90206-6)
761 [8502\(88\)90206-6](https://doi.org/10.1016/0021-8502(88)90206-6), 1988.
- 762 Schwier, A. N., Rose, C., Asmi, E., Ebling, A. M., Landing, W. M., Marro, S., Pedrotti, M.-L., Sallon, A., Iuculano,
763 F., Agusti, S., Tsiola, A., Pitta, P., Louis, J., Guieu, C., Gazeau, F., and Sellegri, K.: Primary Marine Aerosol
764 Emissions from the Mediterranean Sea During Pre-Bloom and Oligotrophic Conditions: Correlations to Seawater
765 Chlorophyll-a From a Mesocosm Study, *Atmos. Chem. Phys.*, 15, 7961-7976, [https://doi.org/10.5194/acp-15-](https://doi.org/10.5194/acp-15-7961-2015)
766 [7961-2015](https://doi.org/10.5194/acp-15-7961-2015), 2015.
- 767 Schwier, A. N., Sellegri, K., Mas, S., Charrière, B., Pey, J., Rose, C., Temime-Roussel, B., Jaffrezo, J.-L., Parin,
768 D., Picard, D., Ribeiro, M., Roberts, G., Sempéré, R., Marchand, N., and D'Anna, B.: Primary marine aerosol

769 physical flux and chemical composition during a nutrient enrichment experiment in mesocosms in the
770 Mediterranean Sea, *Atmospheric Chemistry and Physics*, 17, 14645-14660, 10.5194/acp-17-14645-2017, 2017.
771 Vali, G., DeMott, P. J., Möhler, O., and Whale, T. F.: Technical Note: A proposal for ice nucleation terminology,
772 *Atmospheric Chemistry and Physics*, 15, 10263-10270, 10.5194/acp-15-10263-2015, 2015.

773

774

A Two-Component Parameterization of Marine Ice Nucleating Particles Based on Seawater Biology and Sea Spray Aerosol Measurements in the Mediterranean Sea

Jonathan V. Trueblood¹, Alesia Nicosia¹, Anja Engel², Birthe Zäncker², Matteo Rinaldi³, Evelyn Freney¹, Melilotus Thyssen⁴, Ingrid Obernosterer⁵, Julie Dinasquet^{5,6}, Franco Belosi³, Antonio Tovar-Sánchez⁷, Araceli Rodriguez-Romero⁷, Gianni Santachiara³, Cécile Guieu⁵, and Karine Sellegri¹

¹ Université Clermont Auvergne, CNRS, Laboratoire de Météorologie Physique (LaMP) F-63000 Clermont-Ferrand, France

² GEOMAR, Helmholtz Centre for Ocean Research Kiel, 24105 Kiel, Germany

³ Institute of Atmospheric Sciences and Climate, National Research Council, 40129 Bologna, Italy

⁴ Mediterranean Institute of Oceanography, 163 avenue de Luminy, Marseille, France

⁵ CNRS, Sorbonne Université, Laboratoire d'Océanographie de Villefranche, UMR7093, Villefranche-sur-Mer

⁶ Marine Biology Research Division, Scripps Institution of Oceanography, 92037 La Jolla, US

⁷ Department of Ecology and Coastal Management, Institute of Marine Sciences of Andalusia (ICMAN-CSIC), 07190 Puerto Real, Spain

Correspondence to: K.Sellegri@opgc.cnrs.fr

Abstract. Ice nucleating particles (INP) have a large impact on the climate-relevant properties of clouds over the oceans. Studies have shown that sea spray aerosols (SSA), produced upon bursting of bubbles at the ocean surface, can be an important source of marine INP, particularly during periods of enhanced biological productivity. Recent mesocosm experiments using natural seawater spiked with nutrients have revealed that marine INP are derived from two separate classes of organic matter in SSA. Despite this finding, existing parameterizations for marine INP abundance are based solely on single variables such as SSA organic carbon (OC) or SSA surface area, which may mask specific trends in the separate classes of INP. The goal of this paper is to improve the understanding of the connection between ocean biology and marine INP abundance by reporting results from a field study and proposing a new parameterization of marine INP that accounts for the two associated classes of organic matter. The PEACETIME cruise took place from May 10 to June 10, 2017 in the Mediterranean Sea. Throughout the cruise, INP concentrations in the surface microlayer (INP_{SML}) and in SSA (INP_{SSA}) produced using a plunging aquarium apparatus were continuously monitored while surface seawater (SSW) and SML biological properties were measured in parallel. The organic content of artificially generated SSA was also evaluated. INP_{SML} and INP_{SSA} concentrations were found lower than in the literature, presumably due to the oligotrophic nature of the Mediterranean Sea. A dust wet deposition event that occurred during the cruise increased the INP concentrations measured in the SML by an order of magnitude, in line with increases of iron in the SML and bacterial abundances. Increases of INP_{SSA} were not observed until after a delay of three days compared to increases in the SML, and are likely a result of a strong influence of bulk SSW INP for the temperatures investigated ($T = -18^\circ\text{C}$ for SSA, $T = -15^\circ\text{C}$ for SSW). Results confirmed that INP_{SSA} are divided into two classes depending on their associated organic matter. Here we find that warm ($T \geq -22^\circ\text{C}$) INP_{SSA} concentrations are correlated with water soluble organic matter (WSOC) in the SSA, but also to SSW parameters (POC_{SSW} and $INP_{SSW,-16^\circ\text{C}}$) while cold INP_{SSA} ($T < -22^\circ\text{C}$) are correlated with SSA water-insoluble organic carbon (WIOC), and SML dissolved organic carbon (DOC) concentration. A relationship was also found between cold INP_{SSA} and SSW nano- and micro-phytoplankton cell abundances, indicating that these species might be a source of water insoluble organic matter with surfactant properties and specific IN activities. Guided by these results, we formulated and tested multiple parameterizations for the abundance of INP in marine SSA, including a single component model based on POC_{SSW} and a two-component model based on SSA WIOC and OC. We also altered two previous models based on SSA surface area and OC_{SSA} content to account for oligotrophy of the Mediterranean Sea. We then compared these formulations with the previous models. These new parameterizations should improve attempts to incorporate marine INP emissions into numerical models.

817 **1 Introduction**

818 Ice nucleating particles are a subset of aerosol particles that are required for the heterogeneous nucleation of ice particles in
819 the atmosphere. While extremely rare (Rogers et al., 1998), INP greatly control the ice content of clouds, which is crucial to a
820 range of climate-relevant characteristics including precipitation onset, lifetime, and radiative forcing (Verheggen et al., 2007).
821 Despite their importance, the knowledge of INP sources and concentrations, particularly in marine regions, remains low as
822 evidenced by the large uncertainties in modelled radiative properties of clouds (McCoy et al., 2015; McCoy et al., 2016;
823 Franklin et al., 2013).

824 While the ice nucleating (IN) ability of marine SSA particles is less efficient than their terrestrial counterparts (DeMott et
825 al., 2016), modelling studies have shown that marine INP are of particular importance in part due to the lack of other INP
826 sources in such remote regions (Burrows et al., 2013; Vergara-Temprado et al., 2017). For this reason, recent studies have
827 been conducted to better understand which SSA particles contribute to the marine INP population as well as the relationship
828 between SSA emission and ecosystem productivity. Results from these studies suggest that the IN ability of SSA is linked to
829 the biological productivity of source waters, with higher productivity leading to greater IN activity (DeMott et al., 2016; Bigg,
830 1973; Schnell and Vali, 1976). For example, it has been shown that both the cell surface and organic exudate of the marine
831 diatom *Thalassiosira pseudonana* can promote freezing at conditions relevant to mixed-phase clouds (Knopf et al., 2011;
832 Wilson et al., 2015). More recently, mesocosm studies on phytoplankton blooms using two separate in-lab SSA-generation
833 techniques have furthered the understanding of the connection between ocean biology and the IN activity of SSA (McCluskey
834 et al., 2017). In-depth chemical analysis of the artificially generated SSA during this set of experiments has revealed marine
835 INP may be related to two classes of organic matter: a regularly occurring surface-active molecule type related to DOC and
836 long-chain fatty acids, and an episodic heat-labile microbially-derived type (McCluskey et al., 2018b).

837 As the understanding of the connection between ocean biology and marine INP has improved, parameterizations for
838 predicting marine INP abundance using readily available ocean parameters have been proposed. Wilson and co-authors
839 (Wilson et al., 2015) identified a temperature-dependent relationship between TOC and ice nucleating entities (INE) number
840 concentrations in the SML from samples collected in the North Atlantic and Arctic ocean basins. They then extended this
841 relationship from the ocean to the atmosphere to predict the abundance of INP in SSA based on model estimates of marine
842 organic carbon aerosol concentrations. The parameterization was tested for the first time on field measurements of marine
843 aerosol over the North Atlantic at Mace Head and was found to overestimate INP abundance in pristine marine aerosol by a
844 factor of 4 to 100 at -15°C and -20°C (McCluskey et al., 2018c). In the same study, a new parameterization based on SSA
845 surface area and temperature was proposed (McCluskey et al., 2018c). However, this parameterization did not incorporate the
846 recently observed heat labile organic INPs. Most recently, this parameterization was compared with observations of INP over
847 the Southern Ocean, showing reasonable agreement between predictions and observations at -25°C (McCluskey et al., 2019).

848 Despite the recent progress made in the understanding of marine INP, there remains much room for improvement. To
849 date, previous parameterizations have only been tested in the two field studies mentioned in the previous paragraph,
850 underscoring the need for more real-world observations. Furthermore, the field studies conducted so far have taken place in
851 regions of the ocean where biological productivity is high (i.e., North Atlantic and Southern Ocean). As modelling work has
852 shown that the link between ocean biology and SSA organic content properties in oligotrophic waters differs from those in
853 highly productive regions (Burrows et al., 2014) there is need for more measurements in waters with low primary productivity.
854 Finally, despite the finding that marine INP may exist as two separate populations, no model has yet been proposed to account
855 for this.

856 This paper addresses the current gaps in the knowledge of marine INP by 1) testing existing parameterizations of INP on
857 a new set of field measurements by extending the current inventory of field measurements beyond eutrophic waters to more
858 oligotrophic regions for the first time 2) improving the understanding of how INP in the SML and SSA are linked to both

859 seawater biological and SSA organic properties and 3) proposing a new parameterization based on the two-component nature
860 of INP. Here we present results from the ProcEss studies at the Air-sEa Interface after dust deposition in the Mediterranean
861 Sea (PEACETIME) cruise. The cruise took place in the central and western Mediterranean Sea from May 10 - June 10, 2017.
862 Observations of INP concentrations both in the SML and SSA were compared with a suite of surface seawater, surface
863 microlayer, and SSA properties to better determine how INP concentrations related to biology.

864 2 Methods

865 In the frame of the PEACETIME project (<http://peacetime-project.org/>), an oceanographic campaign took place aboard
866 the French research vessel (R/V) ‘Pourquoi Pas?’ between May 10-June 10, 2017 with the purpose of investigating the
867 processes that occur at the air-sea interface in the Mediterranean Sea. The cruise started in La Seyne, France and travelled in
868 a clockwise fashion between 35° to 42° latitude and 0° to 20° longitude. The observations and process studies performed on
869 board both in the whole water column and the atmosphere are described elsewhere (Freney et al., 2020). Here, we focus on the
870 measurements conducted to describe the SML, SSW, and aerosol properties.

871 2.1 Surface Seawater (SSW)

872 SSW properties presented here were obtained from sampling at depths of 20 cm and 5 m. First, 21 parameters including
873 various chemical properties, microbial assemblages, hydrological properties, and optical properties were monitored using the
874 ship’s underway system that continuously collected seawater at 5 m under the ship using a large peristaltic pump (Verder VF40
875 with EPDM hose). These measurements included counts of specific microbial classes (e.g., *Synechococcus*, *Prochlorococcus*,
876 picoeukaryotes, nanoeukaryotes, microphytoplankton, high phycoerythrin containing cells, coccolithophores, cryptophytes), as
877 well as seawater biovolume, chlorophyll-*a* (chl-*a*), and POC concentrations. Chl-*a* was determined from the particulate
878 absorption spectrum line-height at 676 nm after adjusting to PEACETIME chl-*a* from high performance liquid chromatography
879 (HPLC). POC was estimated from the particulate attenuation at 660 nm using an empirical relationship specific to
880 PEACETIME ($POC = 1405.1 \times c_p(660) - 52.4$). For enumeration of phytoplankton cells, an automated Cytosense flow
881 cytometer (Cytobuoy, NL) operating at a time resolution of one-hour was connected to the continuous underway seawater
882 system. Particles were carried in a laminar flow filtered seawater sheath fluid and subsequently detected with forward scatter
883 and sideward scatter as well as fluorescence in the red (FLR > 652 nm) and orange (FLO 552-652 nm). Distinction between
884 highly concentrated picophytoplankton and cyanobacteria groups and lower concentrated nano- and microphytoplankton was
885 accomplished using two trigger levels (trigger level FLR 7.34 mV, sampling speed of $4 \text{ mm}^3 \text{ s}^{-1}$ analysing $0.65 \pm 0.18 \text{ cm}^3$ and
886 trigger level FLR 14.87 mV at a speed of $8 \text{ mm}^3 \text{ s}^{-1}$ analysing $3.57 \pm 0.97 \text{ cm}^3$).

887 The second set of SSW measurements were made on seawater collected at ~20 cm depth from a pneumatic boat that was
888 periodically deployed at a distance of 2 km from the R/V to avoid contamination. The SSW was manually collected using acid
889 cleaned borosilicate bottles. From these discrete samples, microbial composition and cell abundance of the SSW was monitored
890 as described in a companion paper (Tovar-Sanchez et al., 2019). Measurements included heterotrophic bacteria counts, high
891 nucleic acid and low nucleic acid bacteria (HNA and LNA bacteria, respectively), total non-cyanobacteria like cells (NCBL),
892 cyanobacteria like cells (CBL), and total phytoplankton concentration (NCBL+CBL). These were further segregated into size
893 classes of small, medium, and large which roughly correspond to the pico-, nano-, and micro- size classifications from the
894 underway measurements. Trace metals (i.e., Cd, Co, Cu, Fe, Ni, Mo, V, Zn, Pb) were analysed by inductively coupled plasma
895 mass spectrometry, although here we only report on Fe. Finally DOC and marine gel-like particles, including abundance of
896 transparent exopolymer particles (TEP) and Coomassie stainable particles (CSP) were also measured as described in literature
897 (Engel, 2009).

898 2.2 Surface Microlayer

899 At the same time SSW samples were manually collected on the pneumatic boat, SML samples were also collected using
900 a glass plate sampling method which has been previously described in the literature (Tovar-Sanchez et al., 2019). The glass
901 plate was cleaned overnight with acid and rinsed with ultrapure Milli-Q water. Roughly 100 dips of the glass were conducted
902 to collect 500 mL of SML water into 0.5 L acid cleaned low-density polyethylene plastic bottles. The samples were then
903 acidified on board to pH<2 with ultrapure-grade hydrochloric acid in a class-100 HEPA laminar flow hood. The same
904 measurements done for the SSW samples (see above, Section 2.1) were then made on the SML samples. Enrichment factor
905 was calculated for relevant properties as the ratio of SML to SSW:

$$906 EF = \frac{SML}{SSW}$$

907 In addition to biological measurements, concentrations of immersion freezing mode INP in SML samples (and a small
908 number of SSW samples, n=4) were measured between May 22 - June 7 using an offline method described previously (Stopelli
909 et al., 2014). Briefly, prior to acidification of the SML samples, additional aliquots were separated and stored in Corning
910 Falcon 15 mL conical tubes and frozen at -20°C until analysis. Before INP measurement, each aliquot was gradually defrosted
911 and distributed into an array of 26 Eppendorf tubes filled up to 200 µL. The array was then immersed inside an LED based Ice
912 Nuclei Detection Apparatus (LINDA) and the number of ice nucleating particles per liter (INP/L) of SML water was following
913 the method described in Stopelli et al. (2014) which was originally formulated by Vali (1971):

$$914 \frac{INP}{volume} = \frac{\ln(N_{total}) - \ln(N_{unfrozen})}{V_{tube}}$$

915 where N_{total} is the total number of tubes, $N_{unfrozen}$ the total number of unfrozen tubes, and V_{tube} the volume of sample in
916 each tube. The number of unfrozen tubes is calculated by first blank correcting the number of frozen tubes, and then subtracting
917 that value from the total number of tubes. We calculated uncertainty as the binomial proportion confidence interval (95%)
918 using the Wilson score interval. Samples were not corrected for salinity in this study.

919 2.3 Artificially Generated Sea Spray Aerosol

920 Sea spray aerosols were generated using a sea spray generation apparatus which has been described previously (Schwier
921 et al., 2015; Schwier et al., 2017). The characteristics of the setup were selected to mimic Fuentes et al. (2010). These
922 parameters (water flow rates, plunging water depth, etc.) have been shown to mimic well nascent SSA. The apparatus consists
923 of a 10 L glass tank with a plunging jet system. A continuous flow of seawater collected at 5 m depth using the ship's underway
924 seawater circulating system (described above) was supplied to the apparatus. Particle free air was passed perpendicular to the
925 water surface at a height of 1 cm to send a constant airflow across the surface of the water. Aerosols were then either dried
926 with a 1 m long silica dryer for online instrumentation (see Section 2.3.3), with a 30 cm silica gel dryer cascade impactor
927 sampling with subsequent chemical analysis, or were sampled directly from the sea spray generator onto filters for INP
928 analysis.

929 2.3.1 Offline PM1 Filter Analysis

930 Aerosol particles were also sampled onto PM1 quartz fiber filters mounted on a 4-stage cascade impactor (10 LPM)
931 on a daily basis (24-hour duration). Samples were then extracted in Milli-Q water by sonication for 30 minutes for the analysis
932 of water-soluble components. Main inorganic ion abundance (i.e., SO_4^{2-} , NO_3^- , NH_4^+ , Na^+ , Cl^- , K^+ , Mg^{2+} , Ca^{2+}) was analysed
933 via ion chromatography. An IonPac CS16 3x 250 mm Dionex separation column with gradient methanesulfonic acid elution
934 was used for cations, while an IonPac AS11 2 x 250 mm Dionex column with gradient potassium hydroxide elution was used
935 for anions. Water soluble organic carbon (WSOC) and water insoluble organic carbon (WIOC) were also determined. WSOC
936 was measured after water extraction using a high-temperature catalytic oxidation instrument (Shimadzu; TOC 5000 A). Total

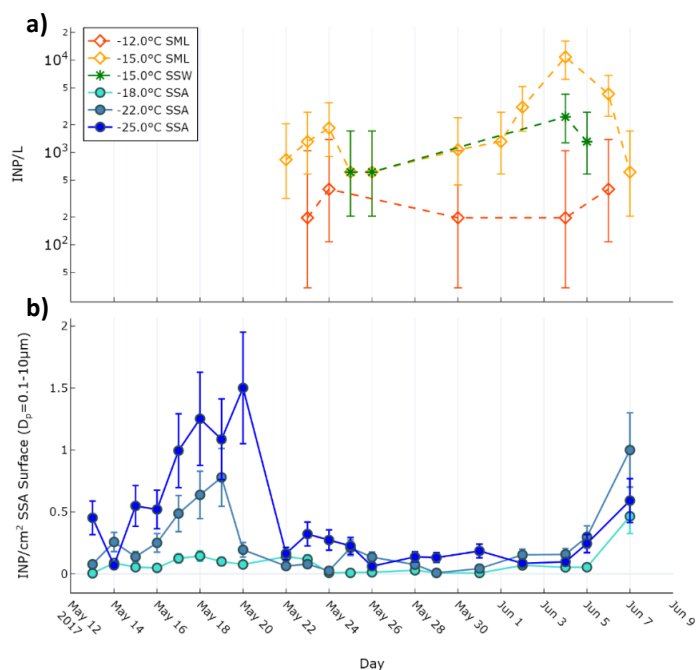
937 organic carbon (which we now refer to as OC), was measured using a Multi N/C 2100 elemental analyzer (Analytik Jena,
938 Germany) with a furnace solids module. The analysis was performed on an 8 mm diameter filter punch, pre-treated with 40
939 μL of H_3PO_4 (20% v/v) to remove contributions from inorganic carbon. WIOC was determined as the difference between OC
940 and WSOC. Finally, we calculated organic mass fraction of SSA (OMSS) by taking the ratio of $\text{OM}/(\text{OM}+\text{SeaSalt})$, where
941 OM is the sum of WSOM and WIOM, calculated as $\text{WSOM} = \text{WSOC} \times 1.8$ and $\text{WIOM} = \text{WIOC} * 1.4$ and SeaSalt is the sum
942 of inorganic ion abundance as determined above.

943 2.3.2 INP

944 INP concentrations were determined from filter-based samples of total suspended particles over a 24-hour duration daily
945 or from the average of two filters (day and night). The concentration of INP in the SSA was determined for the condensation
946 freezing mode using a Dynamic Filter Processing Chamber (DFPC), **which has been used in multiple previous studies and**
947 **found to agree well with other INP monitoring instruments** (DeMott et al., 2018; Hiranuma et al., 2019; McCluskey et al.,
948 2018c). **A full description of the instrument can be found in the literature** (DeMott et al., 2018). Briefly, **bulk** SSA formed
949 using the **plunging aquarium** apparatus were impacted onto 47 mm nitrocellulose filters which were then placed on a metal
950 plate coated with a smooth surface of Vaseline. Air entered the chamber and was sent through a cooling coil allowing it to
951 become saturated with respect to **water**. Different supersaturations with respect to ice and **liquid** water **can be** obtained by
952 controlling the temperatures of the filter and the air flowing across the filter. Filter air temperature combinations were set three
953 different ways, all **resulting in a supersaturation** with respect to **liquid** water of 1.02. The filter temperatures were -18, -22, and
954 -25°C (-15.9, -19.6, and -22.3°C for air temperature). **Under these conditions, condensation freezing is expected to be the**
955 **dominant freezing mode for INP. It has been reported** (Vali et al., 2015) **that condensation freezing and immersion freezing**
956 **are not distinguishable from one another.** Filters were **processed** inside the DFPC for 15 minutes and monitored for formation
957 of ice crystals upon activation of INPs. Based on sampling time and flow rate, the number of INP/volume were calculated. **We**
958 **report an uncertainty of $\pm 30\%$ based on previous reports of the DFPC** (DeMott et al., 2018).

959 2.3.3 Size Distribution Measurements

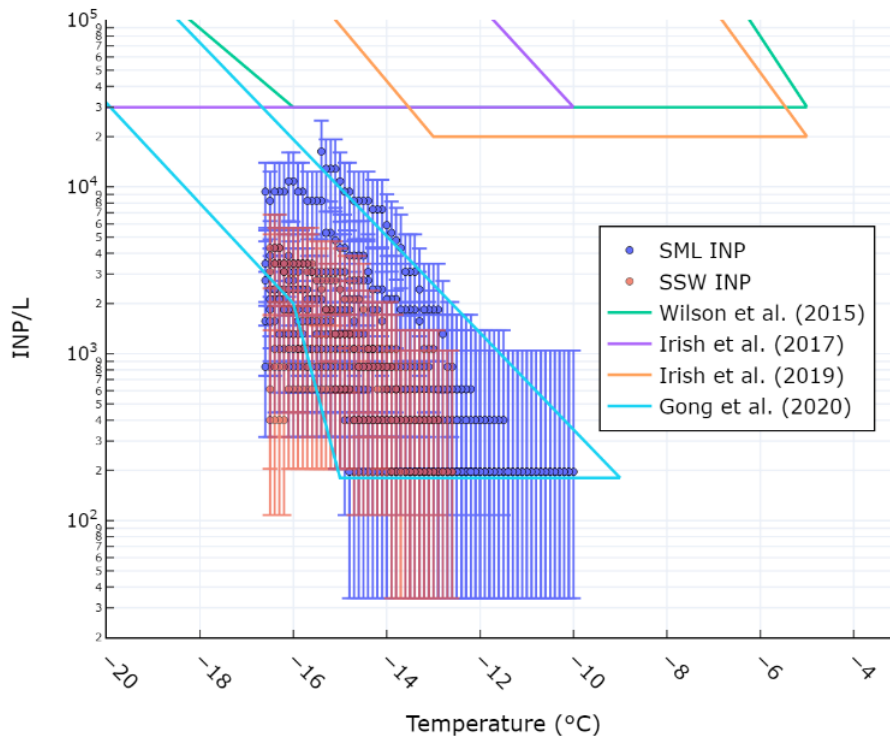
960 Particle size distribution and number concentrations of aerosols generated with the plunging apparatus were
961 monitored using a custom-made differential mobility particle sizer (DMPS) preceded by a 1-micron size-cut impactor and X-
962 ray neutralizer (TSI Inc.). Total counts from the DMPS system were checked using a condensation particle counter (CPC,
963 TSI3010). Using the DMPS, a total of 25 size bins ranging between 10-500 nm (dry particle electrical mobility diameter) were
964 scanned over a 10-minute time period. **We then averaged the size distributions across each DFPC sampling period. For the**
965 **purpose of the present study, surface area of SSA particles were calculated from the number size distributions by assuming**
966 **spherical particles. Theoretical calculation of the number and surface area distributions for particles between .5-10 μm was**
967 **also carried out. The fit from our observed number size distributions from modes 1-4 agreed well with the fit of a sea spray**
968 **aerosol source function consisting 5 lognormal modes based on in-situ particle number concentration measurements at Mace**
969 **Head and open-ocean eddy correlation flux measurements from the Eastern Atlantic (Table S1) (Ovadnevaite et al., 2014). We**
970 **took the ratio of mode 5 to mode 3 from this parameterization and applied it to our fit to calculate a fifth mode accounting for**
971 **particles ranging in size between 500 nm and 10 μm .**



974 **Figure 1. a) INP concentrations observed during the PEACETIME cruise in the SML and SSW as measured using the LINDA**
 975 **instrument. Error bars represent the binomial proportion confidence interval (95%) using the Wilson score interval. b) INP_{SSA}**
 976 **concentrations as observed by the DFPC normalized by SSA surface area. Error bars represent ±30% uncertainty of the DFPC**
 977 **instrument, as cited previously (DeMott et al., 2018).**

978 Ice nucleating particle characteristics were determined for the SSW, SML, and SSA. Figure 1a shows the concentration
 979 of INP in the SML (INP_{SML}) at two different temperatures (-12°C, -15°C) and in the SSW (INP_{SSW}) at -15°C as determined
 980 using the LINDA instrument. An initial increase occurred on May 24 (1.8x10³ INP/L at T=-15°C) relative to May 22 which
 981 was then followed by a further increase on June 4 (1.1x10⁴ INP/L at T=-15°C). The enhancement on June 4 occurred on the
 982 same day as a dust deposition event which led to an enrichment of iron in the SML relative to the underlying water (see Section
 983 3.2). While only four SSW samples were analysed for INP concentrations, they exhibited similar concentrations and trends to
 984 those seen in the SML, with an observed maximum on June 4 (2.4x10³ INP/L at T=-15.0°C). Based on these four samples, no
 985 significant enrichment of INP was observed in the SML compared to SSW, except during the dust deposition event when the
 986 SML concentration was enriched by a factor 4.5.

987 Figure 1b shows the concentration of ice nucleating particles in SSA (INP_{SSA}) normalized by particle surface area for
 988 particles with diameters smaller than 10 μm (0.1 < D_p < 10 μm) at three different temperatures as observed by the DFPC. It
 989 should be noted that INP_{SSA} measurements were conducted at colder temperatures than for the INP_{SML} measurements due to
 990 differences between the LINDA and DFPC instruments. In general, the highest concentrations of INP_{SSA} were observed at the
 991 beginning of the voyage, with an initial value of 0.45 INP_{SSA,-25C}/cm² observed on May 13, increasing to a maximum observed
 992 value of 1.5 INP_{SSA,-25C}/cm² on May 20. After May 20, a considerable drop in INP_{SSA,-25C} concentrations was observed.
 993 Concentrations remained at low, albeit with slight fluctuations, before increasing again to 0.59 INP_{SSA,-25C}/cm² on June 7. It is
 994 also worth noting that the highest concentrations of INP active at -18°C (INP_{SSA,-18C}/cm²) were observed on this day. The
 995 increase of INP concentrations around the time of the dust deposition event in early June is similar to the trend observed for
 996 seawater INP, albeit with a lag of at least one day (no observations of INP_{SSA} were made on June 6).

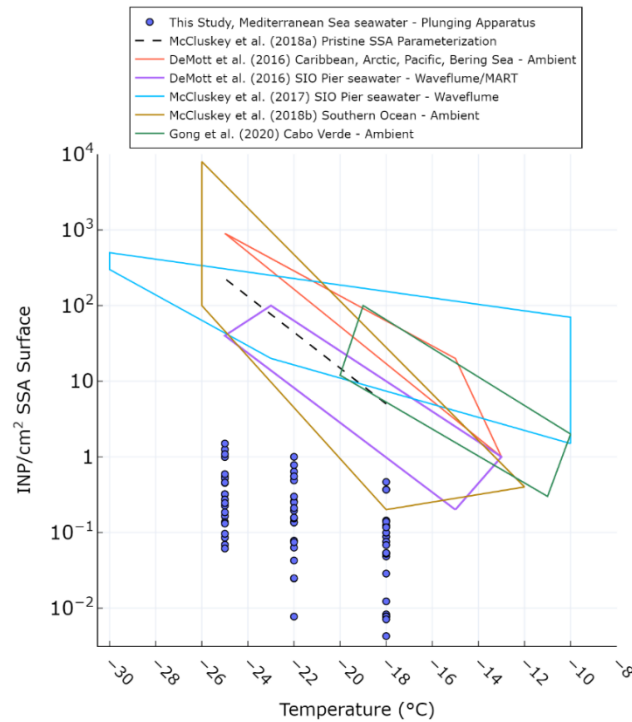


997 **Figure 2. Comparison of observed SSW (blue markers) and SML (red markers) INP concentrations with previous studies. Error**
 998 **bars represent the binomial proportion confidence interval (95%) using the Wilson score interval.**

999 Figure 2 shows the comparison of observed INP concentrations at various temperatures in the SML and SSW with
 000 those reported in previous studies. The concentrations we report here are lower than those from Arctic seawater samples
 001 reported by Irish et al. (2017; 2019) and from Arctic and North Atlantic seawater samples reported in Wilson et al. (2015).
 002 The difference can likely be attributed to the fact that eutrophic Arctic and North Atlantic seawater is more biologically active
 003 than the oligotrophic Mediterranean Sea. Our values agree well with those reported by Gong et al. (2020) who calculated INP
 004 concentrations in mid-latitude seawater off the coast of Cabo Verde. The authors of that study also posited that the low INP
 005 concentrations relative to Irish et al. (2017; 2019) and Wilson et al. (2015) was due to the lower biological activity of the
 006 oligotrophic seawater near Cabo Verde.

007 Figure 3 compares the INP per cm² of SSA surface during the PEACETIME cruise with values reported in previous
 008 studies. DeMott et al. (2016) reported INP concentrations from ambient measurements over the Caribbean, Arctic, Pacific, and
 009 Bering Sea. DeMott et al. (2016) and McCluskey et al. (2017) both reported INP concentrations from separate experiments in
 010 which SSA was artificially generated using nutrient-spiked seawater collected off the Scripps Institute of Oceanography (SIO)
 011 Pier with either a marine aerosol reference tank (MART) or an indoor waveflume. McCluskey et al. (2018a) reported ambient
 012 INP concentrations measured over the Southern Ocean. Finally, Gong et al. (2020) reported INP concentrations as measured
 013 off the coast of Cabo Verde. Our observed values are below those in all studies cited. The differences in our values compared
 014 to those in the literature can be attributed to a number of factors, including differences in trophic state of source waters,
 015 influences from terrestrial sources, and differences in INP analysis instruments. For example, Gong et al. (2020) state that
 016 most INPs observed in their study were from dust particles, rather than sea spray. Gong et al. (2020) also calculated a theoretical
 017 INP concentration based on the ratio of NaCl mass to INP in air and seawater (not shown in Figure 3). When we perform the
 018 same calculation using observed NaCl values in SSA and salinity measurements of underway seawater, we find that the
 019 INP/NaCl in the SSA is ~3000 times higher than in the SML. This is an important conclusion and points to the need for caution
 020 when using the Gong et al. (2020) approach for calculating a contribution of SSA-derived INP in ambient air aerosols in future
 021 studies. We note that studies in which seawater has been spiked with nutrients (McCluskey et al., 2017; McCluskey et al.,
 022 2018b; DeMott et al., 2016) are expected to have higher levels of biological activity than those observed in the Mediterranean
 023 and other oligotrophic regions. Since the departure of the PEACETIME INP in SML and SSW to the literature values is of the

024 same order of magnitude as the departure of the PEACETIME INP in SSA to the literature, it is reasonable to attribute the low
025 INP_{SSA} values to the oligotrophic nature of the Mediterranean seawater.



026 **Figure 3. INP/cm² SSA surface ($0.1 < D_p < 10 \mu\text{m}$) at various temperatures as measured by the DFPC during the PEACETIME**
027 **cruise (blue circles) compared with values reported in the literature. SSA were generated by continuously passing seawater from**
028 **the ship's underway system into a plunging apparatus. Error bars are not shown as the uncertainty is smaller than the data points.**

029 3.2 Correlations between INP and Biogeochemical Conditions

030 As described in the methods section, various seawater biogeochemical properties were monitored throughout the voyage
031 for the SSW and SML. Plots of selected continuous measurements from the R/V's underway sampling system and discrete
032 measurements from the pneumatic boat of relevant biogeochemical values are found in the supporting information (Figure S1
033 and Figure S2, respectively). Biogeochemical properties are described in more detail in our companion papers (Freney et al.,
034 2020; Tovar-Sanchez et al., 2019) and seawater gel properties will be discussed in an upcoming paper. Here, we present a
035 broad summary of observed conditions.

036 In general, surface waters were characterized by oligotrophic conditions as expected for the season. Bacteria
037 concentrations ranged between 2×10^5 and 7×10^5 cells/mL in the SSW and were greatest at the start and end periods of the
038 voyage. NCBL abundance followed a similar trend and ranged between 4.0×10^2 – 4.0×10^3 cells/mL. Observed DOC values
039 ranged between 700–900 $\mu\text{gC/L}$ and POC between 42–80 $\mu\text{gC/L}$ and were within the range of expected values for the
040 oligotrophic Mediterranean (540–860 $\mu\text{gC/L}$ for DOC and 9.6–104 $\mu\text{gC/L}$ for POC) (Pujo-Pay et al., 2011). SSW TEP
041 concentrations ranged between 1.2×10^6 and 1.1×10^7 particles/L, with CSP between 5.6×10^6 and 9.3×10^6 particles/L, and will
042 be discussed in a future paper.

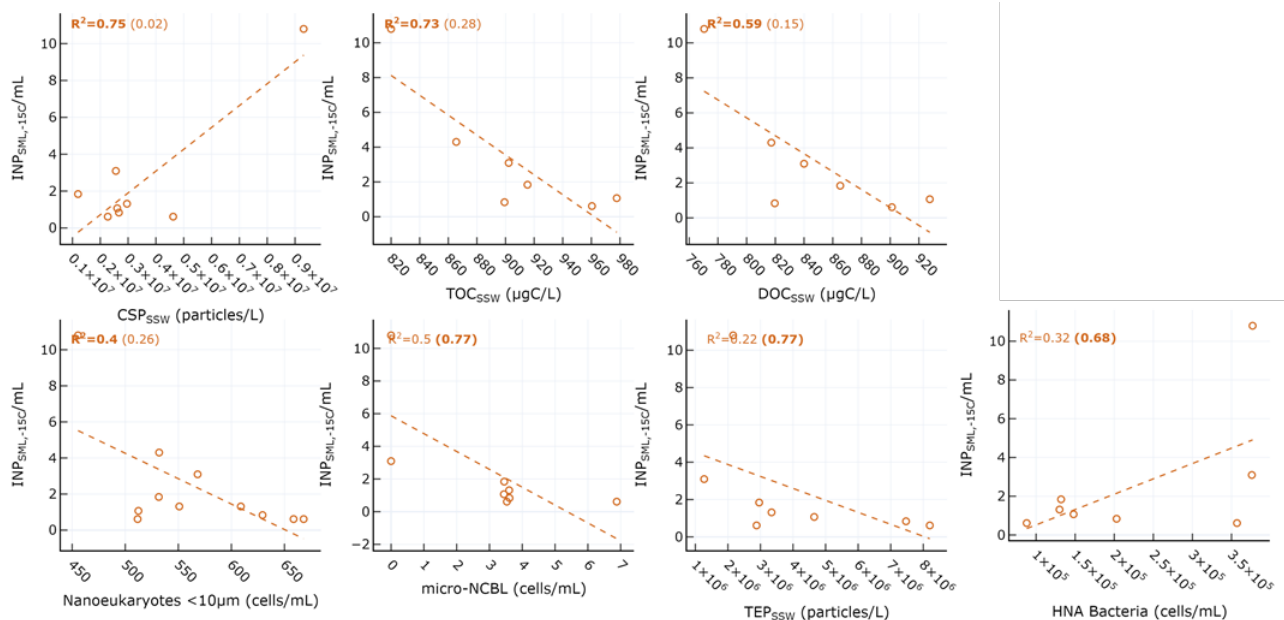
043 Enrichment factors (EF) in the SML relative to the SSW remained low with an average of 1.10 for DOC, 1.07 for bacteria,
044 and 1.17 for NCBL. As POC was not measured in the SML, we cannot report its EF. TEP was typically enriched relative to
045 the SSW, with an average EF of 4.5, while CSP EF was on average 2.7. Of importance, the dust deposition event that occurred
046 on June 4 lead to a drastic increase in SML dissolved iron relative to the SSW (EF ~800). This deposition event had important
047 impacts on the biology of the surface seawaters, which is the focus of another paper (Freney et al., 2020). As a result, TEP EF
048 increased to 17, bacteria EF increased to 1.5, and NBCL to 2.4. We next discuss the correlations between INP abundances and
049 biogeochemical properties in the following sections.

050 **3.2.1 Correlations Between INP_{SML} Abundance and Seawater Properties**

051 **Table 1. Correlation statistics between INP_{SML,-15C} and seawater properties in the SML and SSW, where p is the p-value test for**
 052 **significance and r is the Pearson correlation coefficient. Values in parentheses are calculated for days before the dust deposition**
 053 **event (i.e., days before June 4). Values that are not statistically significant (p > .05) are italicized.**

Variable	Pall days (p _{pre-dust})	r _{all days} (r _{pre-dust})
SSW		
CSP	0.005 (0.78)	0.87 (-0.15)
TOC _{SSW}	0.015 (0.36)	-0.85 (-0.53)
DOC _{SSW}	0.045 (0.52)	-0.76 (-0.39)
Nanoeukaryotes <10µm	0.038 (0.20)	-0.63 (-0.51)
Micro-NCBL	0.051 (0.021)	-0.70 (-0.88)
TEP	0.25 (0.022)	-0.46 (-0.88)
Bacteria HNA	0.14 (0.043)	0.57 (0.83)
SML		
Dissolved Iron	.0000021 (.012)	0.99 (0.91)
TEP EF	0.00032 (0.42)	0.95 (0.41)
Total Bacteria EF	0.00075 (0.82)	0.93 (-0.12)
CSP	0.0053 (0.25)	0.87 (-0.56)
Total NCBL	0.0053 (0.34)	0.87 (0.48)
Pico-NCBL	0.0088 (0.43)	0.84 (0.40)
Total Bacteria	0.016 (0.17)	0.81 (0.64)
Phytoplankton (NCBL+CBL)	0.021 (0.68)	0.78 (-0.22)
NCBL EF	0.022 (0.92)	0.78 (0.054)
DOC EF	0.041 (0.38)	0.78 (-0.51)
Nano-NCBL	0.027 (0.42)	0.77 (0.41)
Bacteria HNA	0.012 (0.068)	0.83 (0.78)
Bacteria LNA	0.037 (0.54)	0.74 (0.32)
TOC _{SML}	0.50 (0.020)	0.31 (-0.93)

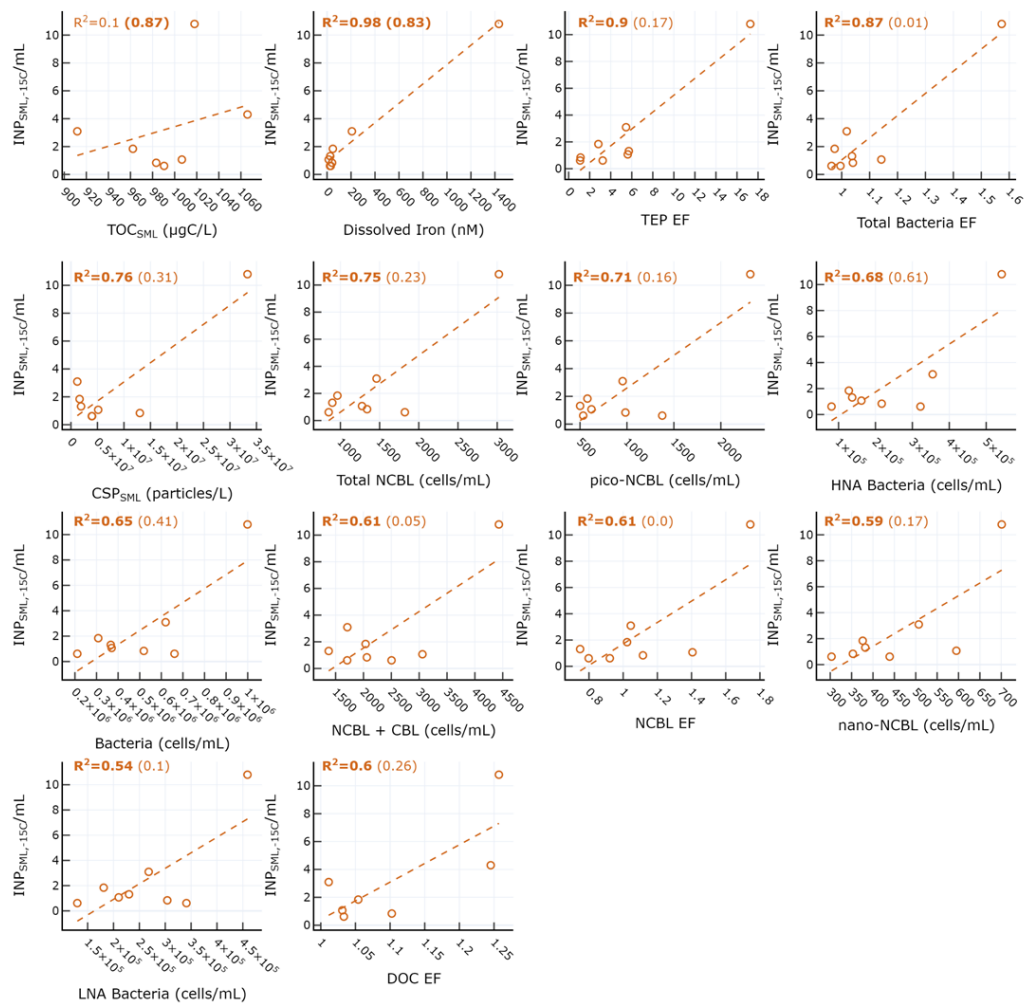
054
 055 Table 1 shows the correlation statistics between INP_{SML,-15C} and selected observed seawater properties (SSW and
 056 SML), calculated either for all days of the PEACETIME experiment or only for days before the dust deposition event (i.e.,
 057 days before June 4). Relationships are only listed in Table 1 if they were significant (p<.05) for either all days or pre-dust only
 058 days. Figure 4 shows the corresponding scatterplots of INP_{SML,-15C} abundance and SSW properties. We note a statistically
 059 significant correlation between INP_{SML,-15C} and CSP (r=0.87) as measured from the underway system. When considering only
 060 days before the dust deposition event, INP_{SML,-15C} were significantly correlated with HNA bacteria (r=0.83) while the
 061 correlation with CSP is no longer statistically significant. INP_{SML,-15C} are actually negatively correlated with most of the
 062 measured SSW properties either when excluding the dust event (for micro-NCBL_{SSW} and TEP_{SSW}) or due to the dust event (for
 063 TOC_{SSW}, DOC_{SSW} and nanoeukaryotes cell abundances). This points to a non-proportional transfer of each species from the
 064 bulk seawater to the SML relative to one another. Given the high p-values and weak correlation coefficients, it appears to be
 065 difficult to reliably relate INP_{SML} to properties of the underlying SSW. Rather, we posit that INP in the SML are more reliably
 066 dictated by SML properties, as shown in the following paragraph.



067 **Figure 4. Scatter plot of INP in the SML and various biogeochemical parameters in the SSW. R^2 for all days are shown in each plot,**
 068 **with R^2 calculated for only days before the dust event shown in parentheses. Statistically significant relationships are shown in bold.**

069 **Figure 5 shows scatterplots of statistically significant relationships between $INP_{SML,-15C}$ concentrations and various SML**
 070 **properties.** $INP_{SML,-15C}$ were most strongly positively correlated with dissolved iron ($r=0.99$), TEP EF ($r=0.95$), and bacteria
 071 EF ($r=0.93$). However, these relationships are skewed by the outlier due to the drastic increase in iron observed on June 4
 072 (Figure S2a) from the dust deposition event, as described previously. **It is difficult to discriminate between the dust and**
 073 **biological impact on the $INP_{SML,-15C}$, as dust is known to have good INP properties while also being capable of fertilizing the**
 074 **surface ocean with dissolved iron, leading to concomitant increases in biological activity. It is also possible that the dust**
 075 **deposition led to increased abundance of terrestrial OC, which would exhibit different INP activity.** When considering days
 076 before the dust event, $INP_{SML,-15C}$ is only significantly correlated with dissolved iron ($r=0.91$) and TOC in the SML ($r=-0.93$).
 077 We note that while no longer statistically significant for pre-dust days, moderate correlations were still observed between
 078 $INP_{SML,-15C}$ and total NCBL ($r=0.48$), HNA bacteria ($r=0.78$), and total bacteria ($r=0.64$). Previous reports examining the
 079 correlation between INP and microbial abundance have yielded mixed results. For example, a report of INP in Arctic SML
 080 and SSW found no statistically significant relationship between the temperature at which 10% of droplets had frozen and
 081 bacteria or phytoplankton abundances in bulk SSW and SML samples (Irish et al., 2017). However, recent mesocosm studies
 082 using nutrient-enriched seawater found that INP abundances between $-15^{\circ}C$ and $-25^{\circ}C$ in the aerosol phase were positively
 083 correlated with aerosolized bacterial abundance (McCluskey et al., 2017).

084
 085

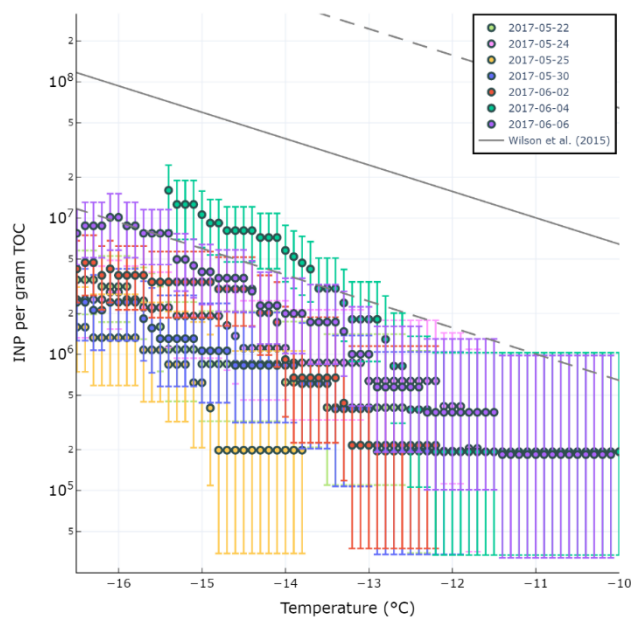


086 **Figure 5. Scatter plot of INP in the SML and various biogeochemical properties in the SML. R^2 for all days are shown in each plot,**
 087 **with R^2 calculated for only days before the dust event shown in parentheses. Statistically significant R^2 values are shown in bold.**

088 A previous study by Wilson and co-authors presented an INP parameterization (hereafter termed W15) based on a
 089 positive relationship between seawater TOC and INP abundance in Arctic, North Pacific, and Atlantic SML and SSW (Wilson
 090 et al., 2015). Total organic carbon in the SML (TOC_{SML} $\mu\text{gC/L}$), derived here as the sum of POC in the SSW (POC_{SSW}) and
 091 DOC in the SML (DOC_{SML}), was poorly correlated with $\text{INP}_{\text{SML},-15\text{C}}$ ($r=0.31$, $p=0.50$). Figure 7 shows the observed $\text{INP}_{\text{SML},-15\text{C}}/$
 092 TOC_{SML} ratio (INP per gram of TOC) for various temperatures and days of the experiment compared with the W15
 093 parameterization (grey line). Our results show observed $\text{INP}_{\text{SML}}/\text{TOC}_{\text{SML}}$ ratios below those expected by the model proposed
 094 by W15, indicating the TOC_{SML} in Mediterranean waters is less IN active at these temperatures than predicted by the W15
 095 parameterization.

096 In agreement with our findings, a recent study found that the W15 model over-predicted observed INP concentrations
 097 in the aerosol phase during two separate mesocosm experiments (McCluskey et al., 2017) by assuming the INP/TOC ratio in
 098 the SML was preserved in the aerosol phase. The authors of that study speculated that the overprediction by the W15 model
 099 was due to the fact that it does not account for the complex transfer mechanism of organic matter from the SML to the aerosol
 100 phase. Our results here show that the overprediction by W15 persists even when calculating INP in the SML and therefore the
 101 overprediction may be due to other factors beyond the transfer of organic matter from the SML to the atmosphere. We stress
 102 however, that the TOC value used in this study was derived using DOC_{SML} and POC_{SSW} values as POC measurements in the
 103 SML were not conducted. As there typically exists an enrichment of organic matter in the SML relative to the bulk seawater,
 104 it is possible that the POC_{SSW} we used to calculate TOC_{SML} was below the actual POC content in the SML, thus underestimating
 105 TOC_{SML} . However, if this was the case, a higher abundance of TOC_{SML} would only further increase the overprediction of W15

106 relative to our observations. Finally, it is possible that the oligotrophic nature of Mediterranean waters results in a pool of TOC
 107 with a different chemical composition than what is observed in more biologically productive waters such as the Arctic and
 108 Atlantic. For example, the pool of TOC during this study was dominated by DOC and featured low POC content, presumably
 109 due to low biological productivity.



110 **Figure 6. Observed INP/TOC ratio in the SML during PEACETIME experiment for different temperatures. The gray line is the fit**
 111 **from Wilson et al., 2015.**

112 In summary, $INP_{SML,-15C}$ increased with SML microbial cell counts (e.g., NCBL and heterotrophic bacteria), F_{eSML}
 113 and DOC_{EF} during a dust deposition event, but were overall not correlated with TOC nor DOC in the SML. **Compared to**
 114 **previous studies, the INP/TOC ratio observed in the Mediterranean is low.** We surmise that the overprediction of INP/TOC by
 115 the model may either be caused by a different relationship between INP and TOC at warmer temperatures, or possibly be due
 116 to the chemical characteristics of TOC in the oligotrophic Mediterranean. This complicated relationship between seawater
 117 TOC and INP_{SML} highlights the need for further studies focused on the chemical composition of DOC and POC in bulk SSW
 118 and SML. Further experiments during low and high biological productivity are needed in controlled environments to better
 119 determine under what conditions (oligotrophic and eutrophic) and location in the water column (i.e., bulk SSW vs SML) TOC,
 120 bacteria, and phytoplankton are linked to INP across a range of temperatures. **Finally, regardless of the exact mechanism,** the
 121 impact of dust deposition on $INP_{SML,-15C}$ is fairly large, as we observe an increase of by $INP_{SML,-15C}$ by almost an order of
 122 magnitude during the dust event. This impact may have climate implications if $INP_{SML,-15C}$ were efficiently transferred to the
 123 sea spray.

124 3.2.2 Correlations Between INP_{SSA} Abundance and Observed SSA and Seawater Conditions

125 In the following section, we compare INP_{SSA} at various temperatures with seawater and SSA properties. Submicron
 126 particle concentrations ranged between 1000-3000 particles/cm³ (Figure S3) and its dependence of seawater biology is further
 127 explored in a separate manuscript (Sellegrri et al. under revision). For comparison with seawater properties, INP_{SSA} was first
 128 normalized by SSA particle surface area ($0.1 < D_p < 10 \mu m$, Figure S4)(see methodology in Section 2.3.1 for estimation of
 129 SSA surface area for particles larger than $D_p=500$ nm).

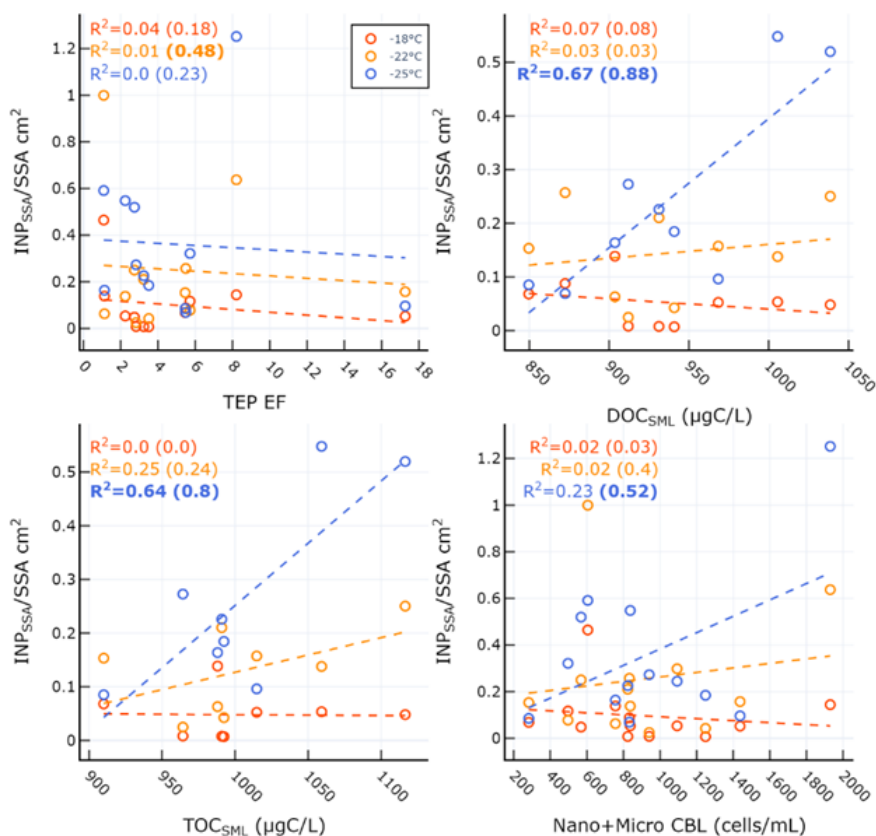
130 Table 2 shows the correlation statistics between INP_{SSA} normalized by SSA particle surface area and select conditions
 131 in the SML for relationships that were statistically significant. Figure 7 shows the corresponding scatter plots for these
 132 relationships. **We also tested for correlations on days not affected by the dust event (i.e., days before June 4), and their statistics**
 133 **are shown in parentheses in Table 2 and Figure 7.** Surprisingly, there were no significant correlations between $INP_{SSA,-18C}$ and

134 conditions in the SML, including TEP and CSP abundance and enrichment factors, bacteria abundance and enrichment factors,
 135 nor with INP_{SML} as measured by the LINDA instrument. This is somewhat unexpected considering INP in the SML at $-15^{\circ}C$
 136 was correlated with SML phytoplankton and bacteria counts, which are all expected to transfer efficiently from the SML to
 137 the aerosol phase, an assumption widely used in the modelling community. Similarly, $-22^{\circ}C$ INP_{SSA} had no significant
 138 correlations with SML variables, except for TEP EF which was positively correlated ($r=0.69$) when only considering days
 139 before the dust deposition event. At $-25^{\circ}C$, INP_{SSA} were found to be significantly correlated with DOC_{SML} and TOC_{SML} on all
 140 days ($r=0.82$ and $r=0.81$ for DOC and TOC, respectively). When examining only pre-dust event days, the significant
 141 correlations included DOC enrichment as well as nano- and micro-CBL.

142 **Table 2. Correlation statistics between INP_{SSA} and properties in the SML, where p is the p-value test for significance and r is the**
 143 **Pearson correlation coefficient. Values in parentheses are calculated for days before the dust deposition event (i.e., days before June**
 144 **4). Values that are not statistically significant ($p > .05$) are italicized.**

Variable	Full days ($p_{pre-dust}$)	Full days ($r_{pre-dust}$)
$-18^{\circ}C$		
<i>No significant correlations</i>		
$-22^{\circ}C$		
TEP EF	<i>0.81 (0.026)</i>	<i>-0.078 (0.69)</i>
$-25^{\circ}C$		
DOC_{SML}	0.0073 (0.00054)	0.82 (0.94)
TOC_{SML}	0.017 (0.0066)	0.81 (0.89)
DOC EF	<i>0.46 (0.014)</i>	<i>0.28 (0.81)</i>
Nano+Micro CBL	<i>0.10 (0.019)</i>	<i>0.47 (0.72)</i>

145



146 **Figure 7. Scatter plots of INP_{SSA} normalized by SSA particle surface area at three temperatures and select conditions in the SML**
 147 **for relationships that were statistically significant. Corresponding correlation parameters are reported Table 2. R^2 values for all**
 148 **days are shown in each plot, with R^2 values for days not including the dust deposition event (i.e., days before June 4) in parentheses.**
 149 **R^2 for statistically significant relationships are shown in bold.**

150

151
152
153

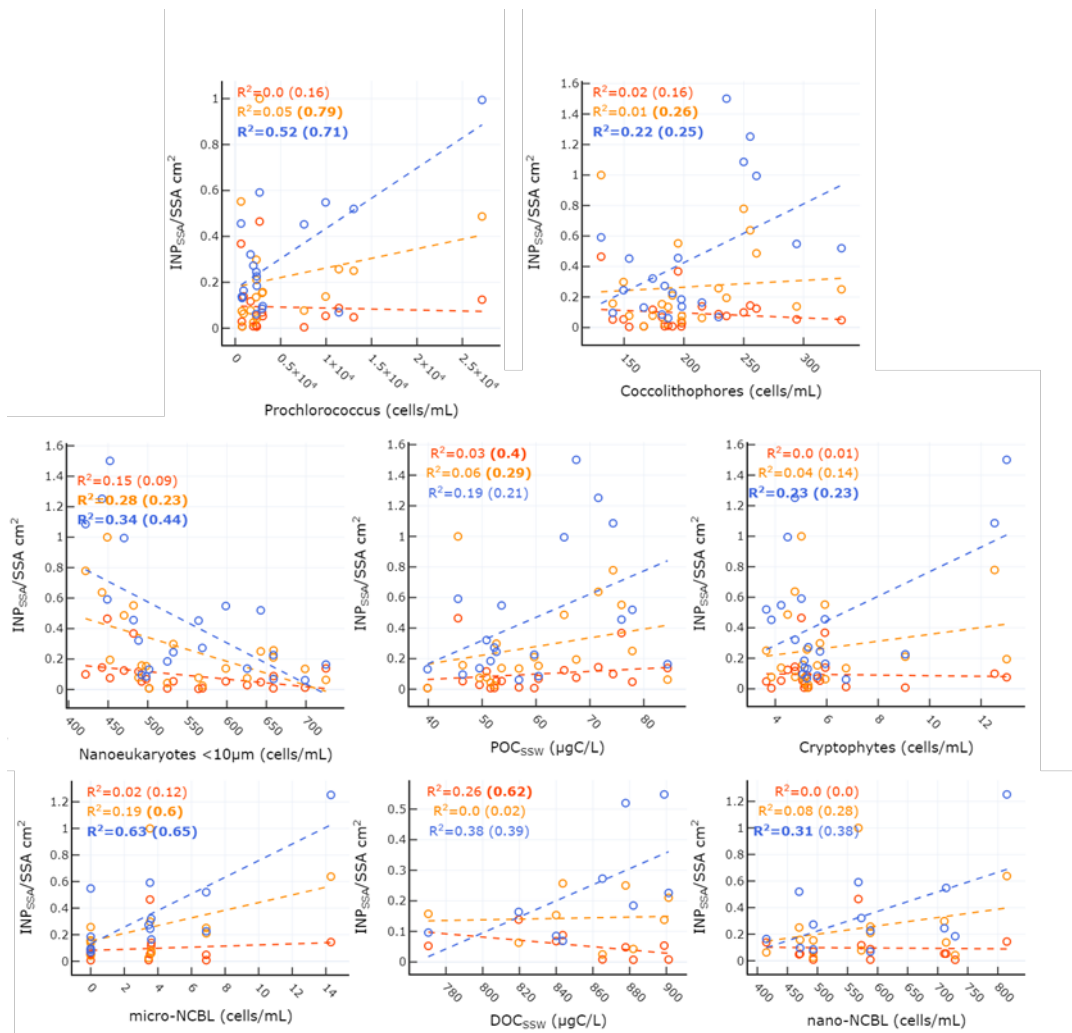
Table 3. Correlation statistics between INP_{SSA} and properties in the SSW, where p is the p-value test for significance and r is the Pearson correlation coefficient. Values in parentheses are calculated for days before the dust deposition event (i.e., days before June 4). Values that are not statistically significant (p > .05) are italicized.

Variable	p_{all days} (p_{pre-dust})	r_{all days} (r_{pre-dust})
	-18°C	
POC _{SSW}	<i>0.46 (0.0064)</i>	<i>0.18 (0.63)</i>
DOC _{SSW}	<i>0.16 (0.020)</i>	<i>-0.51 (-0.79)</i>
	-22°C	
Nanoeukaryotes <10µm	<i>0.014 (0.050)</i>	<i>-0.53 (-0.48)</i>
Prochlorococcus	<i>0.36 (0.000019)</i>	<i>0.23 (0.89)</i>
POC _{SSW}	<i>0.29 (0.037)</i>	<i>0.25 (0.54)</i>
Coccolithophores	<i>0.72 (0.035)</i>	<i>0.084 (0.51)</i>
Micro-NCBL	<i>0.14 (0.0088)</i>	<i>0.43 (0.77)</i>
	-25°C	
Nanoeukaryotes <10µm	<i>0.0055 (0.0040)</i>	<i>-0.58 (-0.66)</i>
Prochlorococcus	<i>0.00076 (0.00015)</i>	<i>0.72 (0.84)</i>
Coccolithophores	<i>0.031 (0.042)</i>	<i>0.47 (0.50)</i>
Cryptophytes	<i>0.028 (0.050)</i>	<i>0.48 (0.48)</i>
Micro-NCBL	<i>0.0012 (0.0049)</i>	<i>0.79 (0.81)</i>
Nano-NCBL	<i>0.048 (0.058)</i>	<i>0.56 (0.62)</i>

154

155 Table 3 and the corresponding scatter plots in Figure 8 show that a weak correlation exists between INP_{SSA} active at
156 -18°C and POC_{SSW} for all days, but becomes significant and strong for days not including the dust event. This points to the
157 possible interference of a different class of organic carbon (e.g., terrestrial OC) or the introduction of some other IN active
158 material (e.g., dissolved iron) which masks the impact of the original pool of POC_{SSW} on INP concentrations. INP_{SSA,-18C} are
159 also significantly correlated INP_{SSW,-16C}, (results not shown) but with a sample size of n=4 this finding requires further
160 validation. Nonetheless, this result could indicate that INP_{SSA} at this temperature come from the bulk water rather than the
161 SML. INP_{SSA} at -22°C show a slightly weaker, yet still significant correlation with POC_{SSW} than INP_{SSA} at -18°C on pre-dust
162 days (r=0.54). Additionally, they have a correlation with Prochlorococcus, coccolithophores, and micro-NCBL. This finding
163 is in agreement with a recent study in which particles generated from lysed Prochlorococcus cultures exhibited good ice
164 nucleating capabilities, albeit at much colder temperatures than observed in our study (i.e., T < -40°C) (Wolf et al., 2019).
165 INP_{SSA} at -25°C were correlated with similar variables as INP_{SSA} at -22°C, with the exception POC_{SSW}. Furthermore, the
166 correlations with the various microbial categories was stronger for INP_{SSA} at -25°C than at warmer temperatures, indicating
167 these parameters are more associated with cold INP. Interestingly, INP_{SSA,-25C} was not correlated with DOC_{SSW}, yet was
168 correlated with DOC_{SML} (Table 2), potentially indicating an important step in the process of transfer of IN active DOC material
169 to the atmosphere is its prior enrichment at the SML.

170



171 **Figure 8. Scatter plots of INP_{SSA} normalized by SSA particle surface area at three temperatures and select conditions in the SSW**
 172 **for relationships that were statistically significant. Corresponding correlation parameters are reported Table 3. R² values for all**
 173 **days are shown in each plot, with R² values for days not including the dust deposition event (i.e., days before June 4) in parentheses.**
 174 **R² for statistically significant relationships are shown in bold.**

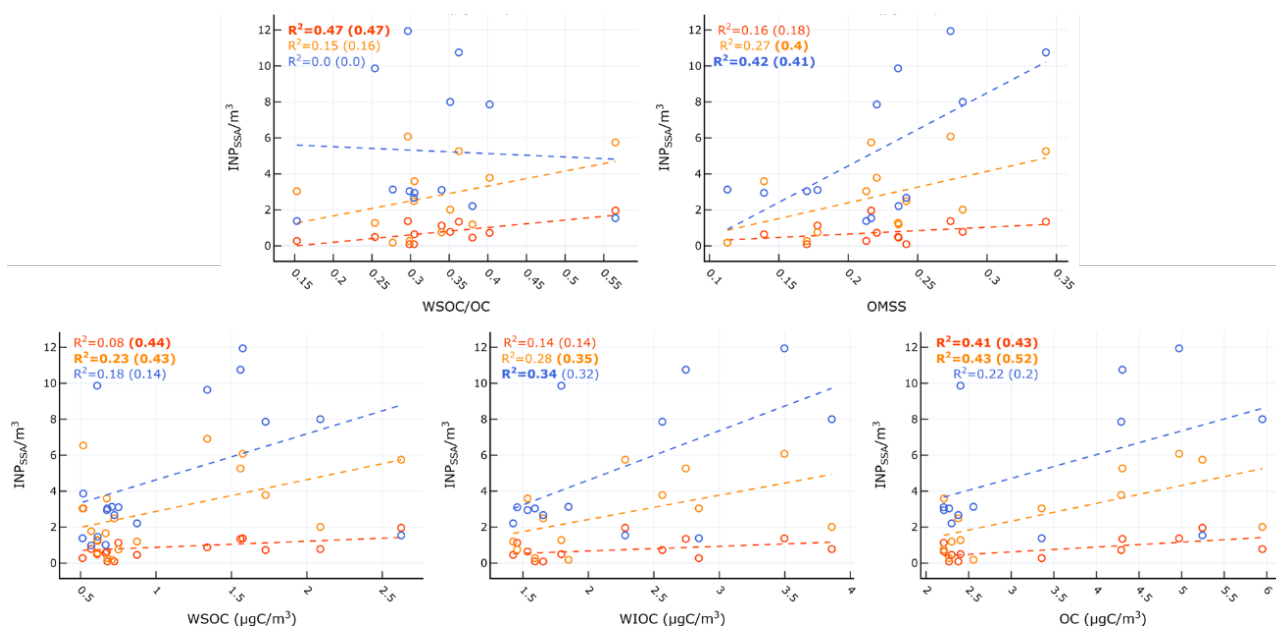
175 Table 4 and Figure 9 show the significant correlations between INP_{SSA} and SSA properties. A positive correlation was observed
 176 between INP_{SSA,-18C} and SSA organic carbon (OC) as well as the ratio of SSA water-soluble organic carbon to organic carbon
 177 (WSOC/OC). The correlation between WSOC/OC and INP_{SSA,-18C} makes sense given the finding that INP_{SSA,-18C} was correlated
 178 with POC_{SSW}. A higher WSOC/OC value would suggest a higher fraction of soluble organics which would be expected to
 179 transfer to the atmosphere from the bulk SSW rather than the SML due to their high solubility.

180 **Table 4. Correlation statistics between INP_{SSA} and SSA properties, where p is the p-value test for significance and r is the Pearson**
 181 **correlation coefficient. Values in parentheses are calculated for days before the dust deposition event (i.e., days before June 4).**
 182 **Values that are not statistically significant (p > .05) are italicized.**

Variable	p all days (p pre-dust)	r all days (r pre-dust)
-18°C		
WSOC/OC	0.0099 (0.014)	0.68 (0.68)
OC	0.018 (0.021)	0.64 (0.65)
WSOC	<i>0.25</i> (0.0074)	<i>0.29</i> (0.66)
-22°C		
WSOC	0.042 (0.0082)	0.48 (0.65)
OC	0.015 (0.0080)	0.66 (0.72)
WIOC	<i>0.061</i> (0.043)	<i>0.53</i> (0.59)
OMSS	<i>0.066</i> (0.028)	<i>0.52</i> (0.63)
-25°C		
WIOC	0.037 (<i>0.057</i>)	0.58 (<i>0.56</i>)
OMSS	0.016 (0.025)	0.65 (0.64)

193
194
195
196
197
198
199
200
201
202
203
204
205

Figure 9 and Table 4 also show that $INP_{SSA,-25C}$ had a significant correlation with WIOC and organic mass fraction of sea spray (OMSS) ($r=0.58$ and $r=0.65$, respectively). As mentioned above, $INP_{SSA,-25C}$ was found to be correlated with various microbes in the SSW, specifically Prochlorococcus, coccolithophores, and nano- and micro-NCBL. Phytoplankton are known for their ability to produce extracellular polymeric substances (Thornton, 2014), and a previous mesocosm experiment showed microbially-derived long-chain fatty acids were efficiently ejected from the seawater as SSA, increasing the fraction of highly-aliphatic, WIOC (Cochran et al., 2017). A separate manuscript discusses the trend and controls on SSA chemical composition, linking the different classes of organic carbon in submicron SSA to seawater chemical and biological properties (Freney et al., 2020). In this work, OMSS was linked to POC_{SSW} and the coccolithophores cell abundance in the SSW. In light of this and given the correlation of $INP_{SSA,-25C}$ with seawater microbial abundance and with SSA OMSS and WIOC, it seems likely that INP_{SSA} at this temperature are related to the exudates of phytoplankton which are concentrated at the SML and then emitted into the SSA as WIOC.



206
207
208

Figure 9. Scatter plots of INP_{SSA} at three temperatures and SSA properties for relationships that were statistically significant. Corresponding correlation statistics are reported Table 2. R^2 values for all days are shown in each plot, with values calculated pre-event (i.e., days before June 4) in parentheses. Statistically significant values are shown in bold.

209
210
211
212
213
214
215
216
217
218

To summarize the results thus far, we have found evidence for the existence of two classes of INP in SSA with separate sources: 1) a class of INP related to POC in the bulk SSW and SSA WIOC and 2) a class of INP related to microbial abundance and POC in the SSW, DOC in the SML, and WIOC in SSA. These findings of a two-component marine INP population agree with a recent study which also reported on the existence of dual classes of INP emitted as SSA during two mesocosm experiments, described as: 1) particulate organic carbon INP coming from intact cells or IN-active microbe fragments and 2) dissolved organic carbon INP composed of IN-active molecules enhanced during periods when the SML is enriched with exudates and cellular detritus (McCluskey et al., 2018b). However, in contrast to that study, we report here the existence of separate temperature regimes at which each INP class is active. Here, the first class of INP consists of INP that are more active at warmer temperatures ($T=-18^{\circ}C$) while the second class of INP are active at colder temperatures ($T=-25^{\circ}C$). INP at $T=-22^{\circ}C$ correlates with items from both warm and cold categories.

219

4 Proposal of New INP Parameterization and Comparison with Previous Models

220
221

To date, parameterizations for the estimation of INP in SSA have not incorporated the knowledge of a two-component INP population. Rather, they have predicted INP based on OC or SSA surface area (W15 and MC18, respectively). To improve

222 upon existing models, we formulated various parameterizations consisting of different time periods, features, and number of
 223 components for temperature ranges. Predictor features were chosen based upon their correlation with INP concentrations as
 224 described in the previous section. Single component parameterizations in which INP across all three temperatures were linked
 225 with the same features were compared with two-component parameterizations in which INP were split into warm and cold
 226 categories, each having their own predictor features. Finally, we developed and compared altered versions of the W15 and
 227 MC18 models to account for the oligotrophic seawater of the Mediterranean Sea, as the existing models were formulated from
 228 observations of eutrophic waters. Each parameterization was recalculated using data across all days of the cruise as well as for
 229 only days before the dust deposition event in order to determine the impact of the dust event on the ability to predict INP. The
 230 complete set of parameterizations and their associated fit metrics (R^2 and R_{adj}^2) are given in Table S2.

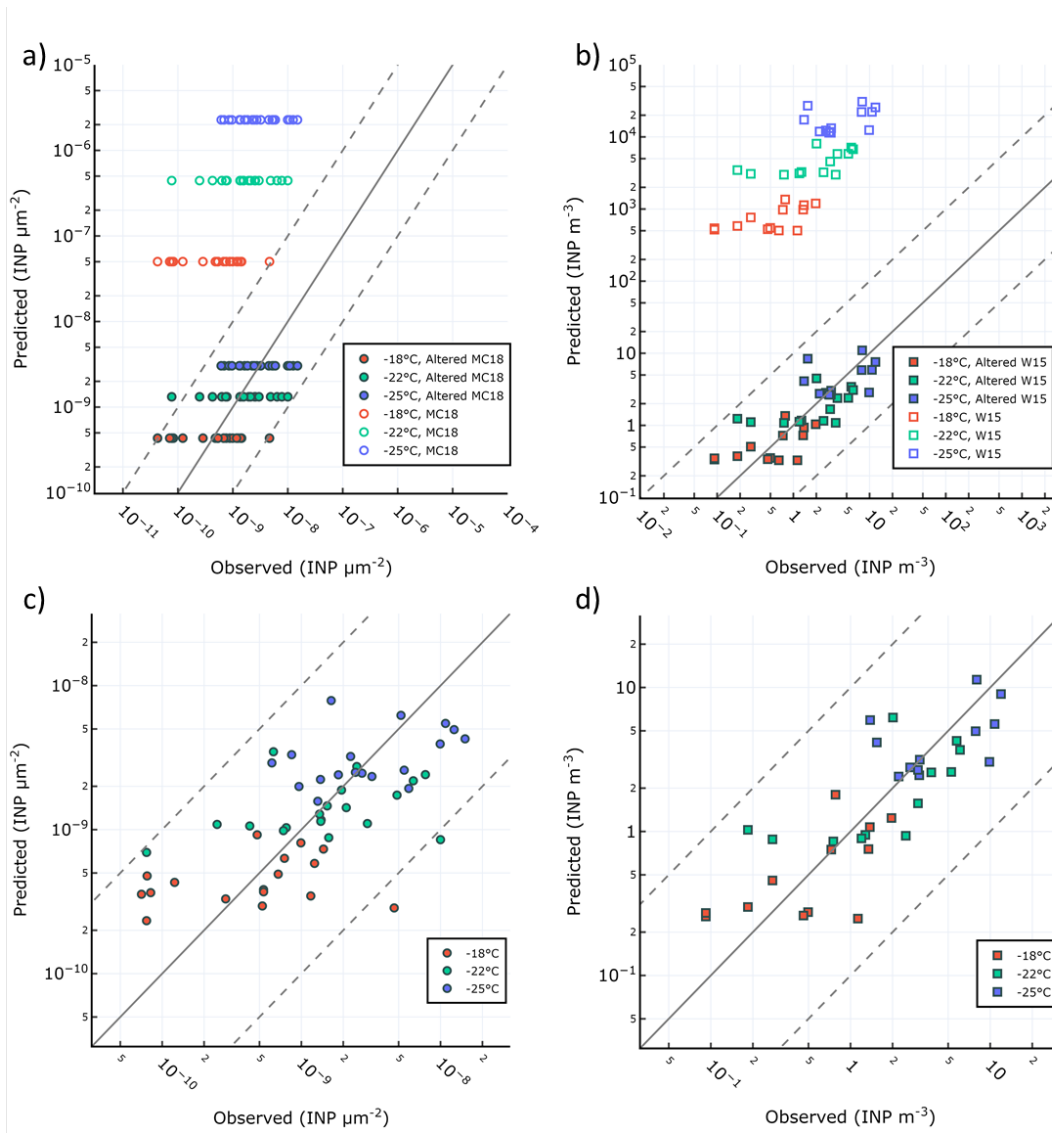
231 Figure 10a shows observed vs predicted INP_{SSA} for the W15 model, while Figure 10b shows the same but using the
 232 MC18 parameterization. Similar to our results for seawater INP (Figure 6), a large overprediction is found relative to our
 233 observations when using W15. Figure 10b shows that while MC18 is a slight improvement over the W15 approach, it still
 234 overpredicts INP by two orders of magnitude. We also present re-calculated best-fit-lines to data using the same features as in
 235 W15 and MC18 (i.e., OC and SSA surface area) in order to account for possible changes due to the oligotrophic nature of the
 236 Mediterranean Sea. We term these two parameterizations the altered Wilson fit for oligotrophy, which is given by:

$$\frac{INP}{m^3} = \exp(-7.332 - (0.2989 * T) + (0.3792 * OC_{SSA}))$$

237 and the altered McCluskey fit for oligotrophy, given as:

$$\frac{INP}{\mu m^2} = \exp(-26.57 - (0.2782 * T))$$

238 The results for these fits are shown in Figure 10a,b alongside the results of the original W15 and MC18 parameterizations.
 239 Both altered models offer improvements over the original parameterizations. The adjusted R^2 of the altered Wilson fit for
 240 oligotrophy on log-transformed INP abundance was $R_{adj}^2=0.59$ and was $R_{adj}^2=0.32$ for the altered McCluskey fit for
 241 oligotrophy. Interestingly, the adjusted Wilson fit for oligotrophy performs better than the adjust McCluskey fit for
 242 oligotrophy, which is the opposite of what was found when comparing the original models.



243 **Figure 10. Different parameterizations for prediction of INP in SSA. a) W15 and refit of same method using PEACETIME**
 244 **observations b) MK18 and refit of same method using PEACETIME observations c) single-component parameterization for**
 245 **INP/ μm^2 SSA surface area where INP at all temperatures are related to POC_{SSW} d) two-component parameterization for INP/ m^3**
 246 **where $\text{INP}_{\geq -22^\circ\text{C}}$ are related to OC and $\text{INP}_{< -22^\circ\text{C}}$ are related to WIOC.**

247 We also tried a range of novel parameterizations based on the observed correlations between INP_{SSA} with seawater
 248 and SSA properties. Below we describe two parameterizations which offered good fits to the data. The single-component
 249 parameterization assumes the abundance of INP per unit surface area of total SSA at each temperature can be predicted from
 250 POC_{SSW} concentrations:

$$\frac{\text{INP}}{\mu\text{m}^2} = \exp(-28.5324 - (0.2729 * T) + (0.0361 * \text{POC}_{\text{SSW}}))$$

251 The second parameterization separates INP into warm and cold classes, where warm INP ($\geq -22^\circ\text{C}$) are related to SSA
 252 OC and cold INP ($< -22^\circ\text{C}$) are related to the concentration of SSA WIOC. This two-component parameterization predicts the
 253 concentration of INP/ m^3 through the following equations:

$$\frac{\text{INP}_{T \geq -22^\circ\text{C}}}{\text{m}^3} = \exp(-7.9857 - (0.3178 * T) + (0.4643 * \text{OC}_{\text{SSA}}))$$

$$\frac{\text{INP}_{T < -22^\circ\text{C}}}{\text{m}^3} = \exp(-6.6606 - (0.2712 * T) + (0.5755 * \text{WIOC}_{\text{SSA}}))$$

254 Figure 10c,d shows the results of our single-component model using POC_{SSW} and the two-part model which uses SSA
 255 WIOC and OC and considers the separate temperature classes of INP. The adjusted R^2 for each model on the log-transformed
 256 INP abundance were $R_{\text{adj}}^2=0.404$ for the single component model using POC_{SSW} and $R_{\text{adj}}^2=0.60$ for the two-component model
 257 using OC and WIOC. This result reveals that they both fit the observations better than the altered McCluskey parameterization

258 for oligotrophy, while the two-component method performs as well as the altered Wilson parameterization. Each
259 parameterization's fit to the data is improved when considering pre-dust days only ($R_{adj}^2=0.63$ for the two-component
260 parameterization and $R_{adj}^2=0.57$ for the single-component parameterization). The improvement is more pronounced for the
261 single-component parameterization using POC_{SSW} , further pointing to the fact that such dust deposition events can alter the
262 INP properties of surface waters and the subsequent SSA, either through introduction of terrestrial OC or by triggering changes
263 to the trophic status of the surface waters, resulting in a different class of biologically produced OC. We note that the ratio of
264 $INP_{SSA,-18C}/OC_{SSA}$ is on average $2.08 \times 10^5 \pm 1.4 \times 10^5$ INP/gC while the ratio of $INP_{SML,-15C}/TOC_{SML}$ as reported in Section 3.2.1
265 is $3.2 \times 10^6 \pm 3.5 \times 10^6$ INP/gC. This points to a depletion in the abundance of INP active material by a factor 16 as it transfers
266 from the seawater to the SSA, which is typically assumed to be negligible in modelling studies. However, when available,
267 using a ratio of INP_{SSW}/TOC_{SSW} to predict sea spray originating INP in the atmosphere seems a better approach than using the
268 ratio $INP_{SSW}/NaCl_{SSW}$. Finally, we remind the readers that the two-component parameterization uses results of SSA chemistry
269 for submicron particles only. As previous studies have shown that the overwhelming majority of SSA OC is found in the
270 submicron phase (Gantt and Meskhidze, 2013), we argue that our analysis of WIOC, WSOC, and OC concentrations in
271 submicron SSA is representative of the whole size range of SSA.

272

273 5 Conclusions

274 In this paper we have presented results from the month-long PEACETIME cruise which took place in the Mediterranean
275 Sea during the spring of 2017, which was characterized with a dust wet deposition event that occurred towards the end of the
276 cruise. First, we find that the INP concentrations measured in the seawater are in agreement with previous studies on
277 oligotrophic waters (Gong et al., 2020). Observed INP cm² of SSA are below those reported in the literature, likely due to
278 differences in biological activity of source waters. We next investigated the relationship between seawater INP concentrations
279 and seawater biogeochemical properties. In the SML, the increase of $INP_{SML,-15C}$ concentrations during the dust deposition
280 event followed the SML microbial cell counts (e.g., NCBL, CBL and heterotrophic bacteria), F_{SML} and DOC_{EF} . Excluding
281 this dust event, $INP_{SML,-15C}$ were still correlated to Fe and bacteria (although not significantly) in the SML. Overall $INP_{SML,-15C}$
282 were not correlated with TOC nor DOC in the SML and compared to previous studies, the INP/TOC in the SML observed
283 during the PEACETIME cruise was low. We surmise that these low INP/TOC is a result of TOC from the oligotrophic
284 Mediterranean being less IN active.

285 The impact of dust deposition on $INP_{SML,-15C}$ is fairly large, as we observe an increase of $INP_{SML,-15C}$ by almost an order
286 of magnitude during this event. This impact of dust deposition could have climate implications if $INP_{SML,-15C}$ were efficiently
287 transferred to the sea spray emitted to the atmosphere. However, we find that INP_{SSA} does not evolve in the same manner as
288 the INP_{SML} does, as an increase of INP_{SSA} is observed with at least a three day delay after the dust wet deposition event. This
289 difference could be attributed to the fact that INP_{SSA} measured at $-18^\circ C$ are more influenced by the INP concentration in the
290 bulk surface seawater (as shown by the correlation between $INP_{SSA,-18C}$ and $INP_{SSW,-16C}$). It is possible that IN active species
291 deposited during the rain event, either dust- related or biology-related, take a few days before entering the bulk surface layer.

292 We also investigated the relationship between INP_{SSA} and various biogeochemical values in the SML, SSW, and SSA. In
293 general, we observed the existence of two classes of INP_{SSA} , each linked to different classes of organic matter. Our results
294 indicate each class is active at separate temperatures. Warm INP ($INP_{SSA,-18C}$) are linked to water soluble organic matter in the
295 SSA, but also to SSW parameters (POC_{SSW} $INP_{SSW,-16C}$). This indicates that INP at this temperature come from the bulk water
296 rather than the SML. Colder INP ($INP_{SSA,-25C}$) are rather correlated with SSA water-insoluble organic carbon, and SML
297 properties (DOC). As the cold INP are also correlated to the SSW nano- and micro-NCBL cell abundance as well, we
298 hypothesize that these classes of phytoplankton produce surface-active water-insoluble organic matter that is active as IN at
299 these temperatures and are transferred to the atmosphere via the SML. Unfortunately, we do not have measurements of the
300 "colder" temperatures INP in the SML to check this hypothesis.

301 We finally proposed a single-component model linking INP/m³ to POC_{SSW} and a two-component model linking warm
302 INP to SSA OC and cold INP to SSA WIOC. Both models utilize features that are readily approximated either from satellite
303 data, biogeochemical models, or from existing parameterizations and observations (Aumont et al., 2015; Rasse et al., 2017;
304 Albert et al., 2010). We then showed these parameterizations fit the data much better than previous single component models
305 based solely on SSA surface area (MC18) or OC content (W15), developed from studies of more biologically active waters.
306 We also re-calculated parameterizations based on SSA surface area and SSA OC content but for the oligotrophic Mediterranean
307 Sea. The parameterization using SSA OC content fits almost as well as the two-component model using SSA OC and WIOC.
308 However, given the results of correlation analysis with SSA properties as well as results from previous studies indicating a
309 dual composition of INP, we believe the two-component model should help improve attempts to incorporate marine INP
310 emissions into numerical models.

311
312 **Acknowledgements** This study is a contribution to the PEACETIME project (<http://peacetime-project.org>), a joint
313 initiative of the MERMEX and ChArMEx components supported by CNRS-INSU, IFREMER, CEA, and Météo-
314 France as part of the programme MISTRALS coordinated by INSU. PEACETIME was endorsed as a process study
315 by GEOTRACES. PEACETIME cruise <https://doi.org/10.17600/17000300>. We thank the captain and the crew of
316 the R/V Pourquoi Pas? for their professionalism and their work at sea. The underway optical instrumentation was
317 provided by Emmanuel Boss's group funded by Nasa Ocean Biology and biogeochemistry. This work has also
318 received funding from the European Research Council (ERC) under the European Union's Horizon 2020 research
319 and innovation program (Sea2Cloud grant agreement No 771369). Sea2Cloud was endorsed by SOLAS.

320

321 References

- 322 Albert, M. F. M. A., Schaap, M., de Leeuw, G., and Buitjes, P. J. H.: Progress in the determination of the sea spray
323 source function using satellite data, *Journal of Integrative Environmental Sciences*, 7, 159-166,
324 [10.1080/19438151003621466](https://doi.org/10.1080/19438151003621466), 2010.
- 325 Aumont, O., Ethé, C., Tagliabue, A., Bopp, L., and Gehlen, M.: PISCES-v2: an ocean biogeochemical model for
326 carbon and ecosystem studies, *Geosci. Model Dev.*, 8, 2465-2513, [10.5194/gmd-8-2465-2015](https://doi.org/10.5194/gmd-8-2465-2015), 2015.
- 327 Bigg, E. K.: Ice Nucleus Concentrations in Remote Areas, *J. Atmos. Sci.*, 30, 1153-1157,
328 [https://doi.org/10.1175/1520-0469\(1973\)030%3C1153:INCIRA%3E2.0.CO;2](https://doi.org/10.1175/1520-0469(1973)030%3C1153:INCIRA%3E2.0.CO;2), 1973.
- 329 Burrows, S. M., Hoose, C., Pöschl, U., and Lawrence, M. G.: Ice Nuclei in Marine Air: Biogenic Particles or Dust?,
330 *ACP*, 13, 245-267, <https://doi.org/10.5194/acp-13-245-2013>, 2013.
- 331 Burrows, S. M., Ogunro, O., Frossard, A. A., Russell, L. M., Rasch, P. J., and Elliott, S. M.: A Physically Based
332 Framework for Modeling the Organic Fractionation of Sea Spray Aerosol from Bubble Film Langmuir Equilibria,
333 *ACP*, 14, 13601-13629, <https://doi.org/10.5194/acp-14-13601-2014>, 2014.
- 334 Cochran, R. E., Laskina, O., Trueblood, J. V., Estillore, A. D., Morris, H. S., Jayarathne, T., Sultana, C. M., Lee, C., Lin,
335 P., Laskin, J., Laskin, A., Dowling, J. A., Qin, Z., Cappa, C. D., Bertram, T. H., Tivanski, A. V., Stone, E. A., Prather, K.
336 A., and Grassian, V. H.: Molecular Diversity of Sea Spray Aerosol Particles: Impact of Ocean Biology on Particle
337 Composition and Hygroscopicity, *Chem*, 2, 655-667, [10.1016/j.chempr.2017.03.007](https://doi.org/10.1016/j.chempr.2017.03.007), 2017.
- 338 DeMott, P. J., Hill, T. C. J., McCluskey, C. S., Prather, K. A., Collins, D. B., Sullivan, R. C., Ruppel, M. J., Mason, R. H.,
339 Irish, V. E., Lee, T., Hwang, C. Y., Rhee, T. S., Snider, J. R., McMeeking, G. R., Dhaniyala, S., Lewis, E. R., Wentzell, J.
340 J. B., Abbatt, J., Lee, C., Sultana, C. M., Ault, A. P., Axson, J. L., Martinez, M. D., Venero, I., Santos-Figueroa, G.,
341 Stokes, D. M., Deane, G. B., Mayol-Bracero, O. L., Grassian, V. H., Bertram, T. H., Bertram, A. K., Moffett, B. F., and
342 Franc, G. D.: Sea Spray Aerosol as a Unique Source of ice Nucleating Particles, *PNAS*, 113, 5797-5803,
343 <https://doi.org/10.1073/pnas.1514034112>, 2016.
- 344 DeMott, P. J., Möhler, O., Cziczo, D. J., Hiranuma, N., Petters, M. D., Petters, S. S., Belosi, F., Bingemer, H. G.,
345 Brooks, S. D., Budke, C., Burkert-Kohn, M., Collier, K. N., Danielczok, A., Eppers, O., Felgitsch, L., Garimella, S.,
346 Grothe, H., Herenz, P., Hill, T. C. J., Höhler, K., Kanji, Z. A., Kiselev, A., Koop, T., Kristensen, T. B., Krüger, K., Kulkarni,

347 G., Levin, E. J. T., Murray, B. J., Nicosia, A., O'Sullivan, D., Peckhaus, A., Polen, M. J., Price, H. C., Reicher, N.,
348 Rothenberg, D. A., Rudich, Y., Santachiara, G., Schiebel, T., Schrod, J., Seifried, T. M., Stratmann, F., Sullivan, R. C.,
349 Suski, K. J., Szakáll, M., Taylor, H. P., Ullrich, R., Vergara-Temprado, J., Wagner, R., Whale, T. F., Weber, D., Welti,
350 A., Wilson, T. W., Wolf, M. J., and Zenker, J.: The Fifth International Workshop on Ice Nucleation phase 2 (FIN-02):
351 laboratory intercomparison of ice nucleation measurements, *Atmospheric Measurement Techniques*, 11, 6231-
352 6257, 10.5194/amt-11-6231-2018, 2018.

353 Engel, A.: Determination of Marine Gel Particles, in: *Practical Guidelines for the Analysis of Seawater*, edited by:
354 Wurl, O., (CRC Press Taylor & Francis Group), Boca Raton, FL, 125-142, 2009.

355 Franklin, C. N., Z. Sun, D. B., Yan, M. D. H., and Bodas-Salcedo, A.: Evaluation of Clouds in ACCESS Using the Satellite
356 Simulator Package COSP: Global, Seasonal, and Regional Cloud Properties, *J. Geophys. Res. Atmos.*, 118, 732-748,
357 <https://doi.org/10.1029/2012JD018469>, 2013.

358 Freney, E., Sellegri, K., Nicosia, A., Trueblood, J. V., Bloss, M., Rinaldi, M., Prevot, A., Slowik, J. G., Thyssen, M.,
359 Gregori, G., Engel, A., Zanker, B., Desboeufs, K., Asmi, E., Lefevre, D., and Guieu, C.: High Time Resolution of
360 Organic Content and Biological Origin of Mediterranean Sea Spray Aerosol, *ACP*, 2020.

361 Fuentes, E., Coe, H., Green, D., de Leeuw, G., and McFiggans, G.: Laboratory-generated primary marine aerosol
362 via bubble-bursting and atomization, *Atmos. Meas. Tech.*, 3, 141-162, 10.5194/amt-3-141-2010, 2010.

363 Gantt, B., and Meskhidze, N.: The physical and chemical characteristics of marine primary organic aerosol: a
364 review, *Atmospheric Chemistry and Physics*, 13, 3979-3996, 10.5194/acp-13-3979-2013, 2013.

365 Gong, X., Wex, H., van Pinxteren, M., Triesch, N., Fomba, K. W., Lubitz, J., Stolle, C., Robinson, T.-B., Müller, T.,
366 Herrmann, H., and Stratmann, F.: Characterization of aerosol particles at Cabo Verde close to sea level and at the
367 cloud level – Part 2: Ice-nucleating particles in air, cloud and seawater, *Atmospheric Chemistry and Physics*, 20,
368 1451-1468, 10.5194/acp-20-1451-2020, 2020.

369 Hiranuma, N., Adachi, K., Bell, D. M., Belosi, F., Beydoun, H., Bhaduri, B., Bingemer, H., Budke, C., Clemen, H.-C.,
370 Conen, F., Cory, K. M., Curtius, J., DeMott, P. J., Eppers, O., Grawe, S., Hartmann, S., Hoffmann, N., Höhler, K.,
371 Jantsch, E., Kiselev, A., Koop, T., Kulkarni, G., Mayer, A., Murakami, M., Murray, B. J., Nicosia, A., Petters, M. D.,
372 Piazza, M., Polen, M., Reicher, N., Rudich, Y., Saito, A., Santachiara, G., Schiebel, T., Schill, G. P., Schneider, J.,
373 Segev, L., Stopelli, E., Sullivan, R. C., Suski, K., Szakáll, M., Tajiri, T., Taylor, H., Tobo, Y., Ullrich, R., Weber, D., Wex,
374 H., Whale, T. F., Whiteside, C. L., Yamashita, K., Zelenyuk, A., and Möhler, O.: A comprehensive characterization
375 of ice nucleation by three different types of cellulose particles immersed in water, *Atmospheric Chemistry and
376 Physics*, 19, 4823-4849, 10.5194/acp-19-4823-2019, 2019.

377 Irish, V. E., Elizondo, P., Chen, J., Chou, C., Charette, J., Lizotte, M., Ladino, L. A., Wilson, T. W., Gosselin, M.,
378 Murray, B. J., Polishchuk, E., Abbatt, J. P. D., Miller, L. A., and Bertram, A. K.: Ice-Nucleating Particles in Canadian
379 Arctic Sea-Surface Microlayer and Bulk Seawater, *Atmos. Chem. Phys.*, 17, 10583-10595,
380 <https://doi.org/10.5194/acp-17-10583-2017>, 2017.

381 Irish, V. E., Hanna, S. J., Xi, Y., Boyer, M., Polishchuk, E., Ahmed, M., Chen, J., Abbatt, J. P. D., Gosselin, M., Chang,
382 R., Miller, L. A., and Bertram, A. K.: Revisiting properties and concentrations of ice-nucleating particles in the sea
383 surface microlayer and bulk seawater in the Canadian Arctic during summer, *Atmospheric Chemistry and Physics*,
384 19, 7775-7787, 10.5194/acp-19-7775-2019, 2019.

385 Knopf, D. A., Alpert, P. A., Wang, B., and Aller, J. Y.: Stimulation of Ice Nucleation by Marine Diatoms, *Nat. Geosci.*,
386 4, 88-90, <https://doi.org/10.1038/ngeo1037>, 2011.

387 McCluskey, C. S., Hill, T. C. J., Malfatti, F., Sultana, C. M., Lee, C., Santander, M. V., Beall, C. M., Moore, K. A.,
388 Cornwell, G. C., Collins, D. B., Prather, K. A., Jayarathne, T., Stone, E. A., Azam, F., Kreidenweis, S. M., and DeMott,
389 P. J.: A Dynamic Link between Ice Nucleating Particles Released in Nascent Sea Spray Aerosol and Oceanic
390 Biological Activity during Two Mesocosm Experiments, *J. Atmos. Sci.*, 74, 151-166, <https://doi.org/10.1175/JAS-D-16-0087.1>, 2017.

392 McCluskey, C. S., Hill, T. C. J., Humphries, R. S., Rauker, A. M., Moreau, S., Stratton, P. G., Chambers, S. D., Williams,
393 A. G., McRobert, I., Ward, J., Keywood, M. D., Harnwell, J., Ponsonby, W., Loh, Z. M., Krummel, P. B., Protat, A.,
394 Kreidenweis, S. M., and DeMott, P. J.: Observations of Ice Nucleating Particles Over Southern Ocean Waters,
395 *Geophysical Research Letters*, 45, 11,989-911,997, 10.1029/2018gl079981, 2018a.

396 McCluskey, C. S., Hill, T. C. J., Sultana, C. M., Laksina, O., Trueblood, J. V., Santander, M. V., Beall, C. M., Michaud,
397 J. M., Kreidenweis, S. M., Prather, K. A., Grassian, V. H., and DeMott, P. J.: A Mesocosm Double Feature: Insights
398 into the Chemical Makeup of Marine Ice Nucleating Particles, *J. Atmos. Sci.*, 75, 2405-2423,
399 <https://doi.org/10.1175/JAS-D-17-0155.1>, 2018b.

400 McCluskey, C. S., Ovadnevaite, J., Rinaldi, M., Atkinson, J., Belosi, F., Ceburnis, D., Marullo, S., Hill, T. C. J.,
401 Lohmann, U., Kanji, Z. A., O'Dowd, C., Kreidenweis, S. M., and DeMott, P. J.: Marine and Terrestrial Organic Ice-

402 Nucleating Particles in Pristine Marine to Continentally Influenced Northeast Atlantic Air Masses, *J. Geophys. Res.*
403 *Atmos.*, 123, 6196-6212, <https://doi.org/10.1029/2017JD028033>, 2018c.

404 McCluskey, C. S., DeMott, P. J., Ma, P. L., and Burrows, S. M.: Numerical Representations of Marine Ice-Nucleating
405 Particles in Remote Marine Environments Evaluated Against Observations, *Geophys. Res. Lett.*, 46, 7838-7847,
406 <https://doi.org/10.1029/2018GL081861>, 2019.

407 McCoy, D. T., Hartmann, D. L., Zelinka, M. D., Ceppi, P., and Grosvenor, D. P.: Mixed-phase Cloud Physics and
408 Southern Ocean Cloud Feedback in Climate Models, *Journal of Geophysical Research: Atmospheres*, 120, 9539-
409 95554, <https://doi.org/10.1175/JAS-D-17-0155.1>, 2015.

410 McCoy, D. T., Tan, I., Hartmann, D. L., Zelinka, M. D., and Storelvmo, T.: On the Relationship Among Cloud Cover,
411 Mixed-phase Partitioning and Planetary Albedo in GCMs, *Journal of Advances in Modeling Earth Systems*, 8, 650-
412 668, <https://doi.org/10.1002/2015MS000589>, 2016.

413 Ovadnevaite, J., Manders, A., de Leeuw, G., Ceburnis, D., Monahan, C., Partanen, A. I., Korhonen, H., and O'Dowd,
414 C. D.: A sea spray aerosol flux parameterization encapsulating wave state, *Atmospheric Chemistry and Physics*,
415 14, 1837-1852, 10.5194/acp-14-1837-2014, 2014.

416 Pujó-Pay, M., Conan, P., Oriol, L., Cornet-Barthaux, V. C., Falco, C., Ghiglione, J.-F., Goyet, C., Moutin, T., and
417 Prieur, L.: Integrated Survey of Elemental Stoichiometry (C, N, P) from the Western to Eastern Mediterranean Sea,
418 *Biogeosciences*, 8, 883-899, <https://doi.org/10.5194/bg-8-883-2011>, 2011.

419 Rasse, R., Dall'Olmo, G., Graff, J., Westberry, T. K., van Dongen-Vogels, V., and Behrenfeld, M. J.: Evaluating Optical
420 Proxies of Particulate Organic Carbon across the Surface Atlantic Ocean, *Frontiers in Marine Science*, 4, 367, 2017.

421 Rogers, D. C., DeMott, P. J., Kreidenweis, S. M., and Chen, Y.: Measurements of Ice Nucleating Aerosols During
422 SUCCESS, *Geophys. Res. Lett.*, 25, 1383-1386, <https://doi.org/10.1029%2F97GL03478>, 1998.

423 Schnell, R. C., and Vali, G.: Biogenic ice Nuclei: Part I. Terrestrial and Marine Sources, *J. Atmos. Sci.*, 33, 1554-1564,
424 [https://doi.org/10.1175/1520-0469\(1976\)033%3C1554:BINPIT%3E2.0.CO;2](https://doi.org/10.1175/1520-0469(1976)033%3C1554:BINPIT%3E2.0.CO;2), 1976.

425 Schwier, A. N., Rose, C., Asmi, E., Ebling, A. M., Landing, W. M., Marro, S., Pedrotti, M.-L., Sallon, A., Iuculano, F.,
426 Agusti, S., Tsiola, A., Pitta, P., Louis, J., Guieu, C., Gazeau, F., and Sellegri, K.: Primary Marine Aerosol Emissions
427 from the Mediterranean Sea During Pre-Bloom and Oligotrophic Conditions: Correlations to Seawater
428 Chlorophyll-a From a Mesocosm Study, *Atmos. Chem. Phys.*, 15, 7961-7976, <https://doi.org/10.5194/acp-15-7961-2015>, 2015.

430 Schwier, A. N., Sellegri, K., Mas, S., Charrière, B., Pey, J., Rose, C., Temime-Roussel, B., Jaffrezo, J.-L., Parin, D.,
431 Picard, D., Ribeiro, M., Roberts, G., Sempéré, R., Marchand, N., and D'Anna, B.: Primary marine aerosol physical
432 flux and chemical composition during a nutrient enrichment experiment in mesocosms in the Mediterranean Sea,
433 *Atmospheric Chemistry and Physics*, 17, 14645-14660, 10.5194/acp-17-14645-2017, 2017.

434 Stopelli, E., Conen, F., Zimmermann, L., Alewell, C., and Morris, C. E.: Freezing Nucleation Apparatus puts New
435 Slant on Study of Biological Ice Nucleators in Precipitation, *Atmos. Meas. Tech.*, 7, 129-134,
436 <https://doi.org/10.5194/amt-7-129-2014>, 2014.

437 Thornton, D. C. O.: Dissolved organic matter (DOM) release by phytoplankton in the contemporary and future
438 ocean, *European Journal of Phycology*, 49, 20-46, 10.1080/09670262.2013.875596, 2014.

439 Tovar-Sanchez, A., Arrieta, J. M., Duarte, C. M., and Sanudo-Wilhelmy, S. A.: Spatial Gradients in Trace Metal
440 Concentrations in the Surface Microlayer of the Mediterranean Sea, *Front. Mar. Sci.*, 1, 1-8,
441 <https://doi.org/10.3389/fmars.2014.00079>, 2019.

442 Vali, G.: Quantitative Evaluation of Experimental Results on the Heterogeneous Freezing Nucleation of
443 Supercooled Liquids, *J. Atmos. Sci.*, 28, 402-409, 1971.

444 Vali, G., DeMott, P. J., Möhler, O., and Whale, T. F.: Technical Note: A proposal for ice nucleation terminology,
445 *Atmospheric Chemistry and Physics*, 15, 10263-10270, 10.5194/acp-15-10263-2015, 2015.

446 Vergara-Temprado, J., Murray, B. J., Wilson, T. W., O'Sullivan, D., Browse, J., Pringle, K. J., O'Sullivan, D., Browse,
447 J. P., K. J., Ardon-Dryer, K., Bertram, A. K., Burrows, S. M., Ceburnis, D., DeMott, P. J., Mason, R. H., O'Dowd, C. D.,
448 Rinaldi, M., and Carslaw, K. S.: Contribution of Feldspar and Marine Organic Aerosols to Global Ice Nucleating
449 Particle Concentrations, *ACP*, 17, 3637-3658, <https://doi.org/10.5194/acp-17-3637-2017>, 2017.

450 Verheggen, B., Cozic, J., Weingartner, E., Bower, K., Mertes, S., Connolly, P., Gallagher, M., Flynn, M., Choulaton,
451 T., and Baltensperger, U.: Aerosol Partitioning Between the Interstitial and the Condensed Phase in Mixed-phase
452 Clouds, *J. Geophys. Res.*, 112, <https://doi.org/10.1029/2007JD008714>, 2007.

453 Wilson, T. W., Ladino, L. A., Alpert, P. A., Breckels, M. N., Brooks, I. M., Browse, J., Burrows, S. M., Carslaw, K. S.,
454 Huffman, J. A., Judd, C., Kilhau, W. P., Mason, R. H., McFiggans, G., Miller, L. A., Nájera, J. J., Polishchuk, E., Rae,
455 S., Schiller, C. L., Si, M., Vergara Temprado, J., Whale, T. F., Wong, J. P. S., Wurl, O., Yakobi-Hancock, J. D., Abbatt,

456 J. P. D., Aller, J. Y., Bertram, A. K., Knopf, D. A., and Murray, D. J.: A Marine Biogenic Source of Atmospheric Ice-
457 Nucleating Particles, *Nature*, 525, 234-238, <https://doi.org/10.1038/nature14986>, 2015.
458 Wolf, M. J., Coe, A., Dove, L. A., Zawadowicz, M. A., Dooley, K., Biller, S. J., Zhang, Y., Chisholm, S. W., and Cziczo,
459 D. J.: Investigating the Heterogeneous Ice Nucleation of Sea Spray Aerosols Using *Prochlorococcus* as a Model
460 Source of Marine Organic Matter, *Environ Sci Technol*, 53, 1139-1149, 10.1021/acs.est.8b05150, 2019.
461